A Statistically-Based Continuum Theory for Polymers with Transient Networks

Manuscript Details

Manuscript number	JMPS_2017_163
Title	A Statistically-Based Continuum Theory for Polymers with Transient Networks
Article type	Full Length Article

Abstract

We present a physics-based theoretical framework to describe the transient mechanical response of polymers undergoing finite deformation. For this, a statistical description of the polymer network is provided by a distribution function that is allowed to evolve in time due to a combination of deformation and chain reconfiguration enabled by transient cross-links. After presenting the evolution law for the chain distribution function, we show that, using classical thermodynamics, one can determine how the entropy, elastic energy and true stress evolve in terms of the network configuration. In particular, we introduce the concept of distribution tensor, that enables a clean transition between the network statistics, its continuum representation and the macroscopic polymer response. In the context of Gaussian statistics, it is further shown that this tensor follows its own evolution law, enabling a simple handling of visco-elastic rubbers. The model degenerates to classical rubber elasticity when cross-links are permanent, while the case of viscous fluids is recovered for fast cross-link kinetics. The generality of the framework as well as its relevance to modeling a number of important dissipative processes occurring in polymers using a continuum approach are also discussed.

Corresponding Author	Franck Vernerey
Order of Authors	Franck Vernerey, Rong Long, Roberto Brighenti
Suggested reviewers	Ellen Arruda, Xuanhe Zhao, Christian Linder

Submission Files Included in this PDF

File Name [File Type]

Cover Letter.pdf [Cover Letter]

response letter.pdf [Response to Reviewers]

Highlights.pdf [Highlights]

revised manuscript_HL.pdf [Manuscript File]

revised manuscript.docx [Supporting File]

To view all the submission files, including those not included in the PDF, click on the manuscript title on your EVISE Homepage, then click 'Download zip file'.

Highlights

- A statistically-based continuum theory is proposed to model the transient response of polymers
- An evolution equation is derived for a distribution tensor that characterize the polymer network
- This tensor enables a direct connection between chain statistics and visco-elastic response.
- The theory can incorporate various elastic and dissipative mechanisms from the molecular scale

A Statistically-Based Continuum Theory for Polymers with Transient Networks

Franck J. Vernerey[1,*], Rong Long[1] and Roberto Brighenti[2]

[1] *Department of Mechanical Engineering*
Program of Materials Science and Engineering
University of Colorado Boulder - USA

[2] *Department of Engineering & Architecture,*
University of Parma - Italy

Abstract

We present a physics-based theoretical framework to describe the transient mechanical response of polymers undergoing finite deformation. For this, a statistical description of the polymer network is provided by a distribution function that is allowed to evolve in time due to a combination of deformation and chain reconfiguration enabled by transient cross-links. After presenting the evolution law for the chain distribution function, we show that, using classical thermodynamics, one can determine how the entropy, elastic energy and true stress evolve in terms of the network configuration. In particular, we introduce the concept of distribution tensor, that enables a clean transition between the network statistics, its continuum representation and the macroscopic polymer response. In the context of Gaussian statistics, it is further shown that this tensor follows its own evolution law, enabling a simple handling of visco-elastic rubbers. The model degenerates to classical rubber elasticity when cross-links are permanent, while the case of viscous fluids is recovered for fast cross-link kinetics. The generality of the framework as well as its relevance to modeling a number of important dissipative processes occurring in polymers using a continuum approach are also discussed.

Keywords: polymer mechanics, visco-elasticity, transient response, dynamic cross-links, statistical theory.

*Corresponding author: franck.vernerey@colorado.edu

1. Introduction

Soft polymeric materials exhibit complex mechanical behaviors, ranging from elastic solids (e.g. crosslinked rubber networks) to viscous fluid (e.g. polymer melts). Tremendous efforts have been devoted to the theoretical modeling of soft polymer mechanics [1-3]. For example, numerous models have been developed in the literature to describe the nonlinear elasticity of soft rubbers capable of large and reversible deformation, following mainly two approaches. In the first approach, phenomenological models are proposed to match experimental data under the constraints derived from continuum mechanics, e.g. frame indifference and material symmetry [4-5]. In contrast, the second approach is based on the statistical mechanics of individual polymer chains [6-10]. When a single chain is stretched, its configurational entropy is reduced which provides the energetic driving force for elastic recovery. Such entropic elasticity can be captured by a number of single chain models, e.g. freely jointed chain (FJC) with Gaussian statistics [11-13]. Because the second approach is rooted in molecular physics of polymer chains, it can be extended to accommodate the nonlinear elastic behaviors of soft polymers in a more guided manner instead of trial-and-error. For example, the concept of Langevin statistics [13] has been used for the FJC model, in place of Gaussian statistics, to capture the strain stiffening effects of soft rubbers at large strains [9, 14]. A necessary component for the second approach is a link between the single chain model and the continuum mechanics of polymer network. A number of models have been proposed to establish such a link, including the 3-chain model [8], the 4-chain model [6-7], the 8-chain model [9], and the full-network model [10, 15] among others. An excellent review of this subject can be found in Boyce and Arruda [1].

Viscoelasticity in soft polymers involves more complex molecular mechanisms such as temporary chain entanglements and chain diffusion [16-17]. The dynamics of chain entanglements and diffusion have been extensively studied in the physics community in the past few decades [13, 16-17]. However, the theoretical insights established in the polymer physics literature have not been fully translated to advancements in continuum models of viscoelasticity. Most existing models, from the simple linear Maxwell or Kelvin-Voigt models [18] to the more sophisticated nonlinear viscoelastic models [19-22], are phenomenological. While in some of these models (e.g. [22]) the continuum-level relaxation or creeping behavior was prescribed with inspirations from chain entanglement dynamics, models that directly connect the molecular physics of chain dynamics and macroscopic viscoelasticity are still not available. A difficulty with building molecular physics-based viscoelasticity models is the lack of a common natural reference configuration for all chains, due to the relaxation processes enabled by disentanglement and chain diffusion.

To accommodate this feature, Green and Tolbosky [23] assumed a conceptual picture when the chains in viscoelastic polymers can detach and reattach, resulting in families of chains with distinct natural reference configurations. This approach was further developed by others [24-29] and also discussed in the continuum mechanics literature as the method of multiple natural configurations, e.g. by Rajagopal and Srinavasa [30]. In this class of models, the chains are assumed to be born at a natural relaxed configuration when reattached to the network. The populations of chains born at different times along the external loading history, thereby possessing different relaxed configurations, are tracked by following the kinetics of chain detachment and reattachment. More recently, the conceptual picture of chain detachment and reattachment was realized in a new class of polymers with dynamic bonds, either through

reversible bonds or bond exchange reactions [31-33]. Macroscopically the network exhibits time-dependent mechanical behaviors, which was found to be well modeled by the approach with multiple natural configurations [28, 34]. Although these models are capable of incorporating the kinetics of dynamic bonds, they still rely on continuum level elasticity models, e.g. neo-Hookean, Arruda-Boyce or Gent model, to describe the mechanics of chains possessing different natural configurations [27-29, 35-36]. As a result, this approach does not provide a direct connection between single chain physics and macroscopic mechanics, and it would be difficult to extend such models to describe more complex molecular mechanisms such as entanglement and chain diffusion. In addition, computational implementation of this type of models can be challenging due to the large number of internal variables required to store chain populations and their respective natural configurations [37]. On the other hand, Tanaka and Edwards [24] developed a model for transient networks [38-39] that links the molecular physics of dynamic chains to the macroscopic mechanical behavior by tracking the evolution of microscopic distribution of chain end-to-end vectors. A rigorous continuum mechanics formulation of this approach in parallel to the 8-chain [9] or the full network model [10] for permanent networks is yet to be developed.

In this work, we introduce a theoretical framework for time-dependent responses of soft polymers that is deeply anchored on the statistical description of the underlying polymer network, based on a similar approach as that adopted by Tanaka and Edwards [24]. Within this framework, the physical state of the polymer is represented by a statistical distribution of the length and direction of chain end-to-end vectors. This distribution can be altered through both the macroscopic deformation and molecular-level events causing chain detachment and re-attachment. For simplicity, we illustrate this framework using an ideal network consisting of long chains with uniform length and dynamic cross-links. We assume that the single chain

behavior follows the entropic elasticity model with Gaussian statistics. Albeit simple, this ideal system closely resembles the 4-arm polyethylene glycol network with reversible metal-ligand cross-links recently developed by Grindy et al. [40] where highly uniform chain length can be achieved.

The manuscript is organized as follows. In Section 2, we first present a statistical description of the chain length and direction within the ideal network. Taking a thermodynamic approach, we then show in Section 3, that the network evolution can be linked to the stress tensor through the so-called distribution tensor, defined as a weighted average of the chain distribution. In Section 4, we show that our model degenerates to the neo-Hookean elastic model, the Maxwell-type viscoelastic model, and the Newtonian viscous fluid model under certain assumptions of the chain kinetics. Generalizations to multiple networks are also discussed. Section 5 highlights the differences between our model and similar models in the literature and the possible extensions of our model. Final conclusions are then provided in Section 6.

2. Statistical mechanics of a polymer chains with dynamic bonds

For the sake of simplicity, we here consider a polymer network made of linear chains that are connected to each-other at cross-linking sites. We are particularly interested in cross-links that display a dynamic response, i.e., they can associate and dissociate in time according to "on" and "off" rates, represented by the constants k_a and k_d , respectively, as shown in Fig. 1a. Figure 1b, on the other hand, illustrates a different type of dynamic bonds based on the bond exchange reactions where the dissociation of a connected chain and association of a new chain is completed in a single step of reaction. In this work, we attempt to describe the mechanical response of such a polymer from a statistical viewpoint.

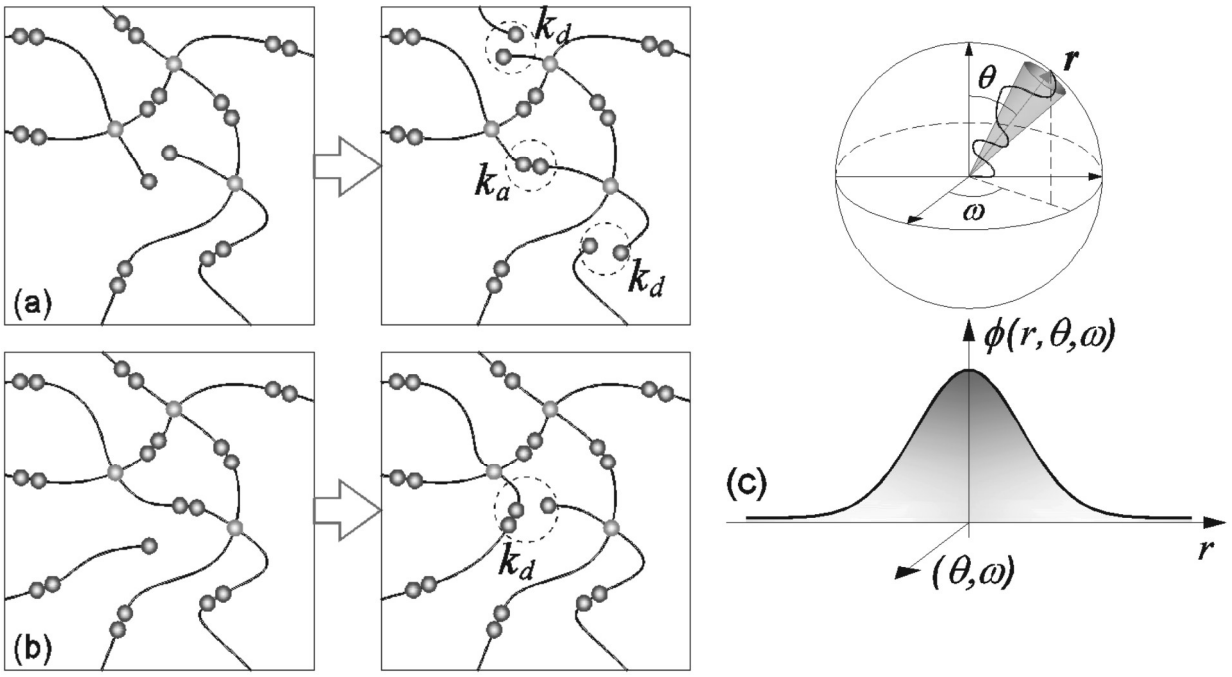

Figure 1. Schematic representation of dynamic bonds in a polymer network with reversible bonds (a) and bond exchange (b). (c) Graphical representation of a polymer chain with end-to-end vector $\mathbf{r} = \mathbf{r}(r,\theta,\omega)$ *and schematic of the distribution function* $\phi(r,\theta,\omega)$ *(Note that in this diagram, the symbol r represents the projection of the end-to-end vector)*

2.1 Statistical description of cross-linked polymer networks

When a polymer network is considered, the orientation of chains that form the network span all possible directions and the end-to-end distance must be replaced by the end-to-end vector that is characterized by both its direction (represented by angles θ and ω in spherical coordinates) and magnitude $r = |\mathbf{r}|$ (or end-to-end distance) as shown in Fig. 1c. The elasticity of the polymer may thus be understood through a statistical description of the end-to-end configuration of each polymer chain within a representative volume element. In this work, these statistics are captured by a distribution function $\phi(\mathbf{r}) = \phi(r,\theta,\omega)$ that allows us to precisely know the configuration of chains in the polymer according to their direction and end-to-end

distance. The probability function P, which represents the probability of a chain to have an end-to-end vector $\boldsymbol{r}$ can further be introduced by normalizing the distribution ϕ as follows:

$$\phi(\boldsymbol{r},t) = c(t)P(\boldsymbol{r},t) \quad \text{where} \quad c = \langle\phi\rangle \tag{1}$$

is the concentration of chains (moles of chains per unit current volume) that are connected to the network at both ends and the operator $\langle\blacksquare\rangle$ is the integral over all chain configurations:

$$\langle\blacksquare\rangle = \int_0^{2\pi}\int_0^{\pi}\left(\int_0^{\infty}\blacksquare r^2 dr\right) sin\theta d\theta d\omega \tag{2}$$

In the following, the energy state of the polymer will always be compared to its natural, or stress-free configuration. Following the standard statistical theory of elasticity, chains in the natural state are assumed to follow a Gaussian distribution around the value $\boldsymbol{r} = \boldsymbol{0}$. For an isotropic polymer, moreover, the chain distribution does not depend on the direction angles θ and ω, and the probability for a chain to have an end-to-end distance $\boldsymbol{r}$ is written as [7, 13]:

$$P_0(\boldsymbol{r}) = \left(\frac{3}{2\pi N b^2}\right)^{\frac{3}{2}} exp\left(-\frac{3|\boldsymbol{r}|^2}{2Nb^2}\right) \tag{3}$$

where N is the number of Kuhn segments of a chain (assumed to be uniform across the network) and b is the Kuhn length. The distribution ϕ_0 of chains in their natural states can therefore be related to the function P_0 by:

$$\phi_0(\boldsymbol{r},t) = c(t)P_0(\boldsymbol{r}) \tag{4}$$

where we purposefully display the argument t to emphasize that c can change with time due to the chain detachment and attachment events. We note that this distribution function is interpreted as the number $dN = \phi_0(r)r^2 sin\theta dr d\theta d\omega$ of chains per unit current volume whose end-to-end distance is between $\boldsymbol{r}$ and $\boldsymbol{r} + d\boldsymbol{r}$ and orientation is between (θ, ω) and $(\theta + d\theta, \omega + d\omega)$.

2.2 Evolution of the chain distribution under deformation.

Let us now evaluate the change in chain distribution when the polymer is subjected to deformation. For this, we consider an arbitrary line element, originally represented by the vector $d\boldsymbol{X}$ that deforms into a new line $d\boldsymbol{x}$ following a linear mapping – represented by the deformation gradient $\boldsymbol{F}$ according to $d\boldsymbol{x} = \boldsymbol{F}d\boldsymbol{X}$**.** In particular, the rate of change $\dot{\boldsymbol{F}}$ of this deformation tensor can be related to the velocity gradient $\boldsymbol{L} = d\dot{\boldsymbol{x}}/d\boldsymbol{x}$ in the form:

$$\dot{\boldsymbol{F}} = \boldsymbol{L} \cdot \boldsymbol{F} \tag{5}$$

When such a deformation is applied to the polymer, chains are distorted such that their end-to-end vector changes from r to $\boldsymbol{r} + \Delta\boldsymbol{r}$ where $\Delta\boldsymbol{r}$ denotes the directional elongation of the chain. Consequently, the chain configuration described by the current chain distribution $\phi(\boldsymbol{r}, t)$ evolves with time. Here, we seek to characterize this evolution based on the knowledge of the macroscopic deformation applied to the polymer. For this, we first note that the change in chain configuration is due to two competing mechanisms: (a) the application of a deformation that distorts each chain's end-to-end vector and (b) the detachment and reattachment of cross-links in different configurational states. The time derivative of $\phi(\boldsymbol{r}, t)$is thus decomposed according to:

$$\frac{\partial\phi(\boldsymbol{r},t)}{\partial t} = \left.\frac{\partial\phi(\boldsymbol{r},t)}{\partial t}\right|_{xl} + \left.\frac{\partial\phi(\boldsymbol{r},t)}{\partial t}\right|_{\boldsymbol{F}} \tag{6}$$

The first term implies that the evolution of $\phi(\boldsymbol{r}, t)$ occurs with no chain detachment and reattachment (the subscript "*xl*" indicates that the crosslinking density is fixed) while the second term represents the change in chain distribution when the deformation is frozen (fixed $\boldsymbol{F}$).

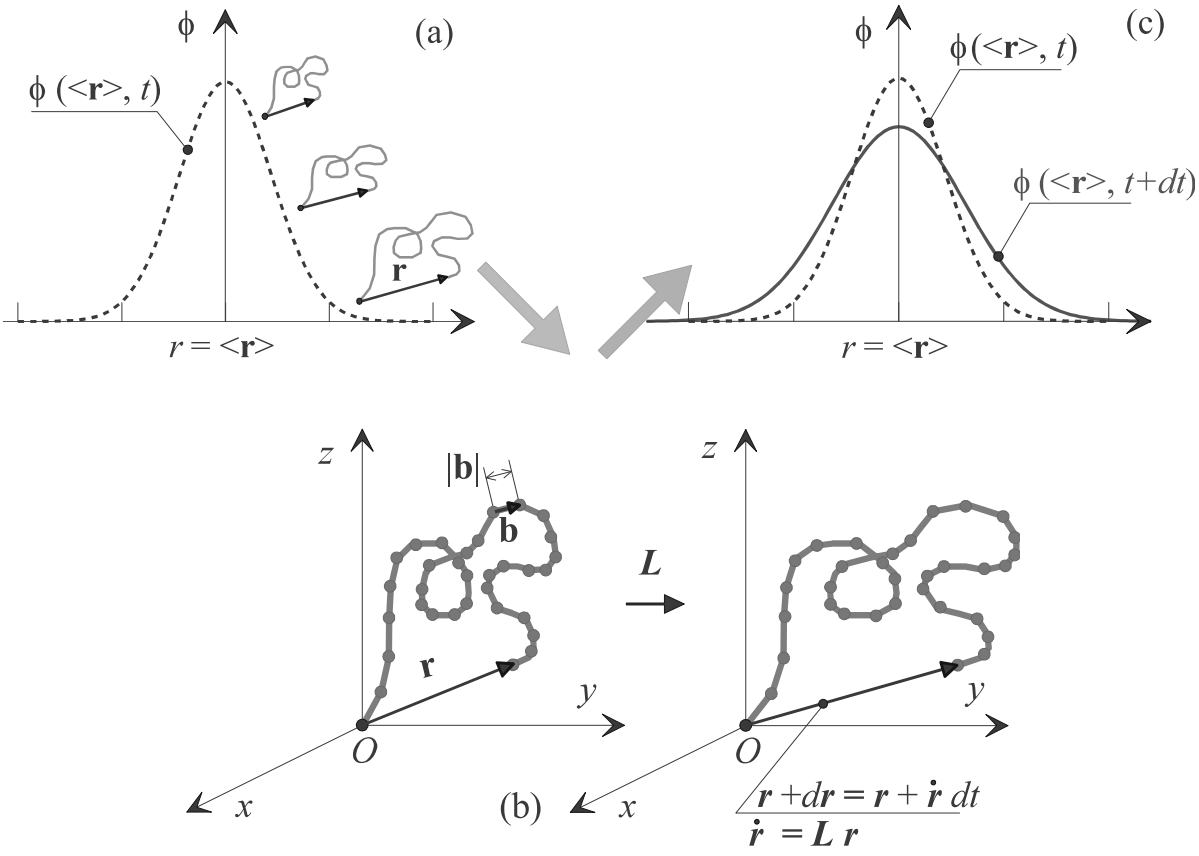

Figure 2. Example of the evolution of the chain distribution during an incremental deformation from t to t+dt represented by the velocity gradient $\boldsymbol{L}$*. The evolution of the distribution* ϕ *at a point is expressed by equation (5).*

To compute the first term, we adopt the affine deformation assumption where the end-to-end vectors of all chains evolve according to the continuum-level deformation gradient $\boldsymbol{F}$. For example, an end-to-end vector $\boldsymbol{r_0}$ before deformation is changed to $\boldsymbol{r} = \boldsymbol{F}\boldsymbol{r_0}$ after deformation (see Fig. 2). As a result, the space spanned by chain end-to-end vectors within a continuum point, referred to as the "chain space" hereafter, is distorted by the deformation gradient $\boldsymbol{F}$ experienced by that continuum point. The time derivative $\partial\phi(\boldsymbol{r},t)/\partial t|_{xl}$ in eq. (5) should be interpreted as

the spatial time derivative in the chain space. To derive how this term is related to the velocity gradient $\boldsymbol{L}$, we consider an arbitrary volume element $V*$ in the chain space and state that under a fixed set of cross-links, the "material time derivative" of the number of connected chains within $V*$ vanishes due to the incompressibility assumption. Here the concept of "material time derivative" is applied to the chain space (formed by the end-to-end vector $\boldsymbol{r}$), instead of the continuum-level physical space (formed by vector $\boldsymbol{X}$). Application of the Reynolds transport theorem in the chain distribution space leads to the following result:

$$\frac{D}{Dt}\int_{V*}\phi(\boldsymbol{r},t)dV=\int_{V*}\left.\frac{\partial\phi(\boldsymbol{r},t)}{\partial t}\right|_{xl}+\nabla_r\cdot(\phi(\boldsymbol{r},t)\dot{\boldsymbol{r}})dV=0 \tag{7}$$

where ∇_r denotes the spatial gradient in the distribution space, and $\dot{\boldsymbol{r}}$ is interpreted as the velocity of a point $\boldsymbol{r}$ in the distribution space**.** Because the distribution space is embedded within a single material point at the continuum level and we have assumed affine deformations, both the deformation gradient $\boldsymbol{F}$ and velocity gradient $\boldsymbol{L}$ can be considered uniform across the distribution space and the rate of chain's deformation becomes $\dot{\boldsymbol{r}}=\boldsymbol{L}\boldsymbol{r}$. Localizing eq. (7) and expanding the divergence term, we obtain,

$$\left.\frac{\partial\phi(\boldsymbol{r},t)}{\partial t}\right|_{xl}=-\left[\frac{\partial\phi(\boldsymbol{r},t)}{\partial r_i}r_j+\phi(\boldsymbol{r},t)\delta_{ij}\right]L_{ij} \tag{8}$$

where the Einstein convention on summation was used. The evolution of $\phi(\boldsymbol{r},t)$ at fixed deformation $\boldsymbol{F}$ can be found by assuming that the rate of detachment of chains with end-to-end vector $\boldsymbol{r}$ is proportional to $\phi(\boldsymbol{r},t)$ following eq. (1). Moreover, similarly to Tanaka and Edwards [24], we assume that these new chains reattach in a stress-free configuration, and thus their configuration is given by the probability function $P_0(\boldsymbol{r})$ shown in equation (3). These considerations yield the evolution law:

$$\left.\frac{\partial \phi(\boldsymbol{r},t)}{\partial t}\right|_{\boldsymbol{F}} = \xi_a P_0(r) - k_d \phi(\boldsymbol{r},t) \tag{9}$$

We see in eq. (9) that the dynamics of association and dissociation are governed by association and dissociation rates represented by the kinetic coefficients ξ_a and k_d, respectively, whose expression depends on the nature of the physical process at play. For a polymer with reversible bonds, the attachment and detachment mechanisms are decoupled and the rate of attachment becomes proportional to the density $c^d = c^t - c$ of detached chains where c^t is the total concentration of chains, including those that are not bonded. The corresponding association rate can therefore be expressed as:

$$\xi_a = k_a(c^t - c) \tag{10a}$$

where k_a is the kinetic coefficient for bond association. For a polymer with bond exchange reaction, an attachment event is immediately followed by a detachment event at a cross-link. This implies that the number of attached chains remains constant and the rate of attachment can be written:

$$\xi_a = \langle k_d \phi(\boldsymbol{r},t) \rangle \tag{10b}$$

Regardless of the mechanisms, the detachment kinetics may depend on external factors such as temperature or the presence of chemical species. Importantly, a force-dependent rate of dissociation is likely to occur, especially in the regime of large strains; for the coefficient k_d can be made a function of end-to-end distance, such that $k_d = k_d(\boldsymbol{r})$. The rate of attachment, however, concerns inactive (or detached) chains which should theoretically be insensitive to strain. For this reason, it is taken as independent of the end-to-end vector $\boldsymbol{r}$ in the reminder of

this study. Using eqs. (8) and (9), the evolution equation (6) for the distribution $\phi(\boldsymbol{r},t)$ finally becomes:

$$\frac{\partial\phi(\boldsymbol{r},t)}{\partial t} = \xi_a P_0(r) - [k_d(\boldsymbol{r}) + L_{ii}]\,\phi(\boldsymbol{r},t) - \frac{\partial\phi(\boldsymbol{r},t)}{\partial r_i} r_j L_{ij} \tag{11}$$

which is similar to the differential equation governing the evolution of chain distribution function in Tanaka and Edwards [24]. As the chain distribution evolves, the density of connected chains c may also change with time. By integrating eq. (11) throughout the chain space following eq. (2) and using the fact that $\langle\dot{\phi}\rangle = \dot{c}$ (see eq. (1a)), the time derivative of the concentration becomes:

$$\dot{c} = k_a(c^t - c) - \bar{k}_d c - c\ tr(\boldsymbol{L}) \tag{12a}$$

with $\bar{k}_d = \langle k_d(r)P(r,t)\rangle$ when reversible bonds are considered (eq. 10a), while

$$\dot{c} = -c\ tr(\boldsymbol{L}) \tag{12b}$$

when polymers with bond exchange reactions are considered (eq. 10b). Note that we consider incompressible polymers and the term $tr(\boldsymbol{L})$ vanishes in the above equations. Furthermore, if the rate constant k_d is independent of $\boldsymbol{r}$ (e.g. for small to moderate strains), we obtain the equality $\bar{k}_d = k_d$ since by definition, the integral of the probability function over the entire configurational space of chains is unity.

3. Macroscopic theory

So far, our description of the polymer evolution is purely statistical, but is related, via the assumption of affine chain deformation, to the macroscopic deformation gradient $\boldsymbol{F}$. In this section, we will make a connection between this statistical view and classical quantities used in continuum mechanics such as stored elastic energy, entropy and the stress tensor. For this, it is

convenient to start by invoking the first and second principle of thermodynamics and apply them to a volume element in the current configuration. In this element, the first principle implies that the material derivative of the internal energy density E_n (per unit current volume) can be expressed by:

$$\dot{E_n} = \boldsymbol{\sigma}\colon \boldsymbol{L} - \nabla \cdot \boldsymbol{q} + s \tag{13}$$

where $\boldsymbol{\sigma}$ is the Cauchy stress tensor in the volume element, $\boldsymbol{L}$ the velocity gradient, $\boldsymbol{q}$ the heat flux across its surface and s is the rate of external heat supply (per unit current volume). The Clausius-Duhem inequality enforcing the second principle of thermodynamics can further be written as:

$$\dot{\vartheta} \geq \frac{s}{T} - \nabla \cdot \left(\frac{\boldsymbol{q}}{T}\right) \tag{14}$$

where ϑ is the entropy per unit current volume and T is the absolute temperature. Introducing the Helmholtz free energy per unit current volume $\Psi = E_n - T\vartheta$, eqs. (13) and (14) yield the inequality:

$$\boldsymbol{\sigma}\colon \boldsymbol{L} - \dot{\Psi} - \dot{T}\vartheta - \frac{\boldsymbol{q}}{T} \cdot \nabla T \geq 0 \tag{15}$$

For convenience, let us consider an incompressible polymer and postulate that the stored elastic energy Ψ_e in the material volume can be computed as the sum of the stored energy in each active chain across their configurational space. If we call $\psi_c(\boldsymbol{r})$ the elastic energy in a single chain with end-to-end vector $\boldsymbol{r}$, the stored elastic energy Ψ_e can be written as:

$$\Psi_e = \langle \phi \psi_c \rangle + p(\det(\boldsymbol{F}) - 1) \tag{16}$$

where the term p represents the Lagrange multiplier enforcing the incompressibility condition, $\det(\boldsymbol{F}) = 1$. Following the freely jointed chain theory with Gaussian statistics [13] under the

assumption that the number of Kuhn segments N in one polymer chain is large (N >>1), we are able to express the elastic energy of a single chain as:

$$\psi_c(\boldsymbol{r}) = \frac{3k_BT}{2Nb^2}|\boldsymbol{r}|^2 = \frac{k_BT}{2}\tilde{r}^2 \tag{17}$$

where k_B is the Boltzmann constant, k_BT is the thermal energy and b is the Kuhn length. We further used the normalized distance defined as $\tilde{r} = |\boldsymbol{r}|/\boldsymbol{\ell}$ where $\ell = b\sqrt{N/3}$ is proportional to the projected mean end-to-end distance $b\sqrt{N}$ of individual chains. We note here that eq. (17) is only accurate for small to moderate chain extension. When extension is more severe, a Langevin chain model can be used to account for the strain stiffening arising from extensive chain stretch [13]. While such an energy functional could be considered here, the above form allows us to work with a simplified model and focus on other aspect of the theory, i.e., the time dependence of the cross-link attachment/detachment. A classical issue with the energy function defined in eq. (16) is that it does not vanish when the polymer is in a stress-free configuration. This can easily be seen by substituting the stress-free probability function eq. (4) into eq. (16). To avoid this, it is preferable to work with the energy difference $\Delta\Psi_e$ between the current state (with distribution $\phi(\boldsymbol{r},t)$) and the stress-free state (with distribution $\phi_0(\boldsymbol{r},t) = c(t)P_0(\boldsymbol{r})$). In this case, we can write:

$$\begin{aligned}\Delta\Psi_e(t) &= \Psi_e - \Psi_e^0 + p(\det(\boldsymbol{F}) - 1)\\ &= \langle(\phi - \phi_0)\psi\rangle + p(\det(\boldsymbol{F}) - 1)\\ &= \frac{ck_BT}{2}\langle(P - P_0)\tilde{r}^2\rangle + p(\det(\boldsymbol{F}) - 1)\end{aligned} \tag{18}$$

We will see below that this energy is implicitly a function of the deformation gradient $\boldsymbol{F}$ since the distribution evolves with applied strains. It is further entirely defined since the distribution

$\phi(\boldsymbol{r}, t)$ can be determined at any time from the evolution law in eq. (10) and the knowledge of the polymer configuration at the initial time.

3.1 Clausius-Duhem inequality

To apply the inequality in eq. (15), we add a term in eq. (18) to account for the change in Helmholtz free energy due to heat absorption, i.e.

$$\Psi = (\gamma - \vartheta_0)(T - T_0) - \gamma T \ln\frac{T}{T_0} + \Delta\Psi_e \tag{19}$$

where γ is the specific heat per unit volume, ϑ_0 is the entropy at the initial stress-free state and T_0 is the initial temperature. Because of the incompressibility assumption, we regard the volumetric specific heat γ as a constant. Taking the material time derivative of the Helmholtz free energy Ψ and using evolution equation (11), we can show that the change in stored elastic energy is (see appendix A.1 for details):

$$\dot{\Psi} = -\dot{T}\left(\gamma\, ln\left(\frac{T}{T_0}\right) + \vartheta_0\right) + p\, tr(\boldsymbol{L}) + \frac{k_B T}{2}\left\{2c[\boldsymbol{\mu} - \boldsymbol{\mu}_0]\colon \boldsymbol{L} + c\frac{\dot{T}}{T}\left(tr(\boldsymbol{\mu} - \boldsymbol{\mu}_0)\right)\right\} - \mathrm{D} \tag{20}$$

where the chain distribution tensor was defined as:

$$\boldsymbol{\mu} = \langle P\tilde{\boldsymbol{r}} \otimes \tilde{\boldsymbol{r}}\rangle \quad \text{and} \quad \boldsymbol{\mu}_0 = \langle P_0\tilde{\boldsymbol{r}} \otimes \tilde{\boldsymbol{r}}\rangle, \tag{21}$$

and the mechanical energy dissipation has the form:

$$\mathrm{D} = \frac{k_B T}{2}\langle k_d c(P - P_0)\tilde{r}^2\rangle \tag{22}$$

Note here that if the rate of dissociation is not a function of chain extension, the dissipation can be rewritten as $\mathrm{D} = k_d\frac{ck_BT}{2}tr(\boldsymbol{\mu} - \boldsymbol{\mu}_0)$. From this expression, it is clear that the rate of mechanical energy dissipation increases with both the dissociation rate and the stored elastic energy in the material. With these new quantities, inequality (15) takes the form:

$$[\boldsymbol{\sigma} - ck_B T(\boldsymbol{\mu} - \boldsymbol{\mu}_0) - p\boldsymbol{I}]: \boldsymbol{L} +$$

$$-\dot{T}\left[\vartheta + \frac{ck_B}{2}\left(tr(\boldsymbol{\mu}) - tr(\boldsymbol{\mu}_0)\right) - \gamma \ln\frac{T}{T_0} - \vartheta_0\right] + \mathrm{D} - \frac{\boldsymbol{q}}{T} \cdot \nabla T \geq 0 \tag{23}$$

This is a macroscopic representation of the Clausius-Duhem inequality, i.e., all quantities involved are defined at the continuum scale.

3.2 The chain distribution tensor

As seen above, the role of chain deformation is captured by the chain distribution tensor $\boldsymbol{\mu}$ defined in eq. (21), a key quantity of the proposed theory. It enables a macroscopic description of the state of the polymer chain network at any instant during the deformation process. In particular, it is of interest to explore the form of this tensor when the polymer network is in a stress-free state, i.e. the end-to-end distance follows the Gaussian distribution shown in eq. (2). Performing the integration, we find that:

$$\boldsymbol{\mu}^0 = \langle P^0 \tilde{\mathbf{r}} \otimes \tilde{\mathbf{r}} \rangle = \left(\frac{2\pi N b^2}{3}\right)^{-\frac{3}{2}} \langle exp(-\tilde{r}^2/2)\tilde{\mathbf{r}} \otimes \tilde{\mathbf{r}} \rangle = \boldsymbol{I} \tag{24}$$

with $\boldsymbol{I}$ being the identity tensor. In other words, using eq. (21), the stored elastic energy (18) in the network can be directly related to the network statistics by the following equation:

$$\Delta\Psi_e = \frac{ck_B T}{2} tr(\boldsymbol{\mu} - \boldsymbol{I}) + p(\det(\boldsymbol{F}) - 1) \tag{25}$$

When it is not evaluated in a stress-free configuration, we see from its definition that the tensor $\boldsymbol{\mu}$ is represented by a symmetric matrix that can better be described by its three independent eigenvalues. Indeed, if we can express $\boldsymbol{\mu}$ in its principal directions to obtain:

$$\boldsymbol{\mu}^{\boldsymbol{d}} = \boldsymbol{Q}^{\boldsymbol{T}}\boldsymbol{\mu}\,\boldsymbol{Q}, \quad \text{in matrix form} \quad [\boldsymbol{\mu}^{\boldsymbol{d}}] = \begin{bmatrix} \mu_1 & 0 & 0 \\ 0 & \mu_2 & 0 \\ 0 & 0 & \mu_3 \end{bmatrix} \tag{26}$$

where $\boldsymbol{Q}$ is the orthogonal matrix of change of basis between the global Cartesian frame and that associated with the principal directions of $\boldsymbol{\mu}$, while the components μ_1, μ_2 and μ_3 are the eigenvalues of the chain distribution tensor. A physical interpretation of these quantities is given by the standard deviation of the end-to-end distance component $\langle r_i^2 \rangle$ in the i-th principal direction, relative to the stress-free value $\langle r_i^2 \rangle = Nb^2/3$. In other words, we can write $\mu_i = 3\langle r_i^2 \rangle / Nb^2$. Conveniently, the distribution tensor can be represented by an ellipsoid with semi-axes μ_i and oriented along the principal direction of $\boldsymbol{\mu}$. This facilitates the visualization of the chain distribution at spatial material points during its deformation history as discussed later in this paper.

Interestingly, the distribution tensor contains the information of average chain stretch. To illustrate this point, we note that the trace of the distribution tensor can be computed as:

$$tr(\boldsymbol{\mu}) = \langle P\tilde{\boldsymbol{r}} \cdot \tilde{\boldsymbol{r}} \rangle = \langle P\tilde{\boldsymbol{r}}^2 \rangle = \frac{\overline{r^2}}{Nb^2/3} \tag{27}$$

In other words, the root mean square of the chain end-to-end distance $r_{rms} = \sqrt{\overline{r^2}}$ can be directly related to $tr(\boldsymbol{\mu})$ by:

$$r_{rms} = \sqrt{N}b\sqrt{\frac{tr(\boldsymbol{\mu})}{3}} \tag{28}$$

In addition, consider an arbitrary direction described by a unit vector $\boldsymbol{n}$, and denote the acute angle between a chain with this direction as θ ($0 \leq \theta \leq \pi/2$) (see Fig. 3a), also named as the chain angle in [41] and [42] we have

$$\boldsymbol{n}\cdot(\boldsymbol{\mu n}) = \langle P\tilde{r}^2 cos^2(\theta)\rangle = \frac{\overline{(rcos\theta)^2}}{Nb^2/3}\ , \tag{29}$$

where $\sqrt{\overline{(rcos\theta)^2}}$ is the root mean square of $rcos\theta$. Based on this result, we define an effective average chain angle γ as

$$\gamma = arccos\left(\sqrt{\frac{\overline{(rcos\theta)^2}}{\overline{r^2}}}\right) = arccos\left(\sqrt{\frac{\boldsymbol{n}\cdot(\boldsymbol{\mu n})}{tr(\boldsymbol{\mu})}}\right). \tag{30}$$

Note that γ is not the direct average of chain angle, as defined in Yang et al. [41], but it also provides a measurement of average chain orientation. To illustrate this point, let us consider a special case where the bonds are permanent and the network is under uniaxial tension. We set $\boldsymbol{n}$ to be the direction of uniaxial tension, and the evolutions of effective average chain angle γ and the root mean square of chain stretch $\lambda_{rms} = r_{rms}/\left(\sqrt{N}b\right)$ with the nominal tensile strain $\lambda - 1$ are shown in Fig.3b. Also plotted in Fig. 3b are the average chain angle θ and stretch λ defined in Yang et al. [42]:

$$\bar{\theta} = \int_0^{\pi/2} tan^{-1}\left(\frac{1}{\lambda_1^{3/2}}tan\theta\right) sin\theta\, d\theta, \tag{31}$$

$$\bar{\lambda} = \int_0^{\pi/2} \sqrt{(\lambda_1 cos\theta)^2 + \lambda_1^{-1} sin^2\theta}\, sin\theta d\theta \tag{32}$$

Although the quantities γ and λ_{rms} are defined differently from $\bar{\theta}$ and $\bar{\lambda}$, they exhibit the same qualitative trends, i.e. on average the chains becomes stretched and also more aligned with $\boldsymbol{n}$.

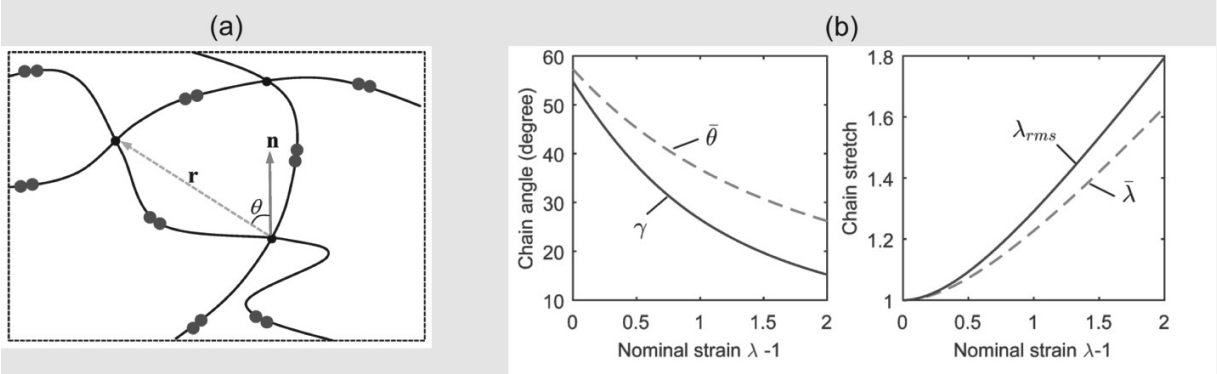

Figure 3. (a) Illustration of the chain end-to-end vector ***r*** *and the angle θ between a single chain and an arbitrary direction characterized by the unit vector* ***n****. (b) Prediction of the averaged chain orientation γ for an elastic network (no dynamic bonds) under uniaxial tension, where the direction vector* ***n*** *is aligned with the tensile direction. This result is compared with the average chain angle* $\bar{\theta}$ *and chain stretch* $\bar{\lambda}$ *defined in eq. (31) and (32). Good qualitative agreement can be observed between the approaches.*

3.3 Stress tensor and entropy

Considering that each process (deformation, heat transfer and bond detachment/reattachment kinetics) occurs independently and assuming that the first two terms in eq. (23) vanish while the last two terms verify the inequality independently, we identify the Cauchy stress as:

$$\boldsymbol{\sigma} = ck_BT(\boldsymbol{\mu} - \mathbf{I}) + p\mathbf{I} \tag{33}$$

where we used the fact that in the stress-free state, $\boldsymbol{\mu}^{\mathbf{0}} = \mathbf{I}$. Similarly, the entropy ϑ is then found as:

$$\vartheta = \vartheta_0 + \gamma \ln\frac{T}{T_0} - \frac{ck_B}{2}(tr(\boldsymbol{\mu}) - 3) \tag{34}$$

The second term on the right-hand side of eq. (34) represents the change in entropy due to heat absorption, while the third term represents the change in the configurational entropy of chains. Note that $-k_B\tilde{r}^2/2$ is the entropy of a single chain, and thus $(ck_B/2)tr(\boldsymbol{\mu}) = (ck_B/2)\langle P\tilde{r}^2\rangle$ is the total entropy of all chains. The last two terms in eq. (23) describe the energy dissipation in the system and imply two inequalities. The first inequality, of the form:

$$\mathrm{D} \geq 0 \tag{35}$$

enforces that the mechanical energy dissipation remains positive. Physically, this statement implies that chain detachment is associated with a decrease in the stored elastic energy and that this loss is proportional to the rate of dissociation k_d and the stored elastic energy expressed in eq. (25)

$$-\frac{\boldsymbol{q}}{T}\cdot\nabla T \geq 0 \tag{36}$$

which eventually implies that the heat flux is written in a form of Fourier's law [43].

3.4 Evolution equation for the distribution tensor

We have seen that elastic energy, entropy and stress can be directly determined from the knowledge of the distribution tensor. It is however not clear yet how this quantity can be evaluated during a macroscopic deformation of the polymer. This can be done by integrating the evolution equation of the distribution function eq. (11) over the chains' configurational space following eq. (1b). After a long but straightforward calculation shown in Appendix A.2, we obtain the following evolution law for $\boldsymbol{\mu}$ (specific to the case of a polymer with reversible bonds whose kinetics follow eq. (10a)):

$$\dot{\boldsymbol{\mu}} = \frac{\xi_a}{c}\boldsymbol{\mu}^{\mathbf{0}} - \overline{\overline{\boldsymbol{k}}}_d - \frac{\dot{c}}{c}\boldsymbol{\mu} + \mathbf{D}\boldsymbol{\mu} + \boldsymbol{\mu}\boldsymbol{D} \tag{37}$$

where the superscript T denotes the transpose operator and the weighted integral of the second moment of the dissociation rates in (37) is given by:

$$\bar{\bar{\boldsymbol{k}}}_d = \langle k_d \, P \, \tilde{\mathbf{r}} \otimes \tilde{\mathbf{r}} \rangle \tag{38}$$

Finally, using eq. (10a) and (10b), we can write the evolution equation for the distribution tensor in the case of reversible bonds and bond exchange reaction, respectively as:

$$\dot{\boldsymbol{\mu}} = k_a \left(\frac{c^t - c}{c} \right) \boldsymbol{I} - \bar{\bar{\boldsymbol{k}}}_d - \frac{\dot{c}}{c} \boldsymbol{\mu} + \boldsymbol{D}\boldsymbol{\mu} + \boldsymbol{\mu}\boldsymbol{D} \tag{39a}$$

$$\dot{\boldsymbol{\mu}} = \bar{k}_d \boldsymbol{I} - \bar{\bar{\boldsymbol{k}}}_d + tr(\boldsymbol{L})\boldsymbol{\mu} + \boldsymbol{D}\boldsymbol{\mu} + \boldsymbol{\mu}\boldsymbol{D} \tag{39b}$$

where we recall that $\bar{k}_d = \langle k_d(r) P(r,t) \rangle$ and $tr(\boldsymbol{L}) = 0$ for incompressible materials. Together with the equation for concentrations (12a) and (12b), equations (39a) and (39b) form a set of coupled first order differential equation for c and $\boldsymbol{\mu}$ whose solution only requires the knowledge of initial conditions $c(t=0)$ and $\boldsymbol{\mu}(t=0)$ as well as the deformation history, represented by the velocity gradient $\boldsymbol{L} = \boldsymbol{L}(t)$. Assuming that the polymer is initially in a stress-free, equilibrium state, the initial conditions for the above two differential equations are: $\mathrm{c}(\mathrm{t}=0) = \mathrm{c}^0$ and $\boldsymbol{\mu}^0(t=0) = \boldsymbol{\mu}^0 = \boldsymbol{I}$. The solution to eq. (39) depends on the form of the relation $\bar{\bar{\boldsymbol{k}}}_d = \bar{\bar{\boldsymbol{k}}}_d(\boldsymbol{\mu})$. In this work, we assume that the rate of dissociation k_d is independent of chain length and orientation (i.e., k_d is constant). Using this assumption in eq. (38) yields the simple form:

$$\bar{\bar{\boldsymbol{k}}}_d = k_d \langle P \, \tilde{\mathbf{r}} \otimes \tilde{\mathbf{r}} \rangle = k_d \, \boldsymbol{\mu} \tag{40}$$

and $\bar{k}_d = k_d$. In this case, eq. (39) becomes a linear differential equation for $\boldsymbol{\mu}$.

3.5 Illustration

We now aim to illustrate the prediction of the above theory by considering the homogeneous deformation, network evolution and mechanical response of a cubic element of polymer. Over a period of time t, the cube is assumed to undergo a series of shear and tensile deformation illustrated in Fig. 4 and more accurately specified as follows. Between 0 and $\tau/20$, the cube is first subjected to a shear deformation into a diamond-shape characterized by a final deformation gradient $F_{12} = 1$ (all other components unchanged). The cube is then let to rest for a period 0.3τ until a tensile deformation is applied quickly during a period $\tau/20$ up to a deformation gradient $F_{22} = 2$ (all other components unchanged). The specimen relaxation is then evaluated for the remainder of the time. For this virtual experiment, we considered a transient network characterized by normalized rates $k = k_a\tau = k_d\tau = 0.07$ and the steady state polymer concentration is taken as unity.

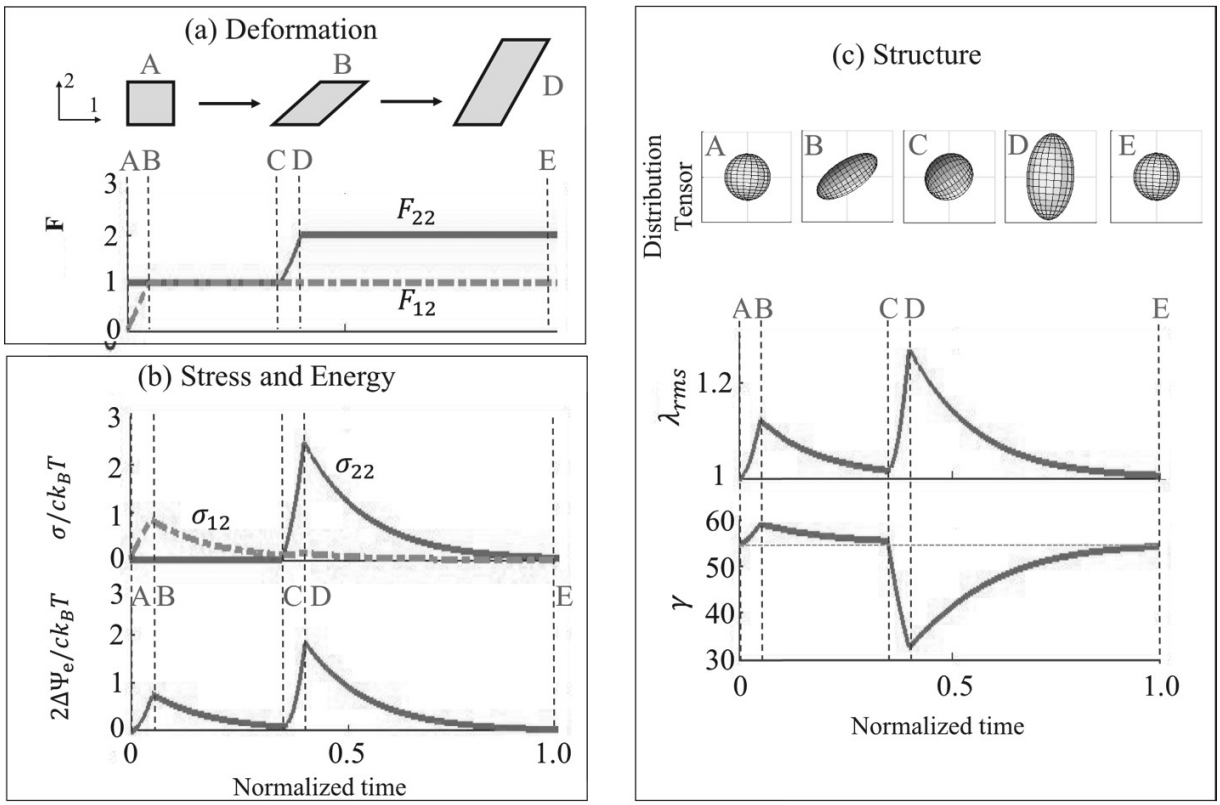

Figure 4. Illustration of (a) the deformation, (b) stress and stored elastic energy and (c) chain statistic response of a polymer characterized by a single network that displays normalized rates $k = k_a\tau = k_d\tau = 0.07$. *Stresses are normalized by* ck_BT *and energies by* $ck_BT/2$. *The polymer structure is characterized by the 3D representation of the distribution tensor, the normalized root mean square end-to-end distance* $\lambda_{rms} = r_{rms}/\sqrt{N}b$ *and the effective average chain angle* γ *with the vertical direction (*$\boldsymbol{n} = [0,1]$ *in the Cartesian coordinate system). Time is expressed in units of* τ.

Fig. 4a presents the evolution of the deformation (components F_{12} and F_{22}), together with the deformation of the corresponding cube. The characteristic times at which the deformation is applied are referred by 5 points (A-E), A being the initial state. The mechanical response of the material is then characterized by the normalized Cauchy stress (components σ_{12} and σ_{22}) and the

overall stored elastic energy $\Delta\Psi_e$ (Fig. 4b) while the evolution of polymer structure is captured by a graphical representation of the distribution tensor $\boldsymbol{\mu}$ over time. This tensor is represented by three quantities: its overall ellipsoidal form as discussed in section 3.2, the normalized root mean square end-to-end distance $r_{rms}/\sqrt{N}b$ (eq. (28)) and the effective average chain angle γ with the vertical direction ($\boldsymbol{n} = [0,1]$) as expressed in eq. (30). We observe via the distribution tensor, that a quickly applied deformation changes the chain's end-to-end distance in directions of maximum stretch. We specifically see that the angle between the chains and the vertical direction increases under shear (from A to B) but significantly decrease under stretch (from C to D) from their isotropic angle $\gamma_{\text{iso}} \approx 55^o$. However, when the deformation is held for some time, the cross-links are allowed to detach and reattach in order for the chains to reconfigure in states that are closer to their stress-free configuration. Eventually, this means that the distribution converges to its stress-free value $\boldsymbol{\mu}^0 = \boldsymbol{I}$, represented by a sphere in the figure and by a chain end-to-end distance $\bar{r}/\sqrt{N}b = 1$ and orientation $\gamma = \gamma_{\text{iso}}$. As stretched chains detach and reattach in stress-free configuration, the internal stresses relaxes over time. This phenomenon can be seen in the drop in the stored elastic energy over time and the stress relaxation whose characteristic time is set by the bond kinetics. Overall, this material response is therefore similar to that predicted by the Maxwell model (viscoelastic fluid), represented by a spring and a dashpot in series.

Experimental observations of such stress relaxation and plastic deformation caused by dynamic bonds have been reported in the literature. A representative example is a polymer network, i.e. vitrimer, with heat activated bond exchange reactions. It was shown in Montarnal et al. [44] (e.g. see Fig. 2 of their paper) that the network can undergo complete stress relaxation under a prescribed deformation. Upon removal of the applied constraint, the polymer is able to maintain the prescribed deformation permanently.

4. Special cases and extension to complex networks

A key advantage of the above theory is that it provides a clear relationship between the kinetics of dynamic bonds, the statistical evolution of the entire network (through the tensor $\boldsymbol{\mu}$) and the overall macroscopic response of the polymer (through the stress tensor $\boldsymbol{\sigma}$). In this section, we investigate how this framework compares to other classical theories that describe the behavior of elastic rubbers (permanent networks), viscoelastic polymers (networks with slow kinetics) and viscous fluid (networks with fast kinetics). We also explore the more general case where the dynamic bond kinetics is characterized by a more complex response in which a spectrum of relaxation time scales can be observed. For this, we describe a route by which to incorporate multiple networks into the formulation, each characterized by their own relaxation time.

4.1 Permanent networks

The evolution of a polymer with permanent cross-links is described by a particular case of the evolution law eq. (11) in the case where $k_a = 0$ (no attachment of new chains over time) and $k_d = 0$ (no chain detachment over time). In this case, the overall concentration c_s of cross-link remains constant and eq. (39) degenerates to the simpler form:

$$\dot{\boldsymbol{\mu}}_s = tr(\boldsymbol{L})\boldsymbol{\mu}_s + \boldsymbol{D}\boldsymbol{\mu}_s + \boldsymbol{\mu}_s\boldsymbol{D} \tag{41}$$

The solution of this tensorial differential equation has the form $\boldsymbol{\mu}_s = J\boldsymbol{F}\boldsymbol{F}^{\mathrm{T}}$ where the deformation gradient **F** (related to the velocity gradient by $\dot{\boldsymbol{F}} = \boldsymbol{L}\boldsymbol{F}$) describes the mapping between the deformed network and its stress-free configuration and $J = \det(\boldsymbol{F})$. In other words,

for a purely elastic material, the chain distribution tensor coincides with the left-Cauchy strain tensor $J\boldsymbol{B} = J\boldsymbol{F}\boldsymbol{F}^{\mathrm{T}}$. Using this result, eq. (25) can be rewritten in the more conventional form:

$$\Delta\Psi_e = \frac{c_S k_B T}{2} J tr(\boldsymbol{F}\boldsymbol{F}^{\mathrm{T}} - \boldsymbol{I}) + p(\det(\boldsymbol{F}) - 1) \tag{42}$$

In other words, in the absence of dynamic bonds, the stored elastic energy degenerates to that predicted by the neo-Hookean model in classical rubber elasticity [4, 11] and the Cauchy stress expressed in eq. (33) becomes:

$$\boldsymbol{\sigma}_s = c_S^0 k_B T(\boldsymbol{F}\boldsymbol{F}^{\mathrm{T}} - \boldsymbol{I}) + p\boldsymbol{I} \tag{43}$$

Where the quantity $c_S^0 = J c_S$ is the nominal concentration, defined per unit reference volume of the dry polymer in agreement with the early work of Treloar [45] and Kuhn and Grun [46]. From eq. (43), it is clear here that when the deformation vanishes, the deformation gradient becomes $\boldsymbol{F} = \boldsymbol{I}$ and the first term on the right-hand side has no contribution. The remaining term p plays the role of a pressure enforcing the material's incompressibility, such that the hydrostatic pressure is $p^h = \frac{1}{3} tr(\boldsymbol{\sigma}_s) = c_S^0 k_B T(tr(\boldsymbol{F}\boldsymbol{F}^{\mathrm{T}})/3 - 1) + p$.

4.2 Relation to standard viscoelasticity

To explore how the statistically-based continuum theory degenerates to standard viscoelasticity, we first make the assumption that the kinetic coefficient k_d is independent of the stretch/force on each individual chain. In this case, we have seen that:

$$\bar{k}_d = k_d \quad \text{and} \quad \bar{\bar{\boldsymbol{k}}}_d = k_d \boldsymbol{\mu} \tag{44}$$

Let us further assume the density of active cross-link density c has achieved a steady state ($\dot{c} = 0$). From eq. (12) this steady state is:

$$c = \frac{k_a}{k_a + k_d} c^t \tag{45}$$

In this case, the evolution equation for the distribution moment degenerates to the simpler form:

$$\dot{\boldsymbol{\mu}} = k_d(\boldsymbol{I} - \boldsymbol{\mu}) + \boldsymbol{D\mu} + \boldsymbol{\mu D} \tag{46}$$

Now using identity that $\boldsymbol{D\mu} + \boldsymbol{\mu D} = \boldsymbol{L\mu} + (\boldsymbol{L\mu})^{\boldsymbol{T}}$, and the fact that the velocity gradient $\boldsymbol{L}$ can be expressed in terms of the deformation gradient tensor $\boldsymbol{F}$ by $\boldsymbol{L} = \dot{\boldsymbol{F}}\boldsymbol{F}^{-1}$, eq. (45) becomes:

$$\dot{\boldsymbol{\mu}} = k_d(\boldsymbol{I} - \boldsymbol{\mu}) + \dot{\boldsymbol{F}}\boldsymbol{F}^{-1}\boldsymbol{\mu} + \boldsymbol{\mu}^{\boldsymbol{T}}\boldsymbol{F}^{-\mathrm{T}}\dot{\boldsymbol{F}}^{\mathrm{T}} \tag{47}$$

Defining $\boldsymbol{A} = \boldsymbol{F}^{-1}\boldsymbol{\mu}\boldsymbol{F}^{-\mathrm{T}}$, the above equation can finally be rewritten as a first-order ordinary differential equation which can be analytically solved:

$$\dot{\boldsymbol{A}} + k_d\boldsymbol{A} = k_d\boldsymbol{F}^{-1}\boldsymbol{F}^{-\mathrm{T}} \tag{48}$$

The initial condition is $\boldsymbol{A}(t = 0) = \boldsymbol{I}$ since initially both $\boldsymbol{\mu}$ and $\boldsymbol{F}$ are identity tensors. The general solution of eq. (48) is [47].

$$\boldsymbol{A} = e^{-k_d t}\boldsymbol{I} + \int_0^t k_d\boldsymbol{F}^{-1}(\tau)\boldsymbol{F}^{-T}(\tau)e^{-k_d(t-\tau)}d\tau \tag{49}$$

Therefore, the general solution of the distribution tensor $\boldsymbol{\mu}$ is:

$$\boldsymbol{\mu}(t) = e^{-k_d t}\boldsymbol{F}(t)\boldsymbol{F}^{T}(t) + \int_0^t k_d[\boldsymbol{F}(t)\boldsymbol{F}^{-1}(\tau)\boldsymbol{F}^{-T}(\tau)\boldsymbol{F}^{T}(t)]\, e^{-k_d(t-\tau)}d\tau \tag{50}$$

To illustrate how the theory degenerates to standard viscoelasticity, let us take the particular case of the uniaxial tension of a polymer specimen along the x_1 direction. In this context, the non-vanishing terms of $\boldsymbol{F}$ are $F_{11} = \lambda$, and $F_{22} = F_{22} = \lambda^{-1/2}$. In addition, if we assume small deformation, the stretch ratio takes the form $\lambda(t) = 1 + \varepsilon(t)$ where ($\varepsilon \ll 1$) is the

linearized unidirectional strain. The tensile stress can be written in the following form (see Appendix A.2)

$$\frac{\sigma_{11}(t)}{ck_bT} = 3\int_{-\infty}^{t} e^{-k_d(t-\tau)}\frac{d\varepsilon}{d\tau}d\tau \tag{51}$$

If we set $E_0 = 3ck_BT$ as the instantaneous Young's modulus and $E(t) = E_0\, e^{-k_d t}$ is the relaxation modulus, then eq. (51) can be written as

$$\sigma_{11}(t) = \int_{-\infty}^{t} E(t-\tau)\frac{d\varepsilon}{d\tau}d\tau \tag{52}$$

This expression is consistent with linear viscoelasticity, specifically a Maxwell model given the form of $E(t)$. We finally note that since the mechanical loading starts at $t = 0$ and we allow an instantaneous application of strain, eq. (52) can also be written as

$$\sigma_{11}(t) = E(t)\cdot\varepsilon(t = 0^+) + \int_{0^+}^{t} E(t-\tau)\,\frac{d\varepsilon}{d\tau}d\tau \tag{53}$$

The above derivation shows that our model degenerates to the Maxwell model under the assumption of constant kinetic parameters k_d and small deformation. This indicates that under a fixed strain, the stress would decay exponentially with time and the characteristic decay time is governed by the dynamic bond kinetics (e.g. the coefficient k_d). Such exponential stress relaxation has been observed in a number of previous studies on networks with bond exchange reactions [27, 42, 44].

To further test our model against experimental data, we note that our assumption of uniform kinetic coefficients k_d and k_a requires a homogeneously structured network, otherwise the polymer may exhibit a spectrum of relaxation times. This was achieved in a recently developed

hydrogel with 4-arm polyethylene glycol (PEG) units with reversible metal ligand crosslinks [40, 48-49]. The time-dependent mechanical behaviors of such gels due to the dynamic metal ion crosslinks were measured by frequency-sweep rheological tests at small shear strains (e.g. 1% for the data in Fig. 5a,b). Because of the homogeneous network structure, we expect our result in this section is applicable to this type of gel, i.e. the rheological data can be well captured by the Maxwell model. This is indeed the case as shown in Fig. 5. According to the Maxwell model, the storage and loss modulus G' and G'' are

$$G' = G_0 \frac{t_R^2 \Omega^2}{1 + t_R^2 \Omega^2}, \quad G'' = G_0 \frac{t_R^2 \Omega}{1 + t_R^2 \Omega^2} \tag{54}$$

where G_0 is the instantaneous shear modulus, t_R is the characteristic relaxation time and Ω is the angular frequency of the oscillatory rheological test. In our case,

$$G_0 = c k_B T, \qquad \text{and} \quad t_R = \frac{1}{k_d} \tag{55}$$

Figure 5ab show the experimental data of G' and G'' extracted from Grindy et al. [40] for two different gels with distinct metal ion crosslinks, i.e. Ni^{2+} and Cu^{2+}, as well as the fit of our model. Overall the Maxwell model well captures the experimental data. For the Ni^{2+} based gel, we found $G_0 = 18.621\ kPa$ and $t_R = 6.2\ s$, while for the Cu^{2+} based gel, $G_0 = 8.318\ kPa$ and $t_R = 1.12\times10^{-3}\ s$. Interestingly, the values of G_0 for the Ni^{2+} and Cu^{2+} based gels are quite different, even though the molar concentration of the 4-arm PEG units is the same in the two gels: $0.01\ mol/L$, which implies a total chain density of $0.02\ mol/L$ or $c^t = 1.204\times10^{22}\ /L$, since on average each 4-arm PEG unit can contribute 2 chains to the network. This is because the modulus G_0 is proportional to the density of active chains c, instead of total chain density c^t. Using the value of c^t, temperature $T = 278\ K$ (5°C reported in Grindy et al. [40]), and eqs. (45) and (54), we are able to determine that for the Ni^{2+} based network, $k_d = 0.1613\ s^{-1}$ and $k_a =$

$0.1044\ s^{-1}$ and for the Cu^{2+} based network, $k_d = 892.9\ s^{-1}$ and $k_a = 190.2\ s^{-1}$. This shows that the kinetics of Cu^{2+} crosslinks is much faster than that of Ni^{2+} crosslinks. In Fig.5cd, we show additional rheological data from a different paper by Tang et al. [49] for a class of 4-arm PEG gels with Zn^{2+} crosslinks. The chemical composition of the metal-ligand crosslink is different from that of Gindy et al. [40] but the gel network structure is similar. By fitting the G' and G'' data using the Maxwell model, we obtain $G_0 = 9.536\ kPa,\ 20.38\ kPa,\ 27.53\ kPa,$ $52.68\ kPa$, and $t_R = 0.47\ s, 0.51\ s, 0.51\ s, 0.59\ s$ for gels with polymer concentration (w/v) of 10%, 15%, 20%, 30%, respectively. Note that G_0 increases with polymer concentration, while t_R is insensitive to polymer concentration. In Fig. 5b and 5d, deviations between the Maxwell model fit and experimental data can be seen at high frequency. The discrepancy has been attributed to additional relaxation mechanisms other than the dynamic metal-ligand crosslinks in Grindy et al. [48], e.g. due to the sticky Rouse mode [49]. The exact nature of such deviation remains to be elucidated.

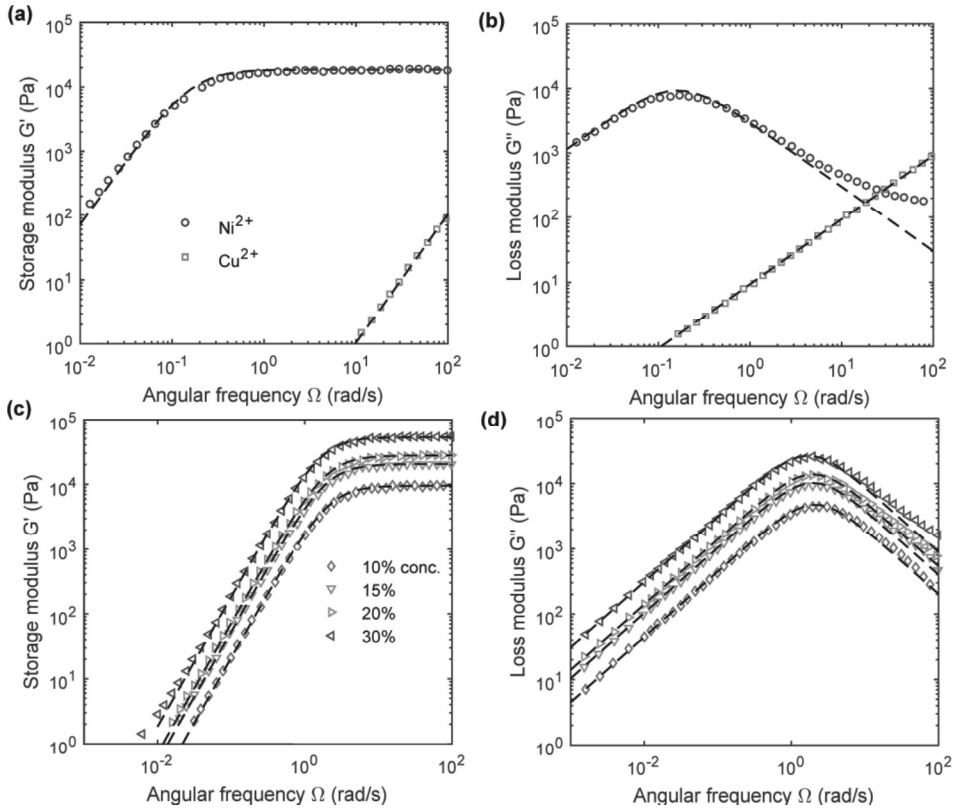

Figure 5. Comparison with rheological data in the literature for 4-arm PEG hydrogels with reversible metal-ligand cross-links. (a-b) Frequency dependence of storage and loss modulus for the PEG hydrogels with two different metal crosslinks: Ni^{2+} and Cu^{2+} [40]. (c-d) Frequency dependence of storage and loss modulus for a Zn^{2+} crosslinked PEG hydrogel with different polymer concentrations (w/v): 10%, 15%, 20% and 30% [49]. The symbols represent experimental data extracted from literature and the dashed lines represent fits by the Maxwell model.

The Maxwell model also implies plastic deformation, and such material is typically referred to as a viscoelastic fluid or viscoplastic solid. This is consistent with the illustrative example in Fig. 4 which shows that the dynamic bonds allow the network to gradually approach a relaxed state under a fixed deformation. As a result, the polymer would not recover its original shape after loading is removed. However, unlike conventional materials (e.g. viscoelastic polymer melts) where the molecular mechanisms for relaxation are complex and the Maxwell model is

phenomenological in nature, here we have derived the Maxwell model from our statistical framework of transient networks, thanks to the relatively simple relaxation mechanism of dynamic bonds. The Maxwell fits of rheological data for the 4-arm PEG gels, as shown in Fig.5, have already been performed in the literature [48-49]. The contribution of our approach is to provide a clear physical picture as to under what circumstances the Maxwell model works well, and to allow molecular interpretation of the material parameters G_0 and t_R.

4.3 Viscous fluid

The case of a perfectly viscous and incompressible fluid may be recovered in two conditions: (a) there are no permanent cross-links and (b) both attachment and dissociation occur at a rate that is much faster than the rate of loading. In this case, the cross-links are in a state of dynamic equilibrium i.e. $\dot{c} = 0$, from eq. (11b) and $\dot{\boldsymbol{\mu}} \approx 0$. Assuming k_d to be independent of load, eq. (40) implies that $\bar{\bar{\boldsymbol{k}}}_d = k_d \boldsymbol{\mu}$ and eq. (39b) becomes:

$$k_d(\boldsymbol{I} - \boldsymbol{\mu}) + \boldsymbol{D}\boldsymbol{\mu} + \boldsymbol{\mu}\boldsymbol{D} = \boldsymbol{0} \tag{56}$$

Now using the fact that the rate of deformation is slow compared to the gel dynamics, i.e. $|\mathbf{D}|/\mathrm{k_d} \ll 1$, a first order perturbation analysis yields $\boldsymbol{\mu} \approx \boldsymbol{I} + 2\boldsymbol{D}/k_d$, and therefore the stress equation (33) becomes:

$$\boldsymbol{\sigma} = ck_BT(\boldsymbol{\mu} - \boldsymbol{I}) + p\boldsymbol{I} = \frac{2ck_BT}{k_d}\boldsymbol{D} + p\boldsymbol{I} \tag{57}$$

where we used the fact that $c^0 = c$ since the cross-link concentration is constant in time. This corresponds to the constitutive relation for a Newtonian fluid, where the Cauchy stress is related to the rate of deformation $\boldsymbol{D}$ via a viscosity parameter:

$$\nu = \frac{2ck_BT}{k_d} = \frac{2k_BTc^t}{k_d}\left(\frac{k_a}{k_d + k_a}\right) \tag{58}$$

We generally see that the apparent viscosity increases with the number of available cross-links c^t and decreases with the rate k_d of crosslink detachment [50].

4.4 Generalization to multiple networks

As discussed above, more general polymers display a variety of characteristic relaxation times and would be better modeled as multiple networks. Literature has also shown that in many cases, polymers possess a permanent network in addition to its transient counterpart [28]. These considerations can be easily incorporated in an additive multiple network model shown here. For this, let us first assume that a polymer is represented by a series of N non-interacting networks, denoted by the index $I = 1, \dots, M$, and associated with their own chain concentration c_I and dynamic bond kinetics k_a^I and k_d^I (assumed to be constants for each network). In addition, the polymer is assumed to possess a permanent network with concentration c_S. In these conditions, the network statistics are represented by M distribution functions P^I and distribution tensors defined as:

$$\boldsymbol{\mu}^I = \langle P^I \tilde{\mathbf{r}} \otimes \tilde{\mathbf{r}} \rangle \tag{59}$$

The evolution equation for the cross-link concentration and the chain distribution is given by:

$$\dot{c}_I = k_a^I(c_I^t - c_I) - k_d^I c_I \tag{60}$$

and the distribution tensor by:

$$\dot{\boldsymbol{\mu}}^I = \frac{\xi_a^I}{c^I}\boldsymbol{I} - \bar{\bar{k}}_d^I - \frac{\dot{c}^I}{c^I}\boldsymbol{\mu} + \boldsymbol{D}\boldsymbol{\mu}^I + \boldsymbol{\mu}^I\boldsymbol{D} \tag{61}$$

Upon calculating these quantities, the total chain concentration can then be calculated as:

$$c = c_S + \sum_{I=1}^{M} c_I \tag{62}$$

and an overall distribution tensor $\boldsymbol{\mu}$ representing the entire network can be defined such that:

$$c\,\boldsymbol{\mu} = \mathrm{c_S} J\boldsymbol{F}\boldsymbol{F}^{\mathrm{T}} + \sum_{I=1}^{M} c_I \boldsymbol{\mu}^I \tag{63}$$

Because the networks do not interact, the stored elastic energy can be additively decomposed in the form:

$$\Delta\,\Psi_e(t) = \frac{k_B T}{2}\left[\, c_S\, J tr(\boldsymbol{F}\boldsymbol{F}^{\mathrm{T}} - \boldsymbol{I}) + \sum_{I=1}^{M} c^I tr(\boldsymbol{\mu}^{\boldsymbol{I}} - \boldsymbol{I}) \,\right] + p(\det(\boldsymbol{F}) - 1) \tag{64}$$

Using the overall concentration and distribution, this can also be written:

$$\Delta\Psi_e(t) = \frac{c k_B T}{2} tr[\,\boldsymbol{\mu} - \boldsymbol{I}] + p(\det(\boldsymbol{F}) - 1) \tag{65}$$

and the Cauchy stress tensor follows directly from eq. (33), with the difference that the distribution tensor is for multiple networks.

4.5 Illustration of a two-network model

For illustration purposes, we consider here the same virtual experiment as discussed in Section 3.4 but now assume that the polymer possesses a permanent network in addition to a dynamic counterpart considered earlier, with concentration $c_S = c$. Fig. 6 shows the theoretical predictions of the stress and energy relaxation as well as the statistical evolution of the two networks. While most of the discussion parallels that provided in Section 3.5 regarding the dynamic network, we see that the distribution tensor, average chain end-to-end distance and chain orientation of the permanent network only changes with the deformation steps, but does not tend to relax back to a stress-free isotropic state. This is expected since chains are unable to

reorganize when permanent cross-links are considered. There is therefore a clear contrast between the chain evolution (end-to-end distance and orientation) of the static and dynamic network (Fig. 6c). Indeed, when a fast deformation is applied, the chain configuration in both network react immediately and in a similar fashion since the rate of deformation is significantly higher than the bond kinetics. However, during the relaxation phase, we see that chains in the dynamic network tend to decrease their average end-to-end distance and become more uniformly distributed ($\theta \rightarrow \theta_{iso}$). The static network is however unable to reconfigure and the chains remain in their stretched configuration. A consequence is that while the stored elastic energy in the dynamic network relaxes to zero, that in the permanent network remains constant for a fixed deformation. An elastic stress therefore exists regardless of the bond dynamics of the transient polymer. In summary, it can therefore be seen that in contrast to the previous example, this double-network only possesses a single stress-free state, which occurs when the $\boldsymbol{F} = \boldsymbol{I}$. In other words, while the material shown in Fig. 4 would maintain the deformed shape once the applied load is removed, the existence of a permanent network gives the present material the ability to gradually creep back to its original shape. This behavior is similar to that predicted by the standard linear solid model where a spring is in parallel to a Maxwell model.

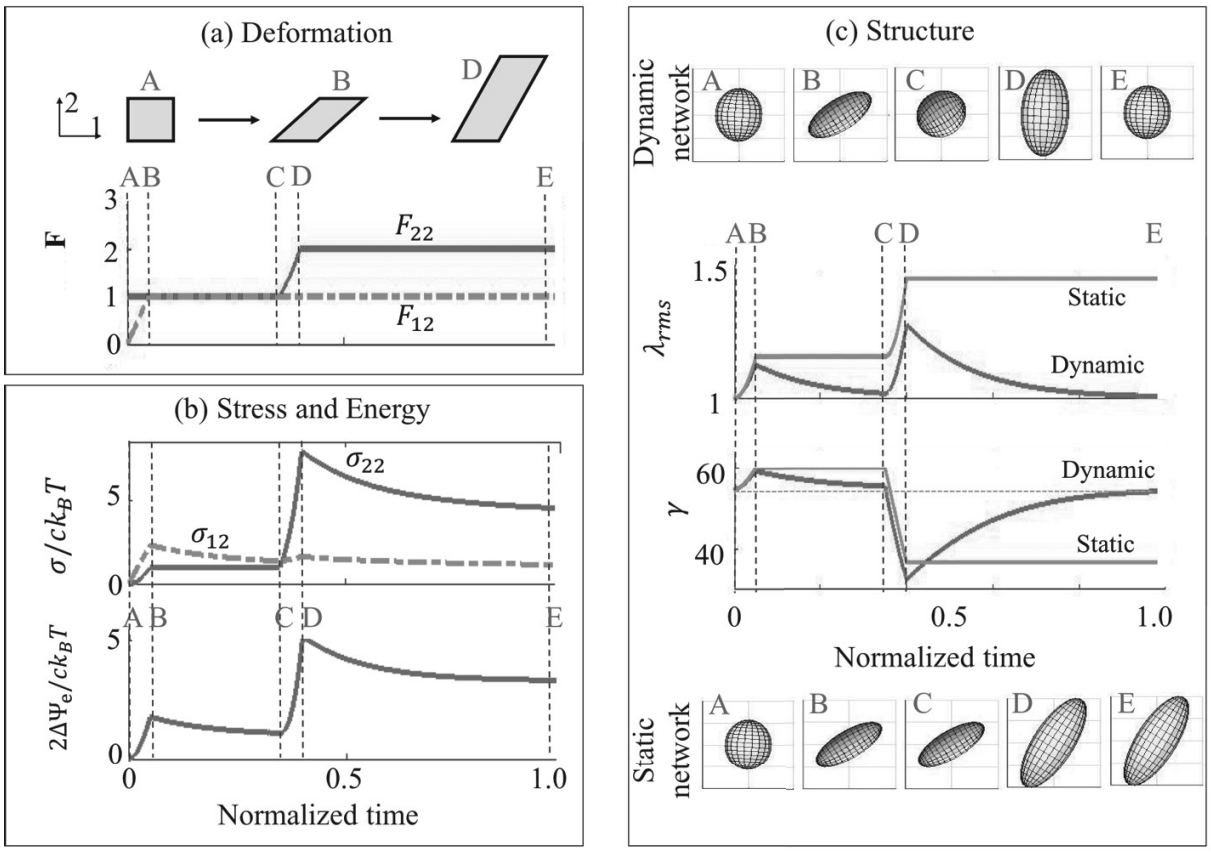

Figure 6. Illustration of (a) the deformation, (b) stress and stored elastic energy and (c) chain statistic response of a polymer characterized by one permanent network and one dynamic network that displays normalized rates $k = k_a\tau = k_d\tau = 0.07$. *The relative concentrations* c_s *and* c *of the permanent and dynamic network, respectively are chosen such that* $c/c_s = 1$ *Stresses are normalized by* $c_s k_B T$ *and energies by* $c_s k_B T/2$. *The structure of each network is characterized by the 3D representation of the distribution tensor, the averaged normalized end-to-end distance* $\lambda_{rms} = r_{rms}/\sqrt{N}b$ *and the average chain angle* γ *with the vertical direction (*$\boldsymbol{n} = [0,1]$ *in the Cartesian coordinate system). Time is expressed in units of* τ.

5. Further discussion

The main contribution of this paper is that our statistical approach illustrates the essential molecular picture that underlies viscoelasticity of soft polymers. This approach allows one to leverage developments in the polymer physics literature to incorporate more complex molecular mechanisms, which may open the door to physics-based nonlinear viscoelastic models. Such models are of fundamental value to many mechanics questions, one example being the fracture of viscoelastic rubbers [51-53]. As pointed out by Knauss [54], one of the limiting factors that hinder further understanding of soft polymer fracture is the lack of an accurate and physics-based nonlinear viscoelastic model.

A number of theories, starting from classical rubber elasticity, attempt to relate the statistical description of polymer chains or fibrous networks to the elastic response of the assembly [1, 9-10, 55]. Such approaches implicitly separate the directional dependence of the chains (or fibers) and the elastic energy stored due to stretch (characterized by the deformation gradient $\boldsymbol{F}$). The total free energy Ψ is therefore expressed in the general form:

$$\Psi = \int_0^{2\pi}\int_0^{\pi} P(\theta,\omega)[\psi_c(\boldsymbol{r}) - \psi_c(\boldsymbol{r}_0)]sin\theta d\theta d\omega \tag{66}$$

Assuming affine deformation, the chain/fiber stretch is expressed in terms of the macroscopic deformation gradient as $\boldsymbol{r} = \boldsymbol{F}\boldsymbol{r}_0$. The proposed approach takes a different route since the chain stretch is now incorporated into the probability function, such that the energy becomes:

$$\Psi = \int_0^{2\pi}\int_0^{\pi}\left(\int_0^{\infty}[P(\boldsymbol{r},t) - P(\boldsymbol{r}_0,t)]\psi_c(\boldsymbol{r})r^2 dr\right)sin\theta d\theta d\omega \tag{67}$$

It is clear here, that in contrast to (66), we here compare the distribution functions of the chains in their "natural" and deformed states and multiply this difference by the corresponding energy

function. A main advantage of this viewpoint is that it allows for the evolution of the probability function $P(\boldsymbol{r},t)$ arising from different physical processes, which may include, for instance the dynamic nature of the chains' attachment and detachment, the degradation of cross-links [56-59] as well as growth processes in biological materials [60] for instance. As a result, a number of dissipative processes can readily be incorporated into the current framework by simply modifying the evolution equation of the probability function shown in eq. (37). From a mathematical standpoint, eq. (67) also implies that one can naturally capture the change in natural (or stress-free) configuration of the material since the term $P(\boldsymbol{r},\Omega)-P(\boldsymbol{r}_0,\Omega)$ can vanish even though $\boldsymbol{F}\neq\boldsymbol{I}$. Consequently, the proposed theory does not rely on the traditional Lagrangian framework used for solid, but can be used to describe elastic fluids and viscous polymer without additional difficulties. Finally, we have shown that in the case of Gaussian statistics, the chain distribution could be described in terms of a distribution tensor, which may be thought of as an extension to the structure's tensor [61-62] that incorporates chain/filament length in its definition. In the following we discuss a number of possible extensions to our statistical approach.

As stated in Section 3, the single chain energy function ψ_c in eq. (17), which is based on the freely jointed chain (FJC) model with Gaussian statistics of segment configurations, is only applicable to small to moderate extensions. At large extensions where the contour length Nb is approached, the resulting chain stiffening can be captured by Langevin statistics. In this case, the single chain energy function is [13]:

$$\Psi_r = Nk_BT\left(\beta L^{-1}(\beta)+\ln\frac{L^{-1}(\beta)}{\sinh[L^{-1}(\beta)]}\right),\quad \beta=\frac{r}{Nb} \tag{68}$$

where $L^{-1}(\beta)$ is the inverse Langevin function that diverges as $\beta \to 1$ or $r \to Nb$. Following the same procedures as described in Section 3, we found that the distribution tensor $\boldsymbol{\mu}$ would become:

$$\boldsymbol{\mu} = \langle \frac{1}{rb} L^{-1}\left(\frac{r}{Nb}\right) P(\boldsymbol{r}, t)\, \boldsymbol{r} \otimes \boldsymbol{r} \rangle \tag{69}$$

and the true stress tensor keeps its original definition as:

$$\boldsymbol{\sigma} = ck_B T(\boldsymbol{\mu} - \boldsymbol{I}) - p\boldsymbol{I} \tag{70}$$

Note that with eq. (69), one can no longer derive a simple time evolution equation for $\boldsymbol{\mu}$, such as that shown in eq. (37). Instead, one needs to calculate the time evolution of the distribution function $\phi(\boldsymbol{r}, t)$ using eq. (11) and numerically perform the integral over all chain configurational states.

In Section 4.1, we have illustrated that our model with Gaussian chains reduces to the elastic neo-Hookean model if permanent cross-links are assumed. It is of interest to see what elastic solid would the Langevin chain model recover under the assumption of permanent cross-links. There are a few hyperelastic models in the literature that are derived from Langevin chains, in particular the Arruda-Boyce 8-chain model [9] and the Wu-van der Giessen (WG) network model [10]. Next we demonstrate that with Langevin chains (eq. (69)) our model degenerates to the WG model. WG adopted the affine deformation assumption for a permanent network which dictates that the end-to-end vector of a chain changes from $\boldsymbol{r}_0$ in the reference configuration to $\boldsymbol{r} = \boldsymbol{F}\boldsymbol{r}_0$ after deformation. However, a key difference between our model and the WG model is that we considered the full distribution in chain end-to-end vector, including both the end-to-end distance r and orientation. This was necessary to incorporate the effect of dynamic cross-links. In contrast, WG only considered the distribution in chain orientation and assumed a uniform

chain end-to-end distance. At the stress-free configuration, all chains are assigned the same mean end-to-end distance $r = \sqrt{N}b$. After deformation, this distance becomes $\lambda\sqrt{N}b$, where λ depends on chain orientation, i.e. $\lambda(\theta, \omega)$ and can be calculated from the affine deformation assumption that $\boldsymbol{r} = \boldsymbol{F}\boldsymbol{r}_0$. This is a special case of our distribution function $P(\boldsymbol{r}, t)$ where the dependence on the end-to-end distance $\boldsymbol{r}$ is through the Dirac δ-function:

$$P(\boldsymbol{r}, t) = \frac{\delta\left(\boldsymbol{r} - \lambda\sqrt{Nb}\right)}{|\boldsymbol{r}|^2} C(\theta, \omega, t) \tag{71}$$

where $C(\theta, \omega, t)$ is a distribution function of chain orientation characterized by the spherical coordinates θ and ω. Substituting eq. (71) into eq. (70), we recover the equation by Wu and van der Giessen (see equation no. (29) in [10]). To the best of our knowledge, the Langevin chain model has not been directly incorporated into continuum models of polymer networks with dynamic bonds. Previous efforts to include the strain stiffening effects were based on continuum elasticity models such the Arruda-Boyce model [9], Gent model [35] or exponentially hardening model [36]. Recently, more sophisticated single chain models have been developed to combine entropic and enthalpic contributions for chain elasticity [63]. The latter describes the effects due to stretching of the carbon bonds on polymer chains. Incorporation of bond stretching can allow one to better capture the irreversible scission of chains due to excessive forces. Such sophisticated single chain models have not been implemented in continuum theories for dynamic networks, and our approach offers a clear path along this direction.

6. Summary

In summary, this paper described a new theoretical framework that can represent the time-dependent responses of soft polymers based on a statistical description of the underlying polymer network. Its root is anchored in a statistical representation of the configuration and evolution of a network of dynamically cross-linked polymer chains as it is subjected to deformation. Using appropriate average operations and thermodynamical arguments, it was possible to relate the chain distribution to the concepts of stress, strain and entropy generation via the so-called distribution tensor. Eventually, a fully macroscopic theory was derived involving an evolution equation for this tensor. The theory provides natural extension of rubber elasticity in the range of inelastic deformation and could be extended to account for multiple networks, or large chain deformation (with Langevin statistics) to name a few. The dynamic bonds considered in this work can be broadly interpreted as the temporary interactions between polymer chains, e.g. entanglements in polymer melts or lightly cross-linked networks. Potentially, one can prescribe physics-based models to describe the kinetics of disentanglements and re-entanglements by taking advantage of the established knowledge in a vast literature on the dynamics of polymer chains [16-17]. Such physical insights may also be drawn from molecular-level simulations. Efforts in this direction may lead to new physics-based nonlinear viscoelasticity model of passive, active and bio-polymers [64-65]. Overall the statistical approach presented in this work can provide a convenient platform to integrate the complex physics of polymer chain dynamics that are otherwise difficult to be implemented into continuum theories.

Acknowledgments

FJV acknowledges the support of the National Science Foundation under the NSF MRSEC DMR

1420736 and the NSF CAREER award 1350090. RL acknowledges the support from the 3M non-Tenured Faculty award.

References

[1] Boyce, M.C., Arruda, E.M., 2000. Constitutive models of rubber elasticity: a review. *Rubber Chemistry and Technology* 73(3), 504–523.

[2] Wineman, A., 2009. Nonlinear viscoelastic solids – A review. *Mathematics and Mechanics of Solids*, 14(3), 300–366.

[3] Puglisi, G., Saccomandi, G., 2016. Multi-scale modelling of rubber-like materials and soft tissues: an appraisal. *Proc. R. Soc. Lond. A* 472: 20160060.

[4] Holzapfel, G.A., 2000. *Nonlinear solid mechanics: A continuum approach for engineering*, Wiley & Sons.

[5] Gurtin, M.A., Fried, E., Anand, L., 2010. *The mechanics and thermodynamics of continua*, Cambridge University Press.

[6] Flory, P.J., Rehner, J., 1943. Statistical mechanics of cross-linked polymer networks. I. Rubberlike elasticity, *J. Chem. Phys*. 11, 512–520.

[7] Treloar, L.R.G., 1946. The elasticity of a network of long-chain molecules –III. *Trans. Faraday Soc.*, 42, 83–94.

[8] Wang, M.C., Guth E., 1952. Statistical theory of networks of non-Gaussian flexible chains, *J. Chem. Phys.* 20, 1144–1157.

[9] Arruda, E.M., Boyce, M.C., 1993. A three-dimensional model for the large stretch behavior of rubber elastic materials. *J. Mech. Phys. Solids*, 41(2), 389–412.

[10] Wu, P.D., Van Der Giessen, E., 1993. On improved network models for rubber elasticity and their applications to orientation hardening in glassy polymers. *J. Mech. Phys. Solids*. 41(3), 427–456.

[11] Treloar, L.R.G., 1943. The elasticity of a network of long-chain molecules. I. *Trans. Faraday Soc.*, 39, 36–41.

[12] Kawakatsu, T., 2004. Gaussian chain model and statistics of polymers. In *Statistical Physics of Polymers*. Springer-Verlag Berlin, Kluwer, 17–99.

[13] Rubinstein, M., Colby, R.H., 2003. *Polymer Physics*. Oxford University Press.

[14] Horgan, C.O., Saccomandi, G., 2006. Phenomenological hyperelastic strain-stiffening constitutive models for rubber. *Rubber Chemistry and Technology* 79(1), 152–169.

[15] Beatty, M.F., 2003. An average-stretch full-network model for rubber elasticity. *J. Elasticity* 70(1), 65–86.

[16] de Gennes, P.G., Leger, L., 1982. Dynamics of entangled polymer chains. *Ann. Rev. Phys. Chem.* 33, 49–61.

[17] Doi, M.; Edwards, S.F., 1988. *The Theory of Polymer Dynamics.* Clarendon Press.

[18] Christensen, R.M., 2010. *Theory of Viscoelasticity*, Second Editon, Dover Publication.

[19] Lubliner, J., 1985. A model of rubber viscoelasticity, *Mech. Res. Comm*. 12, 93–99.

[20] Le Tallec, P., Rahier, C., Kaiss, A., 1993. Three-dimensional incompressible viscoelasticity in large strains: formulation and numerical approximation. *Comp. Meth. Appl. Mech. Eng.* 109, 233–258.

[21] Reese, S., Govindjee S., 1998. A theory of finite viscoelasticity and numerical aspects. *Int. J. Solids Structures* 35, 3455–3482.

[22] Bergstrom, J.S., Boyce, M.C., 1998. Constitutive modeling of the large strain time-dependent behavior of elastomers. *J. Mech. Phys. Solids*, 46, 931–954.

[23] Green, M.S., Tobolsky, A.V., 1946. A new approach to the theory of relaxing polymeric media. *J. Chem. Phys*. 14(2), 80–92.

[24] Tanaka, F., Edwards, S.F., 1992. Viscoelastic properties of physically cross-linked networks -transient network theory. *Macromolecules* 25, 1516–1523.

[25] Drozdov, A.D., 1999. A constitutive model in finite thermoviscoelasticity based on the concept of transient networks. *Acta Mech.* 133, 13–37.

[26] Hui, C.Y., Long, R., 2012. A constitutive model for the large deformation of a self-healing gel. *Soft Matter* 8, 8209–8216.

[27] Long, R., Qi, H.J., Dunn, M.L., 2013. Modeling the mechanics of covalently adaptable polymer networks with temperature-dependent bond exchange reactions. *Soft Matter* 9, 4083–4096.

[28] Long, R., Mayumi, K., Creton, C., Narita, T., Hui, C.Y., 2014. Time dependent behavior of a dual cross-link self-healing gel: theory and experiments. *Macromolecules* 47(20), 7243–7250.

[29] Meng, F., Pritchard, R.H., Terentjev, EM., 2016. Stress relaxation, dynamics, and plasticity of transient polymer networks. *Macromolecules* 49(7), 2843–2852.

[30] Rajagopal, K.R., Srinivasa, A.R., 2004. On the thermomechanics of materials that have multiple natural configurations Part I: viscoelasticity and classical plasticity. *ZAMP* 55, 861–893.

[31] Wojtecki, R.J., Meador, M.A., Rowan, S.J. 2011. Using the dynamic bond to access macroscopically responsive structurally dynamic polymers. *Nature Materials* 10, 14–27.

[32] Jin, Y., Yu, C., Denman, R.J., Zhang, W., 2013. Recent advances in dynamic covalent chemistry. *Chem. Soc. Rev.* 42, 6634–6654.

[33] Kloxin, C.J., Bowman, C.N., 2013. Covalent adaptable networks: smart, reconfigurable and responsive network systems. *Chem. Soc. Rev.* 42, 7161–7173.

[34] Long, R., Mayumi, K., Creton, C., Narita, T., Hui, C.Y., 2015. Rheology of a dual cross-link self-healing gel: theory and measurement using parallel-plate torsional rheometry. *Journal of Rheology* 59(3), 643–665.

[35] Meng, F., Terentjev, E.M., 2016. Transient network at large deformations: elastic-plastic transition and necking instability. *Polymers* 8(4), 108.

[36] Guo, J., Long, R., Mayumi, K., Hui, C-Y., 2016. Mechanics of a dual cross-link gel with dynamic bonds: steady state kinetics and large deformation effects. *Macromolecules* 49(9), 3497–3507.

[37] Long, K.N., Dunn, M.L., Qi, H.J., 2010. Mechanics of soft active materials with phase evolution. *Int. J. Plasticity* 26, 603–616.

[38] Leibler, L., Rubinstein, M., Colby, R.H., 1991. Dynamics of reversible networks. *Macromolecules* 24, 4701–4707.

[39] Sing, M.K., Wang, Z.G., McKinley, G.H., Olsen, B.D., 2015. Celebrating soft matter's 10th anniversary: chain configuration and rate-dependent mechanical properties in transient networks. *Soft Matter* 11, 2085−2096.

[40] Grindy, S.C., Learsch, R., Mozhdehi, D., Cheng, J., Barrett, D.G., Guan, Z., Messersmith, P.B., Holten-Andersen, N., 2015. Control of hierarchical polymer mechanics with bioinspired metal-coordination dynamics. *Nature Materials* 14, 1210−1216.

[41] Bergstrom, J.S.; Boyce, M.C., 2001, Deformation of elastomeric networks: relation between molecular level deformation and classical statistical mechanics models of rubber elasticity. *Macromolecules*, 34, 614-626.

[42] Yang, H., Yu, K., Mu, X., Shi, X., Wei, Y., Guo, Y., Qi, H. J., 2015. A molecular dynamics study of bond exchange reactions in covalent adaptable networks. *Soft Matter*, 11, 6305–6317.

[43] Fourier, J., 1955. *Analytical theory of heat*. Dover Publications, New York.

[44] Montarnal, D., Capelot, M., Tournilhac, F., Leibler, L., 2011. Silica-like malleable materials from permanent organic networks. *Science* 334, 965−968.

[45] Treloar, L.R.G., 1975. *The Physics of Rubber Elasticity*. Oxford University Press, USA.

[46] Kuhn, W., Grün, F., 1946. Statistical behavior of the single chain molecule and its relation to the statistical behavior of assemblies consisting of many chain molecules. *Polym. Chem*. 1(3), 183–199.

[47] Pearson, C.E., 1983. *Handbook of Applied Mathematics*. 2nd edition, Van Nostrand Reinhold.

[48] Grindy, S.C., Lenz, M., Holten-Andersen, N., 2016. Engineering elasticity and relaxation time in metal-coordinate crosslinked hydrogels. *Macromolecules* 49, 8306−8312.

[49] Tang, S., Habicht, A., Li, S., Seiffert, S., Olsen, B.D., 2016. Self-diffusion of associating start-shaped polymers. *Macromolecules* 49, 5599-5608.

[50] Tanaka, F., Edwards, S.F., 1992. Viscoelastic properties of physically crosslinked networks: Part I: Nonlinear stationary viscoelasticity. *J. Non-Newtonian Fluid Mechanics*, 43, 247−271.

[51] Gent, A.N., 1996. Adhesion and strength of viscoelastic solids. Is there a relation between adhesion and bulk properties? *Langmuir* 12, 4492−4496.

[52] de Gennes, P.G., 1996. Soft Adhesives. Langmuir 12, 4497−4500.

[53] Persson, B.N.J., Brener, E.A., 2005. Crack propagation in viscoelastic solids. *Physical Review E* 71, 036123.

[54] Knauss, W.G., 2015. A review of fracture in viscoelastic materials. *Int. J. Fract.* 196, 99−146.

[55] Edwards, S.F., Vilgis, T.A., 1988. The tube model of rubber elasticity. *Rep. Prog. Phys*. 51, 243-297.

[56] Charlesby, A., 1981. Crosslinking and degradation of polymers. *Radiation Physics and Chemistry* 18(1–2), 59–66.

[57] Vernerey, F.J., Greenwald, E.C., Bryant, S.J., 2012. Triphasic mixture model of cell-mediated enzymatic degradation of hydrogels. *Comput. Meth. Biomech. Biomed. Eng.* 15(11), 1197–1210.

[58] Dhote, V., Vernerey, F.J., 2014. Mathematical model of the role of degradation on matrix development in hydrogel scaffold. *Biomech. Model. Mechanobiol*. 13(1), 167–183.

[59] Akalp, U., Bryant, S.J., Vernerey, F.J., 2016. Tuning tissue growth with scaffold degradation in enzyme-sensitive hydrogels: a mathematical model. *Soft Matter* 12(36), 7505–7520.

[60] Vernerey, F.J., 2016. A mixture approach to investigate interstitial growth in engineering scaffolds. *Biomech. Model. Mechanobiol*. 15(2), 259–278.

[61] Cortes, D.H., Elliott, D.M., 2016. Modeling of collagenous tissues using distributed fiber orientations. in *Structure-Based Mechanics of Tissues and Organs*, G. S. Kassab and M. S. Sacks (Eds.), Springer US, 15–39.

[62] Vernerey, F.J., Farsad, M., 2011. A constrained mixture approach to mechano-sensing and force generation in contractile cells. *J. Mech. Behav. Biomed. Mater*. 4(8), 1683–1699.

[63] Mao, Y., Talamini, B., Anand, L., 2017. Rupture of polymers by chain scission. *Extreme Mechanics Letters*, 13, 17−24.

[64] Vernerey, F.J., Akalp, U., 2016. Role of catch bonds in actomyosin mechanics and cell mechanosensitivity. *Phys. Rev. E* 94(1), 012403.

[65] Akalp, U., Schnatwinkel, C., Stoykovich, M.P., Bryant, S.J., Vernerey, F.J., 2017. Structural modeling of mechanosensitivity in non-muscle cells: multiscale approach to understand cell sensing. *ACS Biomater. Sci. Eng.*, in press, DOI:10.1021/acsbiomaterials.6b0069.

Appendix A.1 Derivation of the variation of free energy

Equation (19) in the manuscript represent the variation for the total free energy as a function of macroscopic quantities, including the distribution tensor. Details of its derivation are given below. Starting from the form of the free energy written in eq. (18), it is straightforward to show that $\dot{\Psi}$ can be expressed as:

$$\dot{\Psi} = -\dot{T}\left(\gamma\, ln\left(\frac{T}{T_0}\right) + \vartheta_0\right) + \Delta\dot{\Psi}_e \tag{A1}$$

where $\Delta\dot{\Psi}_e(t)$ can be calculated from eq. (17) as:

$$\Delta\dot{\Psi}_e = \frac{k_B\dot{T}}{2}\langle(\phi - \phi_0)\tilde{r}^2\rangle + \frac{k_BT}{2}\langle\left(\dot{\phi} - \dot{\phi}_0\right)\tilde{r}^2\rangle + ptr(\boldsymbol{L}) \tag{A2}$$

Now using the evolution equation for the distribution function, we can write:

$$\langle\dot{\phi}\tilde{r}^2\rangle = \langle\xi_a P_0\tilde{r}^2\rangle - \langle k_d\phi\tilde{r}^2\rangle - \langle L_{ii}\phi\tilde{r}^2\rangle - \langle\frac{\partial\phi}{\partial r_i}r_j\tilde{r}^2\rangle\, L_{ij} \tag{A3}$$

Using integration by part on the last term, this equation simplifies to:

$$\langle\frac{\partial\phi}{\partial r_i}r_j\tilde{r}^2\rangle\, L_{ij} = -\langle\phi\delta_{ij}\tilde{r}^2\rangle L_{ij} - \langle 2\phi\delta_{ik}\tilde{r}_j\tilde{r}_k\rangle L_{ij} \tag{A4}$$

Substituting in (A3) and using the definition of the chain distribution tensor:

$$\boldsymbol{\mu} = \langle P\tilde{\boldsymbol{r}} \otimes \tilde{\boldsymbol{r}} \rangle \quad \text{and} \quad \boldsymbol{\mu}_0 = \langle P_0\tilde{\boldsymbol{r}} \otimes \tilde{\boldsymbol{r}} \rangle, \tag{A5}$$

we obtain:

$$\langle \dot{\phi}\tilde{r}^2 \rangle = \xi_a tr(\boldsymbol{\mu_0}) - \langle k_d \phi \tilde{r}^2 \rangle + 2c\boldsymbol{\mu}\colon \boldsymbol{L} \tag{A6}$$

Similarly, the time derivative of the chain distribution tensor ϕ_0 from its reference state is:

$$\langle \dot{\phi}_0\tilde{r}^2 \rangle = \xi_a tr(\boldsymbol{\mu_0}) - \langle k_d \phi_0 \tilde{r}^2 \rangle + 2c\boldsymbol{\mu_0}\colon \boldsymbol{L} \tag{A7}$$

Finally substituting eqs (A6) and (A7) into (A2), allows to express the change in elastic energy as:

$$\Delta\dot{\Psi}_e = \frac{k_B T}{2}\left(2c(\boldsymbol{\mu} - \boldsymbol{\mu_0})\colon \boldsymbol{L} - \langle k_d(\phi - \phi_0)\tilde{r}^2 \rangle\right) + \frac{ck_B\dot{T}}{2}\left(tr(\boldsymbol{\mu} - \boldsymbol{\mu}_0)\right) + ptr(\boldsymbol{L}) \tag{A8}$$

which, when plugged into eq (A1) leads to eq. (20) in the main text.

Appendix A.2 Evolution equation for the distribution tensor

Starting from its original definition in eq. (21), let us, for convenience express the time evolution of the tensor $\boldsymbol{\mu}$ in component form as follows:

$$\dot{\mu}_{ij} = \int \dot{P}(\boldsymbol{r})\tilde{r}_i\tilde{r}_j d\boldsymbol{r} = \frac{1}{c}\left(\int \dot{\phi}(\boldsymbol{r})\tilde{r}_i\tilde{r}_j d\boldsymbol{r} - \dot{c}\int P(\boldsymbol{r})\tilde{r}_i\tilde{r}_j d\boldsymbol{r}\right) \tag{A9}$$

Using (10), we then obtain:

$$\dot{\mu}_{ij} = \frac{\xi_a}{c}\mu^0_{ij} - (k_d + L_{kk})\mu_{ij} - L_{lk}M_{klij} - \frac{\dot{c}}{c}\mu_{ij} \tag{A10}$$

where the components of the fourth order tensor M are given by:

$$M_{klij} = \int_r \frac{\partial\phi(\boldsymbol{r})}{\partial r_l}\tilde{r}_k\tilde{r}_i\tilde{r}_j d\boldsymbol{r} \tag{A11}$$

and

$$\bar{\bar{\boldsymbol{k}}}_{ij} = \int_r k_d(\boldsymbol{r})P(\boldsymbol{r})\tilde{r}_i\tilde{r}_j d\boldsymbol{r} \tag{A12}$$

A simple integration by part then leads $M_{ijkl} = -\left(\delta_{ij}\mu_{lk} + \delta_{jk}\mu_{li} + \delta_{jl}\mu_{ik}\right)$ where we assumed that boundary terms vanished. The evolution equation for $\boldsymbol{\mu}$ therefore take the convenient form:

$$\dot{\mu}_{ij} = \frac{\xi_a}{c}\mu^0_{ij} - \bar{\bar{k}}_{d\,ij} + \left(L_{ik}\mu_{kj} + L_{jk}\mu_{ki}\right) - \frac{\dot{c}}{c}\mu_{ij} \tag{A13}$$

In a tensor notation, this relation can be written as:

$$\dot{\boldsymbol{\mu}} = \frac{\xi_a}{c}\boldsymbol{\mu}^0 - \bar{\bar{\boldsymbol{k}}}_d - \frac{\dot{c}}{c}\boldsymbol{\mu} + \boldsymbol{L\mu} + (\boldsymbol{L\mu})^T \tag{A14}$$

where the superscript T denotes the transpose operator. Using the fact that the product of a symmetric and antisymmetric tensor vanishes, the term $\boldsymbol{L\mu}$ can be replaced by $\boldsymbol{D\mu}$ where $\boldsymbol{D} = \left(\boldsymbol{L} + \boldsymbol{L}^T\right)/2$ is the symmetric rate of deformation tensor. This enables to write:

$$\dot{\boldsymbol{\mu}} = \frac{\xi_a}{c}\boldsymbol{\mu^0} - \bar{\bar{\boldsymbol{k}}}_d - \frac{\dot{c}}{c}\boldsymbol{\mu} + \mathbf{D}\boldsymbol{\mu} + \boldsymbol{\mu D} \tag{A15}$$

This equation corresponds to eq. (37) in the main text.

Appendix A.3 Recovering the linear viscoelastic model

Under uniaxial tension, $F_{11} = \lambda$, $F_{22} = F_{33} = \lambda^{-1/2}$, and all other components vanish. Substituting $\boldsymbol{F}$ into eq. (50), we obtain

$$\mu_{11}(t) = e^{-k_d t}\lambda^2(t) + \int_0^t k_d \left[\frac{\lambda^2(t)}{\lambda^2(\tau)}\right] e^{-k_d(t-\tau)}\, d\tau \tag{A16}$$

and

$$\mu_{22}(t) = \mu_{33}(t) = e^{-k_d t}\lambda^{-1}(t) + \int_0^t k_d \left[\frac{\lambda^2(t)}{\lambda^2(\tau)}\right] e^{-k_d(t-\tau)}\, d\tau \tag{A17}$$

To obtain the tensile stress σ_{11}, we use the boundary condition that $\sigma_{22} = \sigma_{33} = 0$ to determine the pressure term p. With some simple algebra, we obtain that

$$\frac{\sigma_{11}(t)}{ck_BT} = e^{-k_d t}\left[\lambda^2(t) - \frac{1}{\lambda(t)}\right] + \int_0^t k_d \left[\frac{\lambda^2(t)}{\lambda^2(\tau)} - \frac{\lambda(\tau)}{\lambda(t)}\right] e^{-k_d(t-\tau)}\, d\tau \tag{A18}$$

with small deformation where $\lambda = 1 + \varepsilon$, we can linearize eq. (A18) and obtain the following equation

$$\begin{aligned} \frac{\sigma_{11}(t)}{ck_BT} &= 3\varepsilon(t)e^{-k_d t} + 3\int_0^t k_d[\varepsilon(t) - \varepsilon(\tau)]e^{-k_d(t-\tau)}\, d\tau \\ &= 3\varepsilon(t)\int_{-\infty}^0 k_d e^{-k_d(t-\tau)}\, d\tau + 3\int_0^t k_d[\varepsilon(t) - \varepsilon(\tau)]e^{-k_d(t-\tau)}\, d\tau \end{aligned} \tag{A19}$$

We assume the mechanical loading starts at $t = 0$, which implies $\varepsilon(\tau) = 0$ for $\tau < 0$. As a result, eq. (A19) can be casted in the following form:

$$\begin{aligned} \frac{\sigma_{11}(t)}{ck_BT} &= 3 \int_{-\infty}^{t} k_d[\varepsilon(t) - \varepsilon(\tau)]e^{-k_d(t-\tau)}\, d\tau \\ &= 3 \int_{-\infty}^{t} e^{-k_d(t-\tau)}\, \frac{d\varepsilon(\tau)}{d\tau} d\tau \end{aligned} \tag{A20}$$

If we recognize that $E_0 = 3ck_BT$ is the instantaneous Young's modulus and $E(t) = E_0 e^{-k_d t}$ is the relaxation modulus, then eq. (A20) can be written as

$$\sigma_{11}(t) = \int_{-\infty}^{t} E(t-\tau)\, \frac{d\varepsilon(\tau)}{d\tau} d\tau \tag{A21}$$

We have reduced to linear viscoelasticity, specifically a Maxwell model given the form of $E(t)$. Since the mechanical loading starts at $t = 0$ and we allow an instantaneous application of strain, eq. (A21) can also be written as

$$\sigma_{11}(t) = E(t)\varepsilon(t = 0^+) + \int_{0^+}^{t} E(t-\tau)\, \frac{d\varepsilon(\tau)}{d\tau} d\tau \tag{A22}$$

A Statistically-Based Continuum Theory for Polymers with Transient Networks

Franck J. Vernerey[1,*], Rong Long[1] and Roberto Brighenti[2]

[1] *Department of Mechanical Engineering*
Program of Materials Science and Engineering
University of Colorado Boulder - USA

[2] *Department of Engineering & Architecture,*
University of Parma - Italy

Abstract

We present a physics-based theoretical framework to describe the transient mechanical response of polymers undergoing finite deformation. For this, a statistical description of the polymer network is provided by a distribution function that is allowed to evolve in time due to a combination of deformation and chain reconfiguration enabled by transient cross-links. After presenting the evolution law for the chain distribution function, we show that, using classical thermodynamics, one can determine how the entropy, elastic energy and true stress evolve in terms of the network configuration. In particular, we introduce the concept of distribution tensor, that enables a clean transition between the network statistics, its continuum representation and the macroscopic polymer response. In the context of Gaussian statistics, it is further shown that this tensor follows its own evolution law, enabling a simple handling of visco-elastic rubbers. The model degenerates to classical rubber elasticity when cross-links are permanent, while the case of viscous fluids is recovered for fast cross-link kinetics. The generality of the framework as well as its relevance to modeling a number of important dissipative processes occurring in polymers using a continuum approach are also discussed.

Keywords: polymer mechanics, visco-elasticity, transient response, dynamic cross-links, statistical theory.

*Corresponding author: franck.vernerey@colorado.edu

1. Introduction

Soft polymeric materials exhibit complex mechanical behaviors, ranging from elastic solids (e.g. crosslinked rubber networks) to viscous fluid (e.g. polymer melts). Tremendous efforts have been devoted to the theoretical modeling of soft polymer mechanics [1-3]. For example, numerous models have been developed in the literature to describe the nonlinear elasticity of soft rubbers capable of large and reversible deformation, following mainly two approaches. In the first approach, phenomenological models are proposed to match experimental data under the constraints derived from continuum mechanics, e.g. frame indifference and material symmetry [4-5]. In contrast, the second approach is based on the statistical mechanics of individual polymer chains [6-10]. When a single chain is stretched, its configurational entropy is reduced which provides the energetic driving force for elastic recovery. Such entropic elasticity can be captured by a number of single chain models, e.g. freely jointed chain (FJC) with Gaussian statistics [11-13]. Because the second approach is rooted in molecular physics of polymer chains, it can be extended to accommodate the nonlinear elastic behaviors of soft polymers in a more guided manner instead of trial-and-error. For example, the concept of Langevin statistics [13] has been used for the FJC model, in place of Gaussian statistics, to capture the strain stiffening effects of soft rubbers at large strains [9, 14]. A necessary component for the second approach is a link between the single chain model and the continuum mechanics of polymer network. A number of models have been proposed to establish such a link, including the 3-chain model [8], the 4-chain model [6-7], the 8-chain model [9], and the full-network model [10, 15] among others. An excellent review of this subject can be found in Boyce and Arruda [1].

Viscoelasticity in soft polymers involves more complex molecular mechanisms such as temporary chain entanglements and chain diffusion [16-17]. The dynamics of chain entanglements and diffusion have been extensively studied in the physics community in the past few decades [13, 16-17]. However, the theoretical insights established in the polymer physics literature have not been fully translated to advancements in continuum models of viscoelasticity. Most existing models, from the simple linear Maxwell or Kelvin-Voigt models [18] to the more sophisticated nonlinear viscoelastic models [19-22], are phenomenological. While in some of these models (e.g. [22]) the continuum-level relaxation or creeping behavior was prescribed with inspirations from chain entanglement dynamics, models that directly connect the molecular physics of chain dynamics and macroscopic viscoelasticity are still not available. A difficulty with building molecular physics-based viscoelasticity models is the lack of a common natural reference configuration for all chains, due to the relaxation processes enabled by disentanglement and chain diffusion.

To accommodate this feature, Green and Tolbosky [23] assumed a conceptual picture when the chains in viscoelastic polymers can detach and reattach, resulting in families of chains with distinct natural reference configurations. This approach was further developed by others [24-29] and also discussed in the continuum mechanics literature as the method of multiple natural configurations, e.g. by Rajagopal and Srinavasa [30]. In this class of models, the chains are assumed to be born at a natural relaxed configuration when reattached to the network. The populations of chains born at different times along the external loading history, thereby possessing different relaxed configurations, are tracked by following the kinetics of chain detachment and reattachment. More recently, the conceptual picture of chain detachment and reattachment was realized in a new class of polymers with dynamic bonds, either through

reversible bonds or bond exchange reactions [31-33]. Macroscopically the network exhibits time-dependent mechanical behaviors, which was found to be well modeled by the approach with multiple natural configurations [28, 34]. Although these models are capable of incorporating the kinetics of dynamic bonds, they still rely on continuum level elasticity models, e.g. neo-Hookean, Arruda-Boyce or Gent model, to describe the mechanics of chains possessing different natural configurations [27-29, 35-36]. As a result, this approach does not provide a direct connection between single chain physics and macroscopic mechanics, and it would be difficult to extend such models to describe more complex molecular mechanisms such as entanglement and chain diffusion. In addition, computational implementation of this type of models can be challenging due to the large number of internal variables required to store chain populations and their respective natural configurations [37]. On the other hand, Tanaka and Edwards [24] developed a model for transient networks [38-39] that links the molecular physics of dynamic chains to the macroscopic mechanical behavior by tracking the evolution of microscopic distribution of chain end-to-end vectors. A rigorous continuum mechanics formulation of this approach in parallel to the 8-chain [9] or the full network model [10] for permanent networks is yet to be developed.

In this work, we introduce a theoretical framework for time-dependent responses of soft polymers that is deeply anchored on the statistical description of the underlying polymer network, based on a similar approach as that adopted by Tanaka and Edwards [24]. Within this framework, the physical state of the polymer is represented by a statistical distribution of the length and direction of chain end-to-end vectors. This distribution can be altered through both the macroscopic deformation and molecular-level events causing chain detachment and re-attachment. For simplicity, we illustrate this framework using an ideal network consisting of long chains with uniform length and dynamic cross-links. We assume that the single chain

behavior follows the entropic elasticity model with Gaussian statistics. Albeit simple, this ideal system closely resembles the 4-arm polyethylene glycol network with reversible metal-ligand cross-links recently developed by Grindy et al. [40] where highly uniform chain length can be achieved.

The manuscript is organized as follows. In Section 2, we first present a statistical description of the chain length and direction within the ideal network. Taking a thermodynamic approach, we then show in Section 3, that the network evolution can be linked to the stress tensor through the so-called distribution tensor, defined as a weighted average of the chain distribution. In Section 4, we show that our model degenerates to the neo-Hookean elastic model, the Maxwell-type viscoelastic model, and the Newtonian viscous fluid model under certain assumptions of the chain kinetics. Generalizations to multiple networks are also discussed. Section 5 highlights the differences between our model and similar models in the literature and the possible extensions of our model. Final conclusions are then provided in Section 6.

2. Statistical mechanics of a polymer chains with dynamic bonds

For the sake of simplicity, we here consider a polymer network made of linear chains that are connected to each-other at cross-linking sites. We are particularly interested in cross-links that display a dynamic response, i.e., they can associate and dissociate in time according to "on" and "off" rates, represented by the constants k_a and k_d, respectively, as shown in Fig. 1a. Figure 1b, on the other hand, illustrates a different type of dynamic bonds based on the bond exchange reactions where the dissociation of a connected chain and association of a new chain is completed in a single step of reaction. In this work, we attempt to describe the mechanical response of such a polymer from a statistical viewpoint.

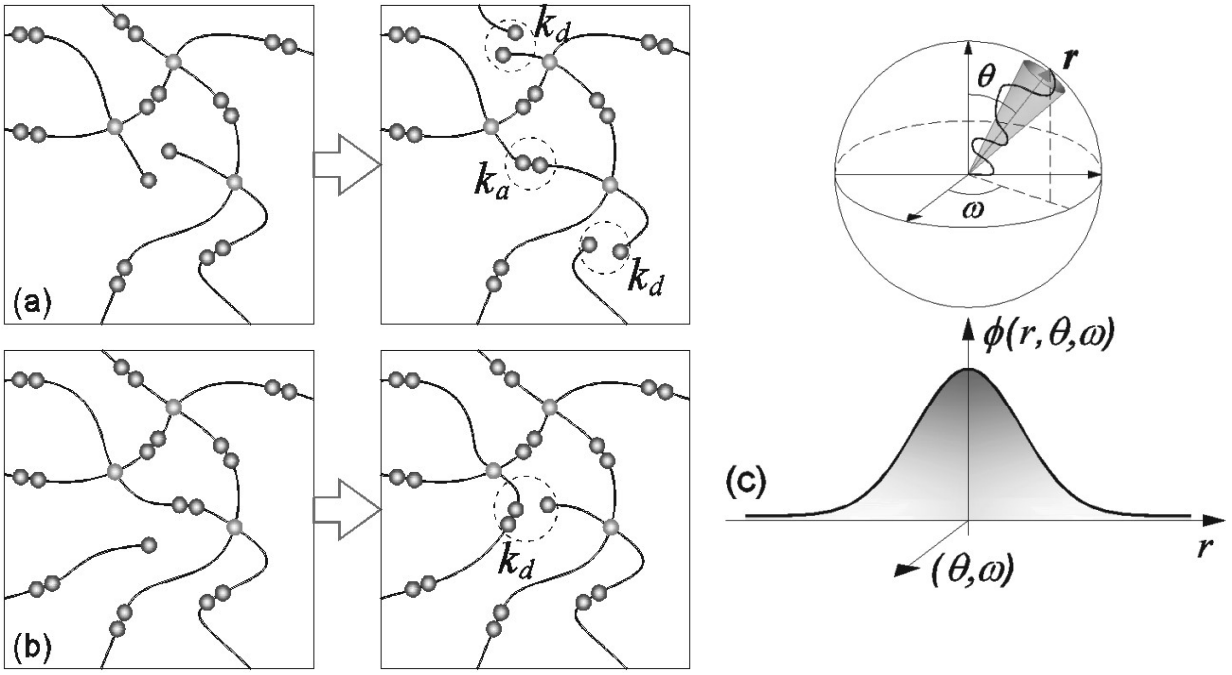

Figure 1. Schematic representation of dynamic bonds in a polymer network with reversible bonds (a) and bond exchange (b). (c) Graphical representation of a polymer chain with end-to-end vector $\boldsymbol{r} = \boldsymbol{r}(r,\theta,\omega)$ *and schematic of the distribution function* $\phi(r,\theta,\omega)$ *(Note that in this diagram, the symbol r represents the projection of the end-to-end vector)*

2.1 Statistical description of cross-linked polymer networks

When a polymer network is considered, the orientation of chains that form the network span all possible directions and the end-to-end distance must be replaced by the end-to-end vector that is characterized by both its direction (represented by angles θ and ω in spherical coordinates) and magnitude $r = |\boldsymbol{r}|$ (or end-to-end distance) as shown in Fig. 1c. The elasticity of the polymer may thus be understood through a statistical description of the end-to-end configuration of each polymer chain within a representative volume element. In this work, these statistics are captured by a distribution function $\phi(\boldsymbol{r}) = \phi(r,\theta,\omega)$ that allows us to precisely know the configuration of chains in the polymer according to their direction and end-to-end

distance. The probability function P, which represents the probability of a chain to have an end-to-end vector $\boldsymbol{r}$ can further be introduced by normalizing the distribution ϕ as follows:

$$\phi(\boldsymbol{r},t) = c(t)P(\boldsymbol{r},t) \quad \text{where} \quad c = \langle\phi\rangle \tag{1}$$

is the concentration of chains (moles of chains per unit current volume) that are connected to the network at both ends and the operator $\langle\blacksquare\rangle$ is the integral over all chain configurations:

$$\langle\blacksquare\rangle = \int_0^{2\pi}\int_0^{\pi}\left(\int_0^{\infty}\blacksquare r^2 dr\right) sin\theta d\theta d\omega \tag{2}$$

In the following, the energy state of the polymer will always be compared to its natural, or stress-free configuration. Following the standard statistical theory of elasticity, chains in the natural state are assumed to follow a Gaussian distribution around the value $\boldsymbol{r} = \boldsymbol{0}$. For an isotropic polymer, moreover, the chain distribution does not depend on the direction angles θ and ω, and the probability for a chain to have an end-to-end distance $\boldsymbol{r}$ is written as [7, 13]:

$$P_0(\boldsymbol{r}) = \left(\frac{3}{2\pi Nb^2}\right)^{\frac{3}{2}} exp\left(-\frac{3|\boldsymbol{r}|^2}{2Nb^2}\right) \tag{3}$$

where N is the number of Kuhn segments of a chain (assumed to be uniform across the network) and b is the Kuhn length. The distribution ϕ_0 of chains in their natural states can therefore be related to the function P_0 by:

$$\phi_0(\boldsymbol{r},t) = c(t)P_0(\boldsymbol{r}) \tag{4}$$

where we purposefully display the argument t to emphasize that c can change with time due to the chain detachment and attachment events. We note that this distribution function is interpreted as the number $dN = \phi_0(r)r^2 sin\theta dr d\theta d\omega$ of chains per unit current volume whose end-to-end distance is betwee $\boldsymbol{r}$ and $\boldsymbol{r} + d\boldsymbol{r}$ and orientation is between (θ,ω) and $(\theta + d\theta,\omega + d\omega)$.

2.2 Evolution of the chain distribution under deformation.

Let us now evaluate the change in chain distribution when the polymer is subjected to deformation. For this, we consider an arbitrary line element, originally represented by the vector $d\boldsymbol{X}$ that deforms into a new line $d\boldsymbol{x}$ following a linear mapping – represented by the deformation gradient $\boldsymbol{F}$ according to $d\boldsymbol{x} = \boldsymbol{F}d\boldsymbol{X}$**.** In particular, the rate of change $\dot{\boldsymbol{F}}$ of this deformation tensor can be related to the velocity gradient $\boldsymbol{L} = d\dot{\boldsymbol{x}}/d\boldsymbol{x}$ in the form:

$$\dot{\boldsymbol{F}} = \boldsymbol{L} \cdot \boldsymbol{F} \tag{5}$$

When such a deformation is applied to the polymer, chains are distorted such that their end-to-end vector changes from r to $\boldsymbol{r} + \Delta\boldsymbol{r}$ where $\Delta\boldsymbol{r}$ denotes the directional elongation of the chain. Consequently, the chain configuration described by the current chain distribution $\phi(\boldsymbol{r},t)$ evolves with time. Here, we seek to characterize this evolution based on the knowledge of the macroscopic deformation applied to the polymer. For this, we first note that the change in chain configuration is due to two competing mechanisms: (a) the application of a deformation that distorts each chain's end-to-end vector and (b) the detachment and reattachment of cross-links in different configurational states. The time derivative of $\phi(\boldsymbol{r},t)$is thus decomposed according to:

$$\frac{\partial\phi(\boldsymbol{r},t)}{\partial t} = \left.\frac{\partial\phi(\boldsymbol{r},t)}{\partial t}\right|_{xl} + \left.\frac{\partial\phi(\boldsymbol{r},t)}{\partial t}\right|_{\boldsymbol{F}} \tag{6}$$

The first term implies that the evolution of $\phi(\boldsymbol{r},t)$ occurs with no chain detachment and reattachment (the subscript "*xl*" indicates that the crosslinking density is fixed) while the second term represents the change in chain distribution when the deformation is frozen (fixed $\boldsymbol{F}$).

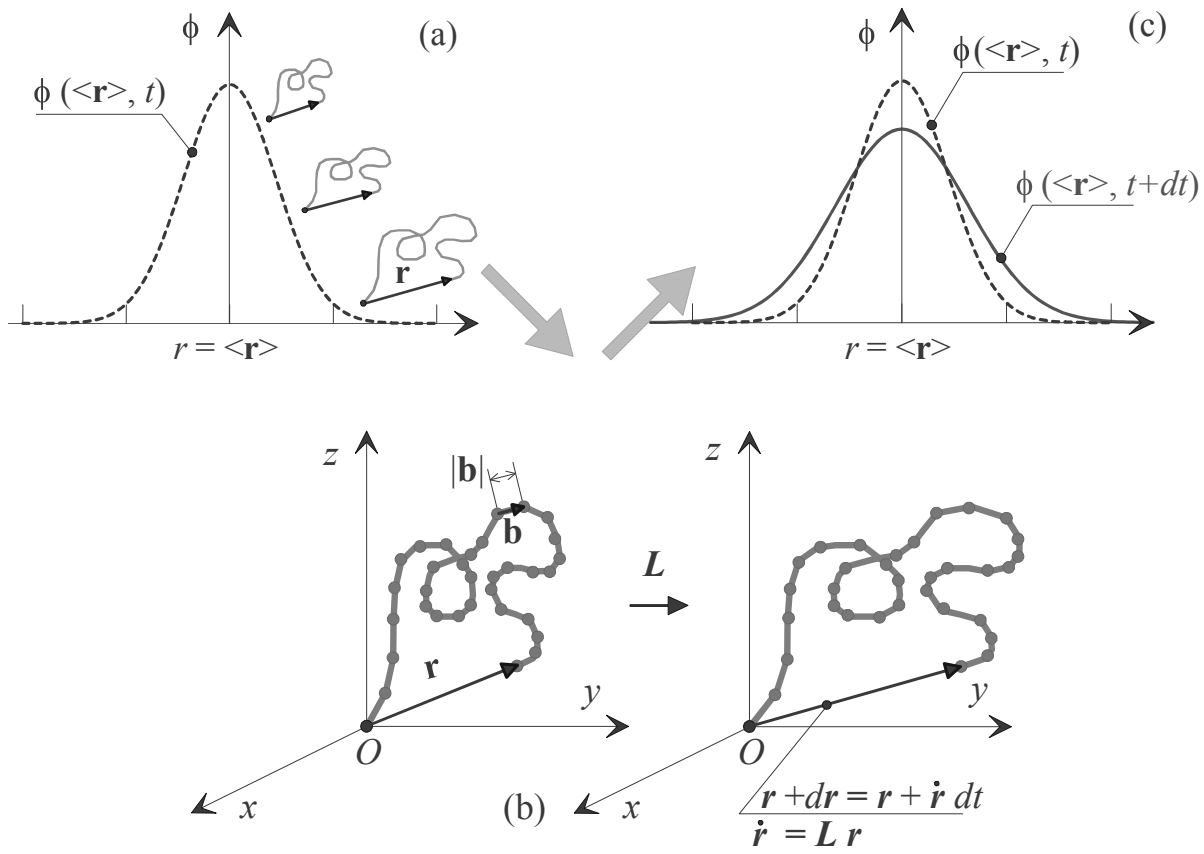

Figure 2. Example of the evolution of the chain distribution during an incremental deformation from t to t+dt represented by the velocity gradient $\boldsymbol{L}$*. The evolution of the distribution* ϕ *at a point is expressed by equation (5).*

To compute the first term, we adopt the affine deformation assumption where the end-to-end vectors of all chains evolve according to the continuum-level deformation gradient $\boldsymbol{F}$. For example, an end-to-end vector $\boldsymbol{r_0}$ before deformation is changed to $\boldsymbol{r} = \boldsymbol{F}\boldsymbol{r_0}$ after deformation (see Fig. 2). As a result, the space spanned by chain end-to-end vectors within a continuum point, referred to as the "chain space" hereafter, is distorted by the deformation gradient $\boldsymbol{F}$ experienced by that continuum point. The time derivative $\partial\phi(\boldsymbol{r},t)/\partial t|_{xl}$ in eq. (5) should be interpreted as

the spatial time derivative in the chain space. To derive how this term is related to the velocity gradient $\boldsymbol{L}$, we consider an arbitrary volume element $V*$ in the chain space and state that under a fixed set of cross-links, the "material time derivative" of the number of connected chains within $V*$ vanishes due to the incompressibility assumption. Here the concept of "material time derivative" is applied to the chain space (formed by the end-to-end vector $\boldsymbol{r}$), instead of the continuum-level physical space (formed by vector $\boldsymbol{X}$). Application of the Reynolds transport theorem in the chain distribution space leads to the following result:

$$\frac{D}{Dt}\int_{V*}\phi(\boldsymbol{r},t)dV=\int_{V*}\left.\frac{\partial\phi(\boldsymbol{r},t)}{\partial t}\right|_{xl}+\nabla_r\cdot(\phi(\boldsymbol{r},t)\dot{\boldsymbol{r}})dV=0 \tag{7}$$

where ∇_r denotes the spatial gradient in the distribution space, and $\dot{\boldsymbol{r}}$ is interpreted as the velocity of a point $\boldsymbol{r}$ in the distribution space**.** Because the distribution space is embedded within a single material point at the continuum level and we have assumed affine deformations, both the deformation gradient $\boldsymbol{F}$ and velocity gradient $\boldsymbol{L}$ can be considered uniform across the distribution space and the rate of chain's deformation becomes $\dot{\boldsymbol{r}}=\boldsymbol{L}\boldsymbol{r}$. Localizing eq. (7) and expanding the divergence term, we obtain,

$$\left.\frac{\partial\phi(\boldsymbol{r},t)}{\partial t}\right|_{xl}=-\left[\frac{\partial\phi(\boldsymbol{r},t)}{\partial r_i}r_j+\phi(\boldsymbol{r},t)\delta_{ij}\right]L_{ij} \tag{8}$$

where the Einstein convention on summation was used. The evolution of $\phi(\boldsymbol{r},t)$ at fixed deformation $\boldsymbol{F}$ can be found by assuming that the rate of detachment of chains with end-to-end vector $\boldsymbol{r}$ is proportional to $\phi(\boldsymbol{r},t)$ following eq. (1). Moreover, similarly to Tanaka and Edwards [24], we assume that these new chains reattach in a stress-free configuration, and thus their configuration is given by the probability function $P_0(\boldsymbol{r})$ shown in equation (3). These considerations yield the evolution law:

$$\left.\frac{\partial \phi(\boldsymbol{r},t)}{\partial t}\right|_{\boldsymbol{F}} = \xi_a P_0(r) - k_d \phi(\boldsymbol{r},t) \tag{9}$$

We see in eq. (9) that the dynamics of association and dissociation are governed by association and dissociation rates represented by the kinetic coefficients ξ_a and k_d, respectively, whose expression depends on the nature of the physical process at play. For a polymer with reversible bonds, the attachment and detachment mechanisms are decoupled and the rate of attachment becomes proportional to the density $c^d = c^t - c$ of detached chains where c^t is the total concentration of chains, including those that are not bonded. The corresponding association rate can therefore be expressed as:

$$\xi_a = k_a(c^t - c) \tag{10a}$$

where k_a is the kinetic coefficient for bond association. For a polymer with bond exchange reaction, an attachment event is immediately followed by a detachment event at a cross-link. This implies that the number of attached chains remains constant and the rate of attachment can be written:

$$\xi_a = \langle k_d \phi(\boldsymbol{r},t) \rangle \tag{10b}$$

Regardless of the mechanisms, the detachment kinetics may depend on external factors such as temperature or the presence of chemical species. Importantly, a force-dependent rate of dissociation is likely to occur, especially in the regime of large strains; for the coefficient k_d can be made a function of end-to-end distance, such that $k_d = k_d(\boldsymbol{r})$. The rate of attachment, however, concerns inactive (or detached) chains which should theoretically be insensitive to

strain. For this reason, it is taken as independent of the end-to-end vector $\boldsymbol{r}$ in the reminder of this study. Using eqs. (8) and (9), the evolution equation (6) for the distribution $\phi(\boldsymbol{r},t)$ finally becomes:

$$\frac{\partial \phi(\boldsymbol{r},t)}{\partial t} = \xi_a P_0(r) - \left[k_d(\boldsymbol{r}) + L_{ii}\right] \phi(\boldsymbol{r},t) - \frac{\partial \phi(\boldsymbol{r},t)}{\partial r_i} r_j L_{ij} \tag{11}$$

which is similar to the differential equation governing the evolution of chain distribution function in Tanaka and Edwards [24]. As the chain distribution evolves, the density of connected chains c may also change with time. By integrating eq. (11) throughout the chain space following eq. (2) and using the fact that $\langle \dot{\phi} \rangle = \dot{c}$ (see eq. (1a)), the time derivative of the concentration becomes:

$$\dot{c} = k_a\left(c^t - c\right) - \overline{k}_d c - c\, tr(\boldsymbol{L}) \tag{12a}$$

with $\overline{k}_d = \langle k_d(r) P(r,t) \rangle$ when reversible bonds are considered (eq. 10a), while

$$\dot{c} = - c\, tr(\boldsymbol{L}) \tag{12b}$$

when polymers with bond exchange reactions are considered (eq. 10b). Note that we consider incompressible polymers and the term $tr(\boldsymbol{L})$ vanishes in the above equations. Furthermore, if the rate constant k_d is independent of $\boldsymbol{r}$ (e.g. for small to moderate strains), we obtain the equality $\overline{k}_d = k_d$ since by definition, the integral of the probability function over the entire configurational space of chains is unity.

3. Macroscopic theory

So far, our description of the polymer evolution is purely statistical, but is related, via the assumption of affine chain deformation, to the macroscopic deformation gradient $\boldsymbol{F}$. In this

section, we will make a connection between this statistical view and classical quantities used in continuum mechanics such as stored elastic energy, entropy and the stress tensor. For this, it is convenient to start by invoking the first and second principle of thermodynamics and apply them to a volume element in the current configuration. In this element, the first principle implies that the material derivative of the internal energy density E_n (per unit current volume) can be expressed by:

$$\dot{E}_n = \boldsymbol{\sigma}:\boldsymbol{L} - \nabla \cdot \boldsymbol{q} + s \tag{13}$$

where $\boldsymbol{\sigma}$ is the Cauchy stress tensor in the volume element, $\boldsymbol{L}$ the velocity gradient, $\boldsymbol{q}$ the heat flux across its surface and s is the rate of external heat supply (per unit current volume). The Clausius-Duhem inequality enforcing the second principle of thermodynamics can further be written as:

$$\dot{\vartheta} \geq \frac{s}{T} - \nabla \cdot \left(\frac{\boldsymbol{q}}{T}\right) \tag{14}$$

where ϑ is the entropy per unit current volume and T is the absolute temperature. Introducing the Helmholtz free energy per unit current volume $\Psi = E_n - T\vartheta$, eqs. (13) and (14) yield the inequality:

$$\boldsymbol{\sigma}:\boldsymbol{L} - \dot{\Psi} - \dot{T}\vartheta - \frac{\boldsymbol{q}}{T} \cdot \nabla T \geq 0 \tag{15}$$

For convenience, let us consider an incompressible polymer and postulate that the stored elastic energy Ψ_e in the material volume can be computed as the sum of the stored energy in each active chain across their configurational space. If we call $\psi_c(\boldsymbol{r})$ the elastic energy in a single chain with end-to-end vector $\boldsymbol{r}$, the stored elastic energy Ψ_e can be written as:

$$\Psi_e = \langle \phi \psi_c \rangle + p(\det(\boldsymbol{F}) - 1) \tag{16}$$

where the term p represents the Lagrange multiplier enforcing the incompressibility condition, $\det(\boldsymbol{F}) = 1$. Following the freely jointed chain theory with Gaussian statistics [13] under the assumption that the number of Kuhn segments N in one polymer chain is large ($N >> 1$), we are able to express the elastic energy of a single chain as:

$$\psi_c(\boldsymbol{r}) = \frac{3k_BT}{2Nb^2}|\boldsymbol{r}|^2 = \frac{k_BT}{2}\tilde{r}^2 \tag{17}$$

where k_B is the Boltzmann constant, k_BT is the thermal energy and b is the Kuhn length. We further used the normalized distance defined as $\tilde{r} = |\boldsymbol{r}|/\boldsymbol{\ell}$ where $\ell = b\sqrt{N/3}$ is proportional to the projected mean end-to-end distance $b\sqrt{N}$ of individual chains. We note here that eq. (17) is only accurate for small to moderate chain extension. When extension is more severe, a Langevin chain model can be used to account for the strain stiffening arising from extensive chain stretch [13]. While such an energy functional could be considered here, the above form allows us to work with a simplified model and focus on other aspect of the theory, i.e., the time dependence of the cross-link attachment/detachment. A classical issue with the energy function defined in eq. (16) is that it does not vanish when the polymer is in a stress-free configuration. This can easily be seen by substituting the stress-free probability function eq. (4) into eq. (16). To avoid this, it is preferable to work with the energy difference $\Delta\Psi_e$ between the current state (with distribution $\phi(\boldsymbol{r},t)$) and the stress-free state (with distribution $\phi_0(\boldsymbol{r},t) = c(t)P_0(\boldsymbol{r})$). In this case, we can write:

$$\begin{aligned}\Delta\Psi_e(t) &= \Psi_e - \Psi_e^0 + p(\det(\boldsymbol{F}) - 1)\\ &= \langle(\phi - \phi_0)\psi\rangle + p(\det(\boldsymbol{F}) - 1)\\ &= \frac{ck_BT}{2}\langle(P - P_0)\tilde{r}^2\rangle + p(\det(\boldsymbol{F}) - 1)\end{aligned} \tag{18}$$

We will see below that this energy is implicitly a function of the deformation gradient $\boldsymbol{F}$ since the distribution evolves with applied strains. It is further entirely defined since the distribution $\phi(\boldsymbol{r},t)$ can be determined at any time from the evolution law in eq. (10) and the knowledge of the polymer configuration at the initial time.

3.1 Clausius-Duhem inequality

To apply the inequality in eq. (15), we add a term in eq. (18) to account for the change in Helmholtz free energy due to heat absorption, i.e.

$$\Psi = (\gamma - \vartheta_0)(T - T_0) - \gamma T \ln\frac{T}{T_0} + \Delta\Psi_e \tag{19}$$

where γ is the specific heat per unit volume, ϑ_0 is the entropy at the initial stress-free state and T_0 is the initial temperature. Because of the incompressibility assumption, we regard the volumetric specific heat γ as a constant. Taking the material time derivative of the Helmholtz free energy Ψ and using evolution equation (11), we can show that the change in stored elastic energy is (see appendix A.1 for details):

$$\dot{\Psi} = -\dot{T}\left(\gamma\, ln\left(\frac{T}{T_0}\right) + \vartheta_0\right) + p\, tr(\boldsymbol{L}) + \frac{k_B T}{2}\left\{2c[\boldsymbol{\mu} - \boldsymbol{\mu}_0]:\boldsymbol{L} + c\frac{\dot{T}}{T}\left(tr(\boldsymbol{\mu} - \boldsymbol{\mu}_0)\right)\right\} - \mathrm{D} \tag{20}$$

where the chain distribution tensor was defined as:

$$\boldsymbol{\mu} = \langle P\tilde{\boldsymbol{r}} \otimes \tilde{\boldsymbol{r}}\rangle \quad \text{and} \quad \boldsymbol{\mu}_0 = \langle P_0\tilde{\boldsymbol{r}} \otimes \tilde{\boldsymbol{r}}\rangle, \tag{21}$$

and the mechanical energy dissipation has the form:

$$\mathrm{D} = \frac{k_B T}{2}\left\langle k_d c(P - P_0)\tilde{r}^2 \right\rangle \tag{22}$$

Note here that if the rate of dissociation is not a function of chain extension, the dissipation can be rewritten as $\mathrm{D} = k_d \frac{c k_B T}{2} tr(\boldsymbol{\mu} - \boldsymbol{\mu}_0)$. From this expression, it is clear that the rate of

mechanical energy dissipation increases with both the dissociation rate and the stored elastic energy in the material. With these new quantities, inequality (15) takes the form:

$$\begin{aligned}&\left[\boldsymbol{\sigma}-ck_BT\left(\boldsymbol{\mu}-\boldsymbol{\mu}_0\right)-p\boldsymbol{I}\right]:\boldsymbol{L}+\\&-\dot{T}\left[\vartheta+\frac{ck_B}{2}\left(tr(\boldsymbol{\mu})-tr\left(\boldsymbol{\mu}_0\right)\right)-\gamma\ln\frac{T}{T_0}-\vartheta_0\right]+\ \mathrm{D}\ -\frac{\boldsymbol{q}}{T}\cdot\nabla T\geq 0\end{aligned}\tag{23}$$

This is a macroscopic representation of the Clausius-Duhem inequality, i.e., all quantities involved are defined at the continuum scale.

3.2 The chain distribution tensor

As seen above, the role of chain deformation is captured by the chain distribution tensor $\boldsymbol{\mu}$ defined in eq. (21), a key quantity of the proposed theory. It enables a macroscopic description of the state of the polymer chain network at any instant during the deformation process. In particular, it is of interest to explore the form of this tensor when the polymer network is in a stress-free state, i.e. the end-to-end distance follows the Gaussian distribution shown in eq. (2). Performing the integration, we find that:

$$\boldsymbol{\mu}^{\,0}=\left\langle P^0\tilde{\mathbf{r}}\otimes\tilde{\mathbf{r}}\right\rangle=\left(\frac{2\pi Nb^2}{3}\right)^{-\frac{3}{2}}\left\langle exp\left(-\tilde{r}^2/2\right)\tilde{\mathbf{r}}\otimes\tilde{\mathbf{r}}\right\rangle=\ \boldsymbol{I}\tag{24}$$

with $\boldsymbol{I}$ being the identity tensor. In other words, using eq. (21), the stored elastic energy (18) in the network can be directly related to the network statistics by the following equation:

$$\Delta\Psi_e=\frac{ck_BT}{2}tr(\boldsymbol{\mu}-\boldsymbol{I})+p(\det\left(\boldsymbol{F}\right)-1)\tag{25}$$

When it is not evaluated in a stress-free configuration, we see from its definition that the tensor $\boldsymbol{\mu}$ is represented by a symmetric matrix that can better be described by its three independent eigenvalues. Indeed, if we can express $\boldsymbol{\mu}$ in its principal directions to obtain:

$$\boldsymbol{\mu^d} = \boldsymbol{Q^T \mu\, Q}, \quad \text{in matrix form} \quad [\boldsymbol{\mu^d}] = \begin{bmatrix} \mu_1 & 0 & 0 \\ 0 & \mu_2 & 0 \\ 0 & 0 & \mu_3 \end{bmatrix} \tag{26}$$

where $\boldsymbol{Q}$ is the orthogonal matrix of change of basis between the global Cartesian frame and that associated with the principal directions of $\boldsymbol{\mu}$, while the components μ_1,μ_2 and μ_3 are the eigenvalues of the chain distribution tensor. A physical interpretation of these quantities is given by the standard deviation of the end-to-end distance component $\langle r_i^2 \rangle$ in the *i*-th principal direction, relative to the stress-free value $\langle r_i^2 \rangle = Nb^2/3$. In other words, we can write $\mu_i = 3\langle r_i^2 \rangle / Nb^2$. Conveniently, the distribution tensor can be represented by an ellipsoid with semi-axes μ_i and oriented along the principal direction of $\boldsymbol{\mu}$. This facilitates the visualization of the chain distribution at spatial material points during its deformation history as discussed later in this paper.

Interestingly, the distribution tensor contains the information of average chain stretch. To illustrate this point, we note that the trace of the distribution tensor can be computed as:

$$tr(\boldsymbol{\mu}) = \langle P\tilde{\boldsymbol{r}} \cdot \tilde{\boldsymbol{r}} \rangle = \langle P\tilde{\boldsymbol{r}}^2 \rangle = \frac{\overline{r^2}}{Nb^2/3} \tag{27}$$

In other words, the root mean square of the chain end-to-end distance $r_{rms} = \sqrt{\overline{r^2}}$ can be directly related to $tr(\boldsymbol{\mu})$ by:

$$r_{rms} = \sqrt{N} b \sqrt{\frac{tr(\boldsymbol{\mu})}{3}} \tag{28}$$

In addition, consider an arbitrary direction described by a unit vector $\boldsymbol{n}$, and denote the acute angle between a chain with this direction as θ ($0 \le \theta \le \pi/2$) (see Fig. 3a), also named as the chain angle in [41] and [42] we have

$$\boldsymbol{n} \cdot (\boldsymbol{\mu n}) = \left\langle \tilde{Pr}^2 cos^2(\theta) \right\rangle = \frac{\overline{(rcos\theta)^2}}{Nb^2/3} \ , \tag{29}$$

where $\sqrt{\overline{(rcos\theta)^2}}$ is the root mean square of $rcos\theta$. Based on this result, we define an effective average chain angle γ as

$$\gamma = arccos\left(\sqrt{\frac{\overline{(rcos\theta)^2}}{\overline{r^2}}}\right) = arccos\left(\sqrt{\frac{\boldsymbol{n} \cdot (\boldsymbol{\mu n})}{tr(\boldsymbol{\mu})}}\right). \tag{30}$$

Note that γ is not the direct average of chain angle, as defined in Yang et al. [41], but it also provides a measurement of average chain orientation. To illustrate this point, let us consider a special case where the bonds are permanent and the network is under uniaxial tension. We set $\boldsymbol{n}$ to be the direction of uniaxial tension, and the evolutions of effective average chain angle γ and the root mean square of chain stretch $\lambda_{rms} = r_{rms}/(\sqrt{N}b)$ with the nominal tensile strain $\lambda - 1$ are shown in Fig.3b. Also plotted in Fig. 3b are the average chain angle θ and stretch λ defined in Yang et al. [42]:

$$\overline{\theta} = \int_0^{\pi/2} tan^{-1}\left(\frac{1}{\lambda_1^{3/2}} tan\theta\right) sin\theta d\theta, \tag{31}$$

$$\overline{\lambda} = \int_0^{\pi/2} \sqrt{\left(\lambda_1 cos\theta\right)^2 + \lambda_1^{-1} sin^2\theta} sin\theta d\theta \tag{32}$$

Although the quantities γ and λ_{rms} are defined differently from $\overline{\theta}$ and $\overline{\lambda}$, they exhibit the same qualitative trends, i.e. on average the chains becomes stretched and also more aligned with $\boldsymbol{n}$.

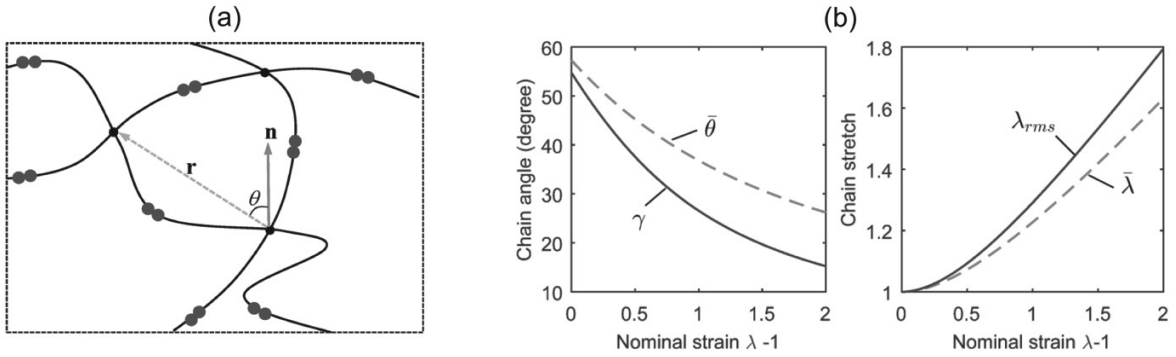

Figure 3. (a) Illustration of the chain end-to-end vector $\boldsymbol{r}$ *and the angle* θ *between a single chain and an arbitrary direction characterized by the unit vector* $\boldsymbol{n}$*. (b) Prediction of the averaged chain orientation* γ *for an elastic network (no dynamic bonds) under uniaxial tension, where the direction vector* $\boldsymbol{n}$ *is aligned with the tensile direction. This result is compared with the average chain angle* $\overline{\theta}$ *and chain stretch* $\overline{\lambda}$ *defined in eq. (31) and (32). Good qualitative agreement can be observed between the approaches.*

3.3 Stress tensor and entropy

Considering that each process (deformation, heat transfer and bond detachment/reattachment kinetics) occurs independently and assuming that the first two terms in eq. (23) vanish while the last two terms verify the inequality independently, we identify the Cauchy stress as:

$$\boldsymbol{\sigma} = ck_BT(\boldsymbol{\mu} - \mathbf{I}) + p\mathbf{I} \tag{33}$$

where we used the fact that in the stress-free state, $\boldsymbol{\mu}^{\mathbf{0}} = \mathbf{I}$. Similarly, the entropy ϑ is then found as:

$$\vartheta = \vartheta_0 + \gamma \ln \frac{T}{T_0} - \frac{ck_B}{2}(tr(\boldsymbol{\mu}) - 3) \tag{34}$$

The second term on the right-hand side of eq. (34) represents the change in entropy due to heat absorption, while the third term represents the change in the configurational entropy of chains. Note that $-k_B\tilde{r}^2/2$ is the entropy of a single chain, and thus $(ck_B/2)tr(\boldsymbol{\mu}) = (ck_B/2)\langle P\tilde{r}^2\rangle$ is the total entropy of all chains. The last two terms in eq. (23) describe the energy dissipation in the system and imply two inequalities. The first inequality, of the form:

$$\mathrm{D} \geq 0 \tag{35}$$

enforces that the mechanical energy dissipation remains positive. Physically, this statement implies that chain detachment is associated with a decrease in the stored elastic energy and that this loss is proportional to the rate of dissociation k_d and the stored elastic energy expressed in eq. (25)

$$-\frac{\boldsymbol{q}}{T} \cdot \nabla T \geq 0 \tag{36}$$

which eventually implies that the heat flux is written in a form of Fourier's law [43].

3.4 Evolution equation for the distribution tensor

We have seen that elastic energy, entropy and stress can be directly determined from the knowledge of the distribution tensor. It is however not clear yet how this quantity can be evaluated during a macroscopic deformation of the polymer. This can be done by integrating the evolution equation of the distribution function eq. (11) over the chains' configurational space following eq. (1b). After a long but straightforward calculation shown in Appendix A.2, we obtain the following evolution law for $\boldsymbol{\mu}$ (specific to the case of a polymer with reversible bonds whose kinetics follow eq. (10a)):

$$\dot{\boldsymbol{\mu}} = \frac{\xi_a}{c}\boldsymbol{\mu}^{\mathbf{0}} - \overline{\boldsymbol{k}}_d - \frac{\dot{c}}{c}\boldsymbol{\mu} + \mathbf{D}\boldsymbol{\mu} + \boldsymbol{\mu}\boldsymbol{D} \tag{37}$$

where the superscript T denotes the transpose operator and the weighted integral of the second moment of the dissociation rates in (37) is given by:

$$\overline{\boldsymbol{k}}_d = \left\langle k_d P\, \tilde{\mathbf{r}} \otimes \tilde{\mathbf{r}} \right\rangle \tag{38}$$

Finally, using eq. (10a) and (10b), we can write the evolution equation for the distribution tensor in the case of reversible bonds and bond exchange reaction, respectively as:

$$\dot{\boldsymbol{\mu}} = k_a\left(\frac{c^t - c}{c}\right)\boldsymbol{I} - \overline{\boldsymbol{k}}_d - \frac{\dot{c}}{c}\boldsymbol{\mu} + \boldsymbol{D}\boldsymbol{\mu} + \boldsymbol{\mu}\boldsymbol{D} \tag{39a}$$

$$\dot{\boldsymbol{\mu}} = \overline{k}_d\boldsymbol{I} - \overline{\boldsymbol{k}}_d + tr(\boldsymbol{L})\boldsymbol{\mu} + \boldsymbol{D}\boldsymbol{\mu} + \boldsymbol{\mu}\boldsymbol{D} \tag{39b}$$

where we recall that $\overline{k}_d = \langle k_d(r)P(r,t)\rangle$ and $tr(\boldsymbol{L}) = 0$ for incompressible materials. Together with the equation for concentrations (12a) and (12b), equations (39a) and (39b) form a set of coupled first order differential equation for c and $\boldsymbol{\mu}$ whose solution only requires the knowledge of initial conditions $c(t=0)$ and $\boldsymbol{\mu}(t=0)$ as well as the deformation history, represented by the velocity gradient $\boldsymbol{L} = \boldsymbol{L}(t)$. Assuming that the polymer is initially in a stress-free, equilibrium state, the initial conditions for the above two differential equations are: $\mathrm{c}(\mathrm{t}=0) = \mathrm{c}^0$ and $\boldsymbol{\mu}^0(t=0) = \boldsymbol{\mu}^0 = \boldsymbol{I}$. The solution to eq. (39) depends on the form of the relation $\overline{\boldsymbol{k}}_d = \overline{\boldsymbol{k}}_d(\boldsymbol{\mu})$. In this work, we assume that the rate of dissociation k_d is independent of chain length and orientation (i.e., k_d is constant). Using this assumption in eq. (38) yields the simple form:

$$\overline{\boldsymbol{k}}_d = k_d\langle P\, \tilde{\mathbf{r}} \otimes \tilde{\mathbf{r}}\rangle = k_d\,\boldsymbol{\mu} \tag{40}$$

and $\overline{k}_d = k_d$. In this case, eq. (39) becomes a linear differential equation for $\boldsymbol{\mu}$.

3.5 Illustration

We now aim to illustrate the prediction of the above theory by considering the homogeneous deformation, network evolution and mechanical response of a cubic element of polymer. Over a period of time t, the cube is assumed to undergo a series of shear and tensile deformation illustrated in Fig. 4 and more accurately specified as follows. Between 0 and $\tau/20$, the cube is first subjected to a shear deformation into a diamond-shape characterized by a final deformation gradient $F_{12} = 1$ (all other components unchanged). The cube is then let to rest for a period 0.3τ until a tensile deformation is applied quickly during a period $\tau/20$ up to a deformation gradient $F_{22} = 2$ (all other components unchanged). The specimen relaxation is then evaluated for the remainder of the time. For this virtual experiment, we considered a transient network characterized by normalized rates $k = k_a\tau = k_d\tau = 0.07$ and the steady state polymer concentration is taken as unity.

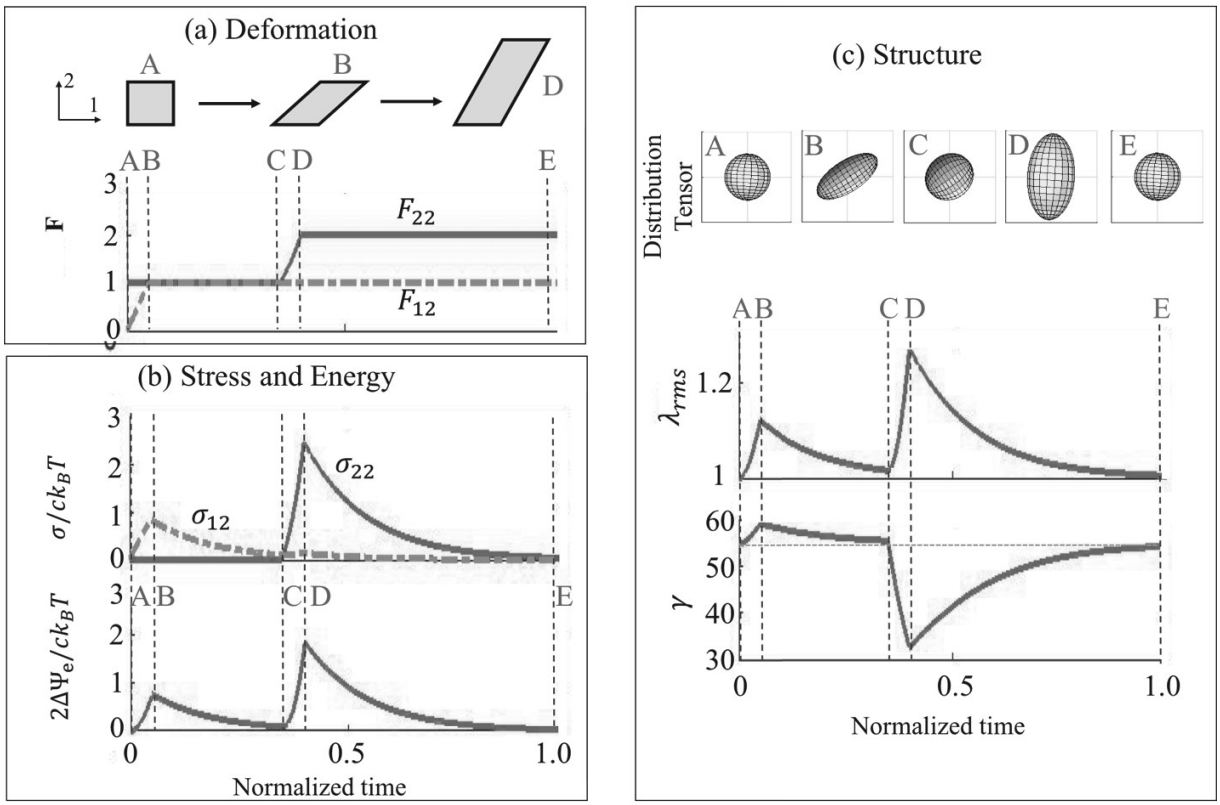

Figure 4. Illustration of (a) the deformation, (b) stress and stored elastic energy and (c) chain statistic response of a polymer characterized by a single network that displays normalized rates $k = k_a\tau = k_d\tau = 0.07$. *Stresses are normalized by* ck_BT *and energies by* $ck_BT/2$. *The polymer structure is characterized by the 3D representation of the distribution tensor, the normalized root mean square end-to-end distance* $\lambda_{rms} = r_{rms}/\sqrt{N}b$ *and the effective average chain angle* γ *with the vertical direction (*$\boldsymbol{n} = [0,1]$ *in the Cartesian coordinate system). Time is expressed in units of* τ.

Fig. 4a presents the evolution of the deformation (components F_{12} and F_{22}), together with the deformation of the corresponding cube. The characteristic times at which the deformation is applied are referred by 5 points (A-E), A being the initial state. The mechanical

response of the material is then characterized by the normalized Cauchy stress (components σ_{12} and σ_{22}) and the overall stored elastic energy $\Delta\Psi_e$ (Fig. 4b) while the evolution of polymer structure is captured by a graphical representation of the distribution tensor $\boldsymbol{\mu}$ over time. This tensor is represented by three quantities: its overall ellipsoidal form as discussed in section 3.2, the normalized root mean square end-to-end distance $r_{rms}/\sqrt{N}b$ (eq. (28)) and the effective average chain angle γ with the vertical direction ($\boldsymbol{n} = [0,1]$) as expressed in eq. (30). We observe via the distribution tensor, that a quickly applied deformation changes the chain's end-to-end distance in directions of maximum stretch. We specifically see that the angle between the chains and the vertical direction increases under shear (from A to B) but significantly decrease under stretch (from C to D) from their isotropic angle $\gamma_{\text{iso}} \approx 55^o$. However, when the deformation is held for some time, the cross-links are allowed to detach and reattach in order for the chains to reconfigure in states that are closer to their stress-free configuration. Eventually, this means that the distribution converges to its stress-free value $\boldsymbol{\mu}^0 = \boldsymbol{I}$, represented by a sphere in the figure and by a chain end-to-end distance $\bar{r}/\sqrt{N}b = 1$ and orientation $\gamma = \gamma_{\text{iso}}$. As stretched chains detach and reattach in stress-free configuration, the internal stresses relaxes over time. This phenomenon can be seen in the drop in the stored elastic energy over time and the stress relaxation whose characteristic time is set by the bond kinetics. Overall, this material response is therefore similar to that predicted by the Maxwell model (viscoelastic fluid), represented by a spring and a dashpot in series.

Experimental observations of such stress relaxation and plastic deformation caused by dynamic bonds have been reported in the literature. A representative example is a polymer network, i.e. vitrimer, with heat activated bond exchange reactions. It was shown in Montarnal et

al. [44] (e.g. see Fig. 2 of their paper) that the network can undergo complete stress relaxation under a prescribed deformation. Upon removal of the applied constraint, the polymer is able to maintain the prescribed deformation permanently.

4. Special cases and extension to complex networks

A key advantage of the above theory is that it provides a clear relationship between the kinetics of dynamic bonds, the statistical evolution of the entire network (through the tensor $\boldsymbol{\mu}$) and the overall macroscopic response of the polymer (through the stress tensor $\boldsymbol{\sigma}$). In this section, we investigate how this framework compares to other classical theories that describe the behavior of elastic rubbers (permanent networks), viscoelastic polymers (networks with slow kinetics) and viscous fluid (networks with fast kinetics). We also explore the more general case where the dynamic bond kinetics is characterized by a more complex response in which a spectrum of relaxation time scales can be observed. For this, we describe a route by which to incorporate multiple networks into the formulation, each characterized by their own relaxation time.

4.1 Permanent networks

The evolution of a polymer with permanent cross-links is described by a particular case of the evolution law eq. (11) in the case where $k_a = 0$ (no attachment of new chains over time) and $k_d = 0$ (no chain detachment over time). In this case, the overall concentration c_S of cross-link remains constant and eq. (39) degenerates to the simpler form:

$$\dot{\boldsymbol{\mu}}_s = tr(\boldsymbol{L})\boldsymbol{\mu}_s + \boldsymbol{D}\boldsymbol{\mu}_s + \boldsymbol{\mu}_s\boldsymbol{D} \tag{41}$$

The solution of this tensorial differential equation has the form $\boldsymbol{\mu}_s = J\boldsymbol{F}\boldsymbol{F}^{\mathrm{T}}$ where the deformation gradient **F** (related to the velocity gradient by $\dot{\boldsymbol{F}} = \boldsymbol{L}\boldsymbol{F}$) describes the mapping between the deformed network and its stress-free configuration and $J = \det(\boldsymbol{F})$. In other words, for a purely elastic material, the chain distribution tensor coincides with the left-Cauchy strain tensor $J\boldsymbol{B} = J\boldsymbol{F}\boldsymbol{F}^{\mathrm{T}}$. Using this result, eq. (25) can be rewritten in the more conventional form:

$$\Delta\Psi_e = \frac{c_S k_B T}{2} J tr\left(\boldsymbol{F}\boldsymbol{F}^{\mathrm{T}} - \boldsymbol{I}\right) + p(\det(\boldsymbol{F}) - 1) \tag{42}$$

In other words, in the absence of dynamic bonds, the stored elastic energy degenerates to that predicted by the neo-Hookean model in classical rubber elasticity [4, 11] and the Cauchy stress expressed in eq. (33) becomes:

$$\boldsymbol{\sigma}_s = c_S^0 k_B T\left(\boldsymbol{F}\boldsymbol{F}^{\mathrm{T}} - \boldsymbol{I}\right) + p\boldsymbol{I} \tag{43}$$

Where the quantity $c_S^0 = J c_S$ is the nominal concentration, defined per unit reference volume of the dry polymer in agreement with the early work of Treloar [45] and Kuhn and Grun [46]. From eq. (43), it is clear here that when the deformation vanishes, the deformation gradient becomes $\boldsymbol{F} = \boldsymbol{I}$ and the first term on the right-hand side has no contribution. The remaining term p plays the role of a pressure enforcing the material's incompressibility, such that the hydrostatic pressure is $p^h = \frac{1}{3} tr(\boldsymbol{\sigma}_s) = c_S^0 k_B T\left(tr\left(\boldsymbol{F}\boldsymbol{F}^{\mathrm{T}}\right)/3 - 1\right) + p$.

4.2 Relation to standard viscoelasticity

To explore how the statistically-based continuum theory degenerates to standard viscoelasticity, we first make the assumption that the kinetic coefficient k_d is independent of the stretch/force on each individual chain. In this case, we have seen that:

$$\overline{k}_d = k_d \quad \text{and} \quad \overline{\overline{\boldsymbol{k}}}_d = k_d \boldsymbol{\mu} \tag{44}$$

Let us further assume the density of active cross-link density c has achieved a steady state ($\dot{c} = 0$). From eq. (12) this steady state is:

$$c = \frac{k_a}{k_a + k_d} c^t \tag{45}$$

In this case, the evolution equation for the distribution moment degenerates to the simpler form:

$$\dot{\mu} = k_d(\boldsymbol{I} - \boldsymbol{\mu}) + D\mu + \mu D \tag{46}$$

Now using identity that $D\mu + \mu D = L\mu + (L\mu)^T$, and the fact that the velocity gradient $\boldsymbol{L}$ can be expressed in terms of the deformation gradient tensor $\boldsymbol{F}$ by $\boldsymbol{L} = \dot{\boldsymbol{F}}\boldsymbol{F}^{-1}$, eq. (45) becomes:

$$\dot{\boldsymbol{\mu}} = k_d(\boldsymbol{I} - \boldsymbol{\mu}) + \dot{\boldsymbol{F}}\boldsymbol{F}^{-1}\boldsymbol{\mu} + \boldsymbol{\mu}^T\boldsymbol{F}^{-T}\dot{\boldsymbol{F}}^T \tag{47}$$

Defining $\boldsymbol{A} = \boldsymbol{F}^{-1}\boldsymbol{\mu}\boldsymbol{F}^{-T}$, the above equation can finally be rewritten as a first-order ordinary differential equation which can be analytically solved:

$$\dot{\boldsymbol{A}} + k_d\boldsymbol{A} = k_d\boldsymbol{F}^{-1}\boldsymbol{F}^{-T} \tag{48}$$

The initial condition is $\boldsymbol{A}(t = 0) = \boldsymbol{I}$ since initially both $\boldsymbol{\mu}$ and $\boldsymbol{F}$ are identity tensors. The general solution of eq. (48) is [47].

$$\boldsymbol{A} = e^{-k_d t}\boldsymbol{I} + \int_0^t k_d\boldsymbol{F}^{-1}(\tau)\boldsymbol{F}^{-T}(\tau)e^{-k_d(t-\tau)}d\tau \tag{49}$$

Therefore, the general solution of the distribution tensor $\boldsymbol{\mu}$ is:

$$\boldsymbol{\mu}(t) = e^{-k_d t}\boldsymbol{F}(t)\boldsymbol{F}^T(t) + \int_0^t k_d[\boldsymbol{F}(t)\boldsymbol{F}^{-1}(\tau)\boldsymbol{F}^{-T}(\tau)\boldsymbol{F}^T(t)]\, e^{-k_d(t-\tau)}d\tau \tag{50}$$

To illustrate how the theory degenerates to standard viscoelasticity, let us take the particular case of the uniaxial tension of a polymer specimen along the x_1 direction. In this context, the non-vanishing terms of $\boldsymbol{F}$ are $F_{11} = \lambda$, and $F_{22} = F_{22} = \lambda^{-1/2}$. In addition, if we assume small deformation, the stretch ratio takes the form $\lambda(t) = 1 + \varepsilon(t)$ where ($\varepsilon \ll 1$) is the linearized unidirectional strain. The tensile stress can be written in the following form (see Appendix A.2)

$$\frac{\sigma_{11}(t)}{ck_bT} = 3\int_{-\infty}^{t} e^{-k_d(t-\tau)}\frac{d\varepsilon}{d\tau}d\tau \tag{51}$$

If we set $E_0 = 3ck_BT$ as the instantaneous Young's modulus and $E(t) = E_0\, e^{-k_d t}$ is the relaxation modulus, then eq. (51) can be written as

$$\sigma_{11}(t) = \int_{-\infty}^{t} E(t-\tau)\frac{d\varepsilon}{d\tau}d\tau \tag{52}$$

This expression is consistent with linear viscoelasticity, specifically a Maxwell model given the form of $E(t)$. We finally note that since the mechanical loading starts at $t = 0$ and we allow an instantaneous application of strain, eq. (52) can also be written as

$$\sigma_{11}(t) = E(t)\cdot\varepsilon\left(t = 0^{+}\right) + \int_{0^{+}}^{t} E(t-\tau)\,\frac{d\varepsilon}{d\tau}d\tau \tag{53}$$

The above derivation shows that our model degenerates to the Maxwell model under the assumption of constant kinetic parameters k_d and small deformation. This indicates that under a fixed strain, the stress would decay exponentially with time and the characteristic decay time is governed by the dynamic bond kinetics (e.g. the coefficient k_d). Such exponential stress

relaxation has been observed in a number of previous studies on networks with bond exchange reactions [27, 42, 44].

To further test our model against experimental data, we note that our assumption of uniform kinetic coefficients k_d and k_a requires a homogeneously structured network, otherwise the polymer may exhibit a spectrum of relaxation times. This was achieved in a recently developed hydrogel with 4-arm polyethylene glycol (PEG) units with reversible metal ligand crosslinks [40, 48-49]. The time-dependent mechanical behaviors of such gels due to the dynamic metal ion crosslinks were measured by frequency-sweep rheological tests at small shear strains (e.g. 1% for the data in Fig. 5a,b). Because of the homogeneous network structure, we expect our result in this section is applicable to this type of gel, i.e. the rheological data can be well captured by the Maxwell model. This is indeed the case as shown in Fig. 5. According to the Maxwell model, the storage and loss modulus $G^{'}$ and $G^{''}$ are

$$G^{'} = G_0 \frac{t_R^2 \Omega^2}{1 + t_R^2 \Omega^2}, \quad G^{''} = G_0 \frac{t_R^2 \Omega}{1 + t_R^2 \Omega^2} \tag{54}$$

where G_0 is the instantaneous shear modulus, t_R is the characteristic relaxation time and Ω is the angular frequency of the oscillatory rheological test. In our case,

$$G_0 = ck_BT\,, \text{ and } \quad t_R = \frac{1}{k_d} \tag{55}$$

Figure 5ab show the experimental data of $G^{'}$ and $G^{''}$ extracted from Grindy et al. [40] for two different gels with distinct metal ion crosslinks, i.e. Ni^{2+} and Cu^{2+}, as well as the fit of our model. Overall the Maxwell model well captures the experimental data. For the Ni^{2+} based gel, we found $G_0 = 18.621\ kPa$ and $t_R = 6.2\ s$, while for the Cu^{2+} based gel, $G_0 = 8.318\ kPa$ and t_R

$= 1.12 \times 10^{-3}\ s$. Interestingly, the values of G_0 for the Ni^{2+} and Cu^{2+} based gels are quite different, even though the molar concentration of the 4-arm PEG units is the same in the two gels: $0.01\ mol/L$, which implies a total chain density of $0.02\ mol/L$ or $c^t = 1.204 \times 10^{22}\ /L$, since on average each 4-arm PEG unit can contribute 2 chains to the network. This is because the modulus G_0 is proportional to the density of active chains c, instead of total chain density c^t. Using the value of c^t, temperature $T = 278\ K$ (5°C reported in Grindy et al. [40]), and eqs. (45) and (54), we are able to determine that for the Ni^{2+} based network, $k_d = 0.1613\ s^{-1}$ and $k_a = 0.1044\ s^{-1}$ and for the Cu^{2+} based network, $k_d = 892.9\ s^{-1}$ and $k_a = 190.2\ s^{-1}$. This shows that the kinetics of Cu^{2+} crosslinks is much faster than that of Ni^{2+} crosslinks. In Fig.5cd, we show additional rheological data from a different paper by Tang et al. [49] for a class of 4-arm PEG gels with Zn^{2+} crosslinks. The chemical composition of the metal-ligand crosslink is different from that of Gindy et al. [40] but the gel network structure is similar. By fitting the $G^{'}$ and $G^{''}$ data using the Maxwell model, we obtain $G_0 = 9.536\ kPa,\ 20.38\ kPa,\ 27.53\ kPa,\ 52.68\ kPa$, and $t_R = 0.47\ s, 0.51\ s, 0.51\ s, 0.59\ s$ for gels with polymer concentration (w/v) of 10%, 15%, 20%, 30%, respectively. Note that G_0 increases with polymer concentration, while t_R is insensitive to polymer concentration. In Fig. 5b and 5d, deviations between the Maxwell model fit and experimental data can be seen at high frequency. The discrepancy has been attributed to additional relaxation mechanisms other than the dynamic metal-ligand crosslinks in Grindy et al. [48], e.g. due to the sticky Rouse mode [49]. The exact nature of such deviation remains to be elucidated.

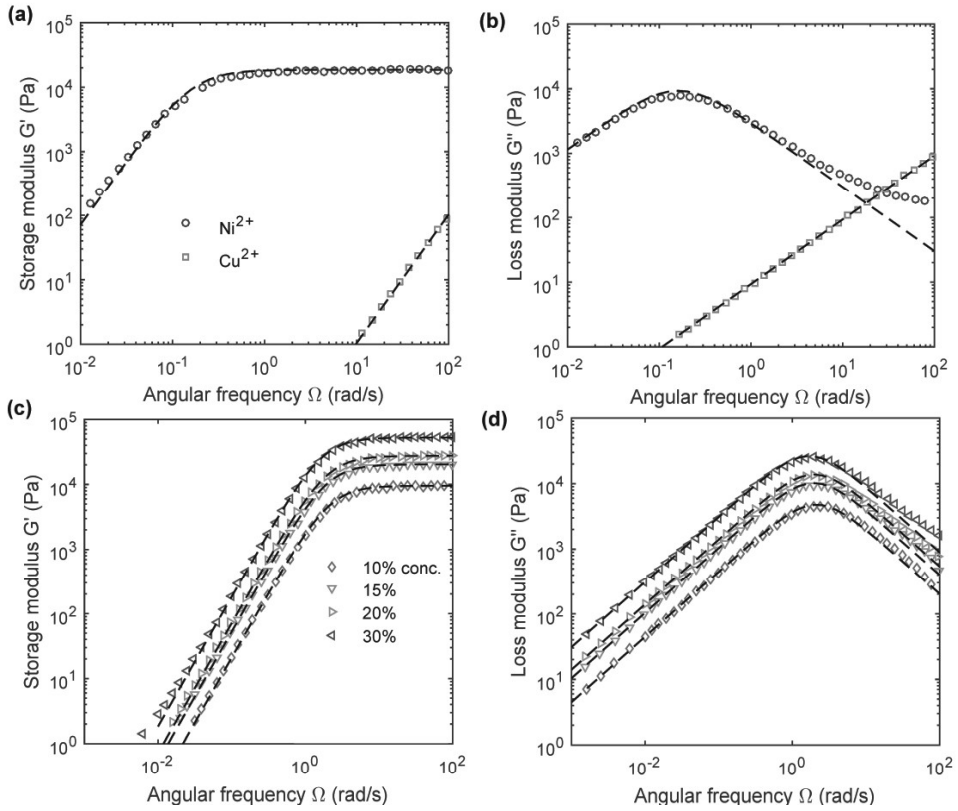

Figure 5. Comparison with rheological data in the literature for 4-arm PEG hydrogels with reversible metal-ligand cross-links. (a-b) Frequency dependence of storage and loss modulus for the PEG hydrogels with two different metal crosslinks: Ni^{2+} and Cu^{2+} [40]. (c-d) Frequency dependence of storage and loss modulus for a Zn^{2+} crosslinked PEG hydrogel with different polymer concentrations (w/v): 10%, 15%, 20% and 30% [49]. The symbols represent experimental data extracted from literature and the dashed lines represent fits by the Maxwell model.

The Maxwell model also implies plastic deformation, and such material is typically referred to as a viscoelastic fluid or viscoplastic solid. This is consistent with the illustrative example in Fig. 4 which shows that the dynamic bonds allow the network to gradually approach a relaxed state under a fixed deformation. As a result, the polymer would not recover its original shape after loading is removed. However, unlike conventional materials (e.g. viscoelastic polymer melts) where the molecular mechanisms for relaxation are complex and the Maxwell model is

phenomenological in nature, here we have derived the Maxwell model from our statistical framework of transient networks, thanks to the relatively simple relaxation mechanism of dynamic bonds. The Maxwell fits of rheological data for the 4-arm PEG gels, as shown in Fig.5, have already been performed in the literature [48-49]. The contribution of our approach is to provide a clear physical picture as to under what circumstances the Maxwell model works well, and to allow molecular interpretation of the material parameters G_0 and t_R.

4.3 Viscous fluid

The case of a perfectly viscous and incompressible fluid may be recovered in two conditions: (a) there are no permanent cross-links and (b) both attachment and dissociation occur at a rate that is much faster than the rate of loading. In this case, the cross-links are in a state of dynamic equilibrium i.e. $\dot{c} = 0$, from eq. (11b) and $\dot{\boldsymbol{\mu}} \approx 0$. Assuming k_d to be independent of load, eq. (40) implies that $\overline{\boldsymbol{k}}_d = k_d\boldsymbol{\mu}$ and eq. (39b) becomes:

$$k_d(\boldsymbol{I} - \boldsymbol{\mu}) + \boldsymbol{D\mu} + \boldsymbol{\mu D} = \boldsymbol{0} \tag{56}$$

Now using the fact that the rate of deformation is slow compared to the gel dynamics, i.e. $|\mathbf{D}|/\mathrm{k_d} \ll 1$, a first order perturbation analysis yields $\mu \approx \mathrm{I} + 2\mathrm{D}/\mathrm{k_d}$, and therefore the stress equation (33) becomes:

$$\boldsymbol{\sigma} = ck_BT(\boldsymbol{\mu} - \boldsymbol{I}) + p\boldsymbol{I} = \frac{2ck_BT}{k_d}\boldsymbol{D} + p\boldsymbol{I} \tag{57}$$

where we used the fact that $c^0 = c$ since the cross-link concentration is constant in time. This corresponds to the constitutive relation for a Newtonian fluid, where the Cauchy stress is related to the rate of deformation $\boldsymbol{D}$ via a viscosity parameter:

$$v = \frac{2ck_BT}{k_d} = \frac{2k_BTc^t}{k_d}\left(\frac{k_a}{k_d + k_a}\right) \tag{58}$$

We generally see that the apparent viscosity increases with the number of available cross-links c^t and decreases with the rate k_d of crosslink detachment [50].

4.4 Generalization to multiple networks

As discussed above, more general polymers display a variety of characteristic relaxation times and would be better modeled as multiple networks. Literature has also shown that in many cases, polymers possess a permanent network in addition to its transient counterpart [28]. These considerations can be easily incorporated in an additive multiple network model shown here. For this, let us first assume that a polymer is represented by a series of N non-interacting networks, denoted by the index $I = 1,..., M$, and associated with their own chain concentration c_I and dynamic bond kinetics k_a^I and k_d^I (assumed to be constants for each network). In addition, the polymer is assumed to possess a permanent network with concentration c_S. In these conditions, the network statistics are represented by M distribution functions P^I and distribution tensors defined as:

$$\boldsymbol{\mu}^I = \langle P^I \tilde{\mathbf{r}} \otimes \tilde{\mathbf{r}} \rangle \tag{59}$$

The evolution equation for the cross-link concentration and the chain distribution is given by:

$$\dot{c}_I = k_a^I\left(c_I^t - c_I\right) - k_d^I c_I \tag{60}$$

and the distribution tensor by:

$$\dot{\boldsymbol{\mu}}^I = \frac{\xi_a^I}{c^I}\boldsymbol{I} - \overline{\boldsymbol{k}}_d^I - \frac{\dot{c}^I}{c^I}\boldsymbol{\mu} + \boldsymbol{D}\boldsymbol{\mu}^I + \boldsymbol{\mu}^I\boldsymbol{D} \tag{61}$$

Upon calculating these quantities, the total chain concentration can then be calculated as:

$$c = c_S + \sum_{I=1}^{M} c_I \tag{62}$$

and an overall distribution tensor $\boldsymbol{\mu}$ representing the entire network can be defined such that:

$$c\,\boldsymbol{\mu} = \mathrm{c}_S J\boldsymbol{F}\boldsymbol{F}^{\mathrm{T}} + \sum_{I=1}^{M} c_I\boldsymbol{\mu}^I \tag{63}$$

Because the networks do not interact, the stored elastic energy can be additively decomposed in the form:

$$\Delta\,\Psi_e(t) = \frac{k_B T}{2}\left[\, c_S J tr\left(\boldsymbol{F}\boldsymbol{F}^{\mathrm{T}} - \boldsymbol{I}\right) + \sum_{I=1}^{M} c^I tr(\boldsymbol{\mu}^I - \boldsymbol{I}) \,\right] + p(\det(\boldsymbol{F}) - 1) \tag{64}$$

Using the overall concentration and distribution, this can also be written:

$$\Delta\Psi_e(t) = \frac{ck_B T}{2} tr[\,\boldsymbol{\mu} - \boldsymbol{I}] + p(\det(\boldsymbol{F}) - 1) \tag{65}$$

and the Cauchy stress tensor follows directly from eq. (33), with the difference that the distribution tensor is for multiple networks.

4.5 Illustration of a two-network model

For illustration purposes, we consider here the same virtual experiment as discussed in Section 3.4 but now assume that the polymer possesses a permanent network in addition to a dynamic counterpart considered earlier, with concentration $c_S = c$. Fig. 6 shows the theoretical predictions of the stress and energy relaxation as well as the statistical evolution of the two

networks. While most of the discussion parallels that provided in Section 3.5 regarding the dynamic network, we see that the distribution tensor, average chain end-to-end distance and chain orientation of the permanent network only changes with the deformation steps, but does not tend to relax back to a stress-free isotropic state. This is expected since chains are unable to reorganize when permanent cross-links are considered. There is therefore a clear contrast between the chain evolution (end-to-end distance and orientation) of the static and dynamic network (Fig. 6c). Indeed, when a fast deformation is applied, the chain configuration in both network react immediately and in a similar fashion since the rate of deformation is significantly higher than the bond kinetics. However, during the relaxation phase, we see that chains in the dynamic network tend to decrease their average end-to-end distance and become more uniformly distributed ($\theta \rightarrow \theta_{iso}$). The static network is however unable to reconfigure and the chains remain in their stretched configuration. A consequence is that while the stored elastic energy in the dynamic network relaxes to zero, that in the permanent network remains constant for a fixed deformation. An elastic stress therefore exists regardless of the bond dynamics of the transient polymer. In summary, it can therefore be seen that in contrast to the previous example, this double-network only possesses a single stress-free state, which occurs when the $\boldsymbol{F} = \boldsymbol{I}$. In other words, while the material shown in Fig. 4 would maintain the deformed shape once the applied load is removed, the existence of a permanent network gives the present material the ability to gradually creep back to its original shape. This behavior is similar to that predicted by the standard linear solid model where a spring is in parallel to a Maxwell model.

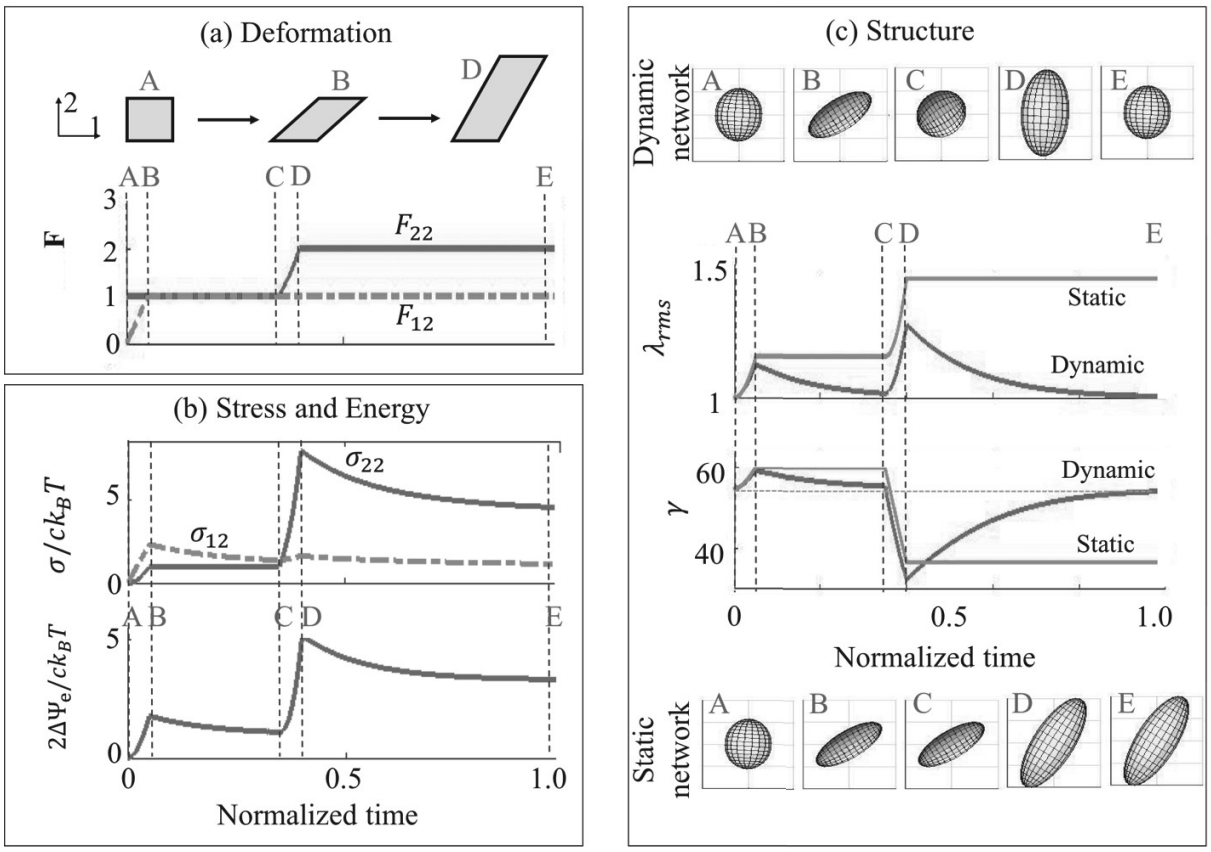

Figure 6. Illustration of (a) the deformation, (b) stress and stored elastic energy and (c) chain statistic response of a polymer characterized by one permanent network and one dynamic network that displays normalized rates $k = k_a\tau = k_d\tau = 0.07$. *The relative concentrations* c_S *and c of the permanent and dynamic network, respectively are chosen such that* $c/c_S = 1$ *Stresses are normalized by* $c_S k_B T$ *and energies by* $c_S k_B T/2$. *The structure of each network is characterized by the 3D representation of the distribution tensor, the averaged normalized end-to-end distance* $\lambda_{rms} = r_{rms}/\sqrt{N}b$ *and the average chain angle* γ *with the vertical direction (*$\boldsymbol{n} = [0,1]$ *in the Cartesian coordinate system). Time is expressed in units of* τ.

5. Further discussion

The main contribution of this paper is that our statistical approach illustrates the essential molecular picture that underlies viscoelasticity of soft polymers. This approach allows one to leverage developments in the polymer physics literature to incorporate more complex molecular mechanisms, which may open the door to physics-based nonlinear viscoelastic models. Such models are of fundamental value to many mechanics questions, one example being the fracture of viscoelastic rubbers [51-53]. As pointed out by Knauss [54], one of the limiting factors that hinder further understanding of soft polymer fracture is the lack of an accurate and physics-based nonlinear viscoelastic model.

A number of theories, starting from classical rubber elasticity, attempt to relate the statistical description of polymer chains or fibrous networks to the elastic response of the assembly [1, 9-10, 55]. Such approaches implicitly separate the directional dependence of the chains (or fibers) and the elastic energy stored due to stretch (characterized by the deformation gradient $\boldsymbol{F}$). The total free energy Ψ is therefore expressed in the general form:

$$\Psi = \int_0^{2\pi}\int_0^{\pi} P(\theta,\omega)\left[\psi_c(\boldsymbol{r}) - \psi_c(\boldsymbol{r}_0)\right] sin\theta d\theta d\omega \tag{66}$$

Assuming affine deformation, the chain/fiber stretch is expressed in terms of the macroscopic deformation gradient as $\boldsymbol{r} = \boldsymbol{F}\boldsymbol{r}_0$. The proposed approach takes a different route since the chain stretch is now incorporated into the probability function, such that the energy becomes:

$$\Psi = \int_0^{2\pi}\int_0^{\pi}\left(\int_0^{\infty}\left[P(\boldsymbol{r},t) - P(\boldsymbol{r}_0,t)\right]\psi_c(\boldsymbol{r})r^2 dr\right) sin\theta d\theta d\omega \tag{67}$$

It is clear here, that in contrast to (66), we here compare the distribution functions of the chains in their "natural" and deformed states and multiply this difference by the corresponding energy function. A main advantage of this viewpoint is that it allows for the evolution of the probability

function $P(\boldsymbol{r},t)$ arising from different physical processes, which may include, for instance the dynamic nature of the chains' attachment and detachment, the degradation of cross-links [56-59] as well as growth processes in biological materials [60] for instance. As a result, a number of dissipative processes can readily be incorporated into the current framework by simply modifying the evolution equation of the probability function shown in eq. (37). From a mathematical standpoint, eq. (67) also implies that one can naturally capture the change in natural (or stress-free) configuration of the material since the term $P(\boldsymbol{r},\Omega) - P(\boldsymbol{r}_0,\Omega)$ can vanish even though $\boldsymbol{F} \neq \boldsymbol{I}$. Consequently, the proposed theory does not rely on the traditional Lagrangian framework used for solid, but can be used to describe elastic fluids and viscous polymer without additional difficulties. Finally, we have shown that in the case of Gaussian statistics, the chain distribution could be described in terms of a distribution tensor, which may be thought of as an extension to the structure's tensor [61-62] that incorporates chain/filament length in its definition. In the following we discuss a number of possible extensions to our statistical approach.

As stated in Section 3, the single chain energy function ψ_c in eq. (17), which is based on the freely jointed chain (FJC) model with Gaussian statistics of segment configurations, is only applicable to small to moderate extensions. At large extensions where the contour length Nb is approached, the resulting chain stiffening can be captured by Langevin statistics. In this case, the single chain energy function is [13]:

$$\Psi_r = Nk_BT\left(\beta L^{-1}(\beta) + \ln\frac{L^{-1}(\beta)}{\sinh\left[L^{-1}(\beta)\right]}\right), \quad \beta = \frac{r}{Nb} \tag{68}$$

where $L^{-1}(\beta)$ is the inverse Langevin function that diverges as $\beta \to 1$ or $r \to Nb$. Following the same procedures as described in Section 3, we found that the distribution tensor $\boldsymbol{\mu}$ would become:

$$\boldsymbol{\mu} = \left\langle \frac{1}{rb} L^{-1}\left(\frac{r}{Nb}\right) P(\boldsymbol{r},t)\, \boldsymbol{r} \otimes \boldsymbol{r} \right\rangle \tag{69}$$

and the true stress tensor keeps its original definition as:

$$\boldsymbol{\sigma} = ck_B T(\boldsymbol{\mu} - \boldsymbol{I}) - p\boldsymbol{I} \tag{70}$$

Note that with eq. (69), one can no longer derive a simple time evolution equation for $\boldsymbol{\mu}$, such as that shown in eq. (37). Instead, one needs to calculate the time evolution of the distribution function $\phi(\boldsymbol{r},t)$ using eq. (11) and numerically perform the integral over all chain configurational states.

In Section 4.1, we have illustrated that our model with Gaussian chains reduces to the elastic neo-Hookean model if permanent cross-links are assumed. It is of interest to see what elastic solid would the Langevin chain model recover under the assumption of permanent cross-links. There are a few hyperelastic models in the literature that are derived from Langevin chains, in particular the Arruda-Boyce 8-chain model [9] and the Wu-van der Giessen (WG) network model [10]. Next we demonstrate that with Langevin chains (eq. (69)) our model degenerates to the WG model. WG adopted the affine deformation assumption for a permanent network which dictates that the end-to-end vector of a chain changes from $\boldsymbol{r}_0$ in the reference configuration to $\boldsymbol{r} = \boldsymbol{F}\boldsymbol{r}_0$ after deformation. However, a key difference between our model and the WG model is that we considered the full distribution in chain end-to-end vector, including both the end-to-end distance r and orientation. This was necessary to incorporate the effect of dynamic cross-links. In contrast, WG only considered the distribution in chain orientation and assumed a uniform chain end-to-end distance. At the stress-free configuration, all chains are assigned the same mean end-to-end distance $r = \sqrt{N}b$. After deformation, this distance becomes $\lambda\sqrt{N}b$, where λ depends on chain orientation, i.e. $\lambda(\theta,\omega)$ and can be calculated from the affine deformation assumption

that $\boldsymbol{r} = \boldsymbol{F}\boldsymbol{r}_0$. This is a special case of our distribution function $P(\boldsymbol{r},t)$ where the dependence on the end-to-end distance $\boldsymbol{r}$ is through the Dirac δ-function:

$$P(\boldsymbol{r},t) = \frac{\delta(\boldsymbol{r} - \lambda\sqrt{Nb})}{|\boldsymbol{r}|^2} C(\theta,\omega,t) \tag{71}$$

where $C(\theta,\omega,t)$ is a distribution function of chain orientation characterized by the spherical coordinates θ and ω. Substituting eq. (71) into eq. (70), we recover the equation by Wu and van der Giessen (see equation no. (29) in [10]). To the best of our knowledge, the Langevin chain model has not been directly incorporated into continuum models of polymer networks with dynamic bonds. Previous efforts to include the strain stiffening effects were based on continuum elasticity models such the Arruda-Boyce model [9], Gent model [35] or exponentially hardening model [36]. Recently, more sophisticated single chain models have been developed to combine entropic and enthalpic contributions for chain elasticity [63]. The latter describes the effects due to stretching of the carbon bonds on polymer chains. Incorporation of bond stretching can allow one to better capture the irreversible scission of chains due to excessive forces. Such sophisticated single chain models have not been implemented in continuum theories for dynamic networks, and our approach offers a clear path along this direction.

6. Summary

In summary, this paper described a new theoretical framework that can represent the time-dependent responses of soft polymers based on a statistical description of the underlying polymer network. Its root is anchored in a statistical representation of the configuration and evolution of a network of dynamically cross-linked polymer chains as it is subjected to deformation. Using

appropriate average operations and thermodynamical arguments, it was possible to relate the chain distribution to the concepts of stress, strain and entropy generation via the so-called distribution tensor. Eventually, a fully macroscopic theory was derived involving an evolution equation for this tensor. The theory provides natural extension of rubber elasticity in the range of inelastic deformation and could be extended to account for multiple networks, or large chain deformation (with Langevin statistics) to name a few. The dynamic bonds considered in this work can be broadly interpreted as the temporary interactions between polymer chains, e.g. entanglements in polymer melts or lightly cross-linked networks. Potentially, one can prescribe physics-based models to describe the kinetics of disentanglements and re-entanglements by taking advantage of the established knowledge in a vast literature on the dynamics of polymer chains [16-17]. Such physical insights may also be drawn from molecular-level simulations. Efforts in this direction may lead to new physics-based nonlinear viscoelasticity model of passive, active and bio-polymers [64-65]. Overall the statistical approach presented in this work can provide a convenient platform to integrate the complex physics of polymer chain dynamics that are otherwise difficult to be implemented into continuum theories.

Acknowledgments

FJV acknowledges the support of the National Science Foundation under the NSF MRSEC DMR 1420736 and the NSF CAREER award 1350090. RL acknowledges the support from the 3M non-Tenured Faculty award.

References

[1] Boyce, M.C., Arruda, E.M., 2000. Constitutive models of rubber elasticity: a review. *Rubber Chemistry and Technology* 73(3), 504–523.

[2] Wineman, A., 2009. Nonlinear viscoelastic solids – A review. *Mathematics and Mechanics of Solids*, 14(3), 300–366.

[3] Puglisi, G., Saccomandi, G., 2016. Multi-scale modelling of rubber-like materials and soft tissues: an appraisal. *Proc. R. Soc. Lond. A* 472: 20160060.

[4] Holzapfel, G.A., 2000. *Nonlinear solid mechanics: A continuum approach for engineering*, Wiley & Sons.

[5] Gurtin, M.A., Fried, E., Anand, L., 2010. *The mechanics and thermodynamics of continua*, Cambridge University Press.

[6] Flory, P.J., Rehner, J., 1943. Statistical mechanics of cross-linked polymer networks. I. Rubberlike elasticity, *J. Chem. Phys*. 11, 512–520.

[7] Treloar, L.R.G., 1946. The elasticity of a network of long-chain molecules –III. *Trans. Faraday Soc.*, 42, 83–94.

[8] Wang, M.C., Guth E., 1952. Statistical theory of networks of non-Gaussian flexible chains, *J. Chem. Phys.* 20, 1144–1157.

[9] Arruda, E.M., Boyce, M.C., 1993. A three-dimensional model for the large stretch behavior of rubber elastic materials. *J. Mech. Phys. Solids*, 41(2), 389–412.

[10] Wu, P.D., Van Der Giessen, E., 1993. On improved network models for rubber elasticity and their applications to orientation hardening in glassy polymers. *J. Mech. Phys. Solids*. 41(3), 427–456.

[11] Treloar, L.R.G., 1943. The elasticity of a network of long-chain molecules. I. *Trans. Faraday Soc.*, 39, 36–41.

[12] Kawakatsu, T., 2004. Gaussian chain model and statistics of polymers. In *Statistical Physics of Polymers*. Springer-Verlag Berlin, Kluwer, 17–99.

[13] Rubinstein, M., Colby, R.H., 2003. *Polymer Physics*. Oxford University Press.

[14] Horgan, C.O., Saccomandi, G., 2006. Phenomenological hyperelastic strain-stiffening constitutive models for rubber. *Rubber Chemistry and Technology* 79(1), 152–169.

[15] Beatty, M.F., 2003. An average-stretch full-network model for rubber elasticity. *J. Elasticity* 70(1), 65–86.

[16] de Gennes, P.G., Leger, L., 1982. Dynamics of entangled polymer chains. *Ann. Rev. Phys. Chem.* 33, 49–61.

[17] Doi, M.; Edwards, S.F., 1988. *The Theory of Polymer Dynamics*. Clarendon Press.

[18] Christensen, R.M., 2010. *Theory of Viscoelasticity*, Second Editon, Dover Publication.

[19] Lubliner, J., 1985. A model of rubber viscoelasticity, *Mech. Res. Comm*. 12, 93–99.

[20] Le Tallec, P., Rahier, C., Kaiss, A., 1993. Three-dimensional incompressible viscoelasticity in large strains: formulation and numerical approximation. *Comp. Meth. Appl. Mech. Eng.* 109, 233–258.

[21] Reese, S., Govindjee S., 1998. A theory of finite viscoelasticity and numerical aspects. *Int. J. Solids Structures* 35, 3455–3482.

[22] Bergstrom, J.S., Boyce, M.C., 1998. Constitutive modeling of the large strain time-dependent behavior of elastomers. *J. Mech. Phys. Solids*, 46, 931–954.

[23] Green, M.S., Tobolsky, A.V., 1946. A new approach to the theory of relaxing polymeric media. *J. Chem. Phys*. 14(2), 80–92.

[24] Tanaka, F., Edwards, S.F., 1992. Viscoelastic properties of physically cross-linked networks -transient network theory. *Macromolecules* 25, 1516–1523.

[25] Drozdov, A.D., 1999. A constitutive model in finite thermoviscoelasticity based on the concept of transient networks. *Acta Mech.* 133, 13–37.

[26] Hui, C.Y., Long, R., 2012. A constitutive model for the large deformation of a self-healing gel. *Soft Matter* 8, 8209–8216.

[27] Long, R., Qi, H.J., Dunn, M.L., 2013. Modeling the mechanics of covalently adaptable polymer networks with temperature-dependent bond exchange reactions. *Soft Matter* 9, 4083–4096.

[28] Long, R., Mayumi, K., Creton, C., Narita, T., Hui, C.Y., 2014. Time dependent behavior of a dual cross-link self-healing gel: theory and experiments. *Macromolecules* 47(20), 7243–7250.

[29] Meng, F., Pritchard, R.H., Terentjev, EM., 2016. Stress relaxation, dynamics, and plasticity of transient polymer networks. *Macromolecules* 49(7), 2843–2852.

[30] Rajagopal, K.R., Srinivasa, A.R., 2004. On the thermomechanics of materials that have multiple natural configurations Part I: viscoelasticity and classical plasticity. *ZAMP* 55, 861–893.

[31] Wojtecki, R.J., Meador, M.A., Rowan, S.J. 2011. Using the dynamic bond to access macroscopically responsive structurally dynamic polymers. *Nature Materials* 10, 14–27.

[32] Jin, Y., Yu, C., Denman, R.J., Zhang, W., 2013. Recent advances in dynamic covalent chemistry. *Chem. Soc. Rev.* 42, 6634–6654.

[33] Kloxin, C.J., Bowman, C.N., 2013. Covalent adaptable networks: smart, reconfigurable and responsive network systems. *Chem. Soc. Rev.* 42, 7161–7173.

[34] Long, R., Mayumi, K., Creton, C., Narita, T., Hui, C.Y., 2015. Rheology of a dual cross-link self-healing gel: theory and measurement using parallel-plate torsional rheometry. *Journal of Rheology* 59(3), 643–665.

[35] Meng, F., Terentjev, E.M., 2016. Transient network at large deformations: elastic-plastic transition and necking instability. *Polymers* 8(4), 108.

[36] Guo, J., Long, R., Mayumi, K., Hui, C-Y., 2016. Mechanics of a dual cross-link gel with dynamic bonds: steady state kinetics and large deformation effects. *Macromolecules* 49(9), 3497–3507.

[37] Long, K.N., Dunn, M.L., Qi, H.J., 2010. Mechanics of soft active materials with phase evolution. *Int. J. Plasticity* 26, 603–616.

[38] Leibler, L., Rubinstein, M., Colby, R.H., 1991. Dynamics of reversible networks. *Macromolecules* 24, 4701–4707.

[39] Sing, M.K., Wang, Z.G., McKinley, G.H., Olsen, B.D., 2015. Celebrating soft matter's 10th anniversary: chain configuration and rate-dependent mechanical properties in transient networks. *Soft Matter* 11, 2085−2096.

[40] Grindy, S.C., Learsch, R., Mozhdehi, D., Cheng, J., Barrett, D.G., Guan, Z., Messersmith, P.B., Holten-Andersen, N., 2015. Control of hierarchical polymer mechanics with bioinspired metal-coordination dynamics. *Nature Materials* 14, 1210−1216.

[41] Bergstrom, J.S.; Boyce, M.C., 2001, Deformation of elastomeric networks: relation between molecular level deformation and classical statistical mechanics models of rubber elasticity. *Macromolecules*, 34, 614-626.

[42] Yang, H., Yu, K., Mu, X., Shi, X., Wei, Y., Guo, Y., Qi, H. J., 2015. A molecular dynamics study of bond exchange reactions in covalent adaptable networks. *Soft Matter*, 11, 6305–6317.

[43] Fourier, J., 1955. *Analytical theory of heat*. Dover Publications, New York.

[44] Montarnal, D., Capelot, M., Tournilhac, F., Leibler, L., 2011. Silica-like malleable materials from permanent organic networks. *Science* 334, 965−968.

[45] Treloar, L.R.G., 1975. *The Physics of Rubber Elasticity*. Oxford University Press, USA.

[46] Kuhn, W., Grün, F., 1946. Statistical behavior of the single chain molecule and its relation to the statistical behavior of assemblies consisting of many chain molecules. *Polym. Chem*. 1(3), 183–199.

[47] Pearson, C.E., 1983. *Handbook of Applied Mathematics*. 2nd edition, Van Nostrand Reinhold.

[48] Grindy, S.C., Lenz, M., Holten-Andersen, N., 2016. Engineering elasticity and relaxation time in metal-coordinate crosslinked hydrogels. *Macromolecules* 49, 8306−8312.

[49] Tang, S., Habicht, A., Li, S., Seiffert, S., Olsen, B.D., 2016. Self-diffusion of associating start-shaped polymers. *Macromolecules* 49, 5599-5608.

[50] Tanaka, F., Edwards, S.F., 1992. Viscoelastic properties of physically crosslinked networks: Part I: Nonlinear stationary viscoelasticity. *J. Non-Newtonian Fluid Mechanics*, 43, 247−271.

[51] Gent, A.N., 1996. Adhesion and strength of viscoelastic solids. Is there a relation between adhesion and bulk properties? *Langmuir* 12, 4492−4496.

[52] de Gennes, P.G., 1996. Soft Adhesives. Langmuir 12, 4497−4500.

[53] Persson, B.N.J., Brener, E.A., 2005. Crack propagation in viscoelastic solids. *Physical Review E* 71, 036123.

[54] Knauss, W.G., 2015. A review of fracture in viscoelastic materials. *Int. J. Fract.* 196, 99−146.

[55] Edwards, S.F., Vilgis, T.A., 1988. The tube model of rubber elasticity. *Rep. Prog. Phys*. 51, 243-297.

[56] Charlesby, A., 1981. Crosslinking and degradation of polymers. *Radiation Physics and Chemistry* 18(1–2), 59–66.

[57] Vernerey, F.J., Greenwald, E.C., Bryant, S.J., 2012. Triphasic mixture model of cell-mediated enzymatic degradation of hydrogels. *Comput. Meth. Biomech. Biomed. Eng.* 15(11), 1197–1210.

[58] Dhote, V., Vernerey, F.J., 2014. Mathematical model of the role of degradation on matrix development in hydrogel scaffold. *Biomech. Model. Mechanobiol*. 13(1), 167–183.

[59] Akalp, U., Bryant, S.J., Vernerey, F.J., 2016. Tuning tissue growth with scaffold degradation in enzyme-sensitive hydrogels: a mathematical model. *Soft Matter* 12(36), 7505–7520.

[60] Vernerey, F.J., 2016. A mixture approach to investigate interstitial growth in engineering scaffolds. *Biomech. Model. Mechanobiol*. 15(2), 259–278.

[61] Cortes, D.H., Elliott, D.M., 2016. Modeling of collagenous tissues using distributed fiber orientations. in *Structure-Based Mechanics of Tissues and Organs*, G. S. Kassab and M. S. Sacks (Eds.), Springer US, 15–39.

[62] Vernerey, F.J., Farsad, M., 2011. A constrained mixture approach to mechano-sensing and force generation in contractile cells. *J. Mech. Behav. Biomed. Mater*. 4(8), 1683–1699.

[63] Mao, Y., Talamini, B., Anand, L., 2017. Rupture of polymers by chain scission. *Extreme Mechanics Letters*, 13, 17–24.

[64] Vernerey, F.J., Akalp, U., 2016. Role of catch bonds in actomyosin mechanics and cell mechanosensitivity. *Phys. Rev. E* 94(1), 012403.

[65] Akalp, U., Schnatwinkel, C., Stoykovich, M.P., Bryant, S.J., Vernerey, F.J., 2017. Structural modeling of mechanosensitivity in non-muscle cells: multiscale approach to understand cell sensing. *ACS Biomater. Sci. Eng*., in press, DOI:10.1021/acsbiomaterials.6b0069.

Appendix A.1 Derivation of the variation of free energy

Equation (19) in the manuscript represent the variation for the total free energy as a function of macroscopic quantities, including the distribution tensor. Details of its derivation are given below. Starting from the form of the free energy written in eq. (18), it is straightforward to show that $\dot{\Psi}$ can be expressed as:

$$\dot{\Psi} = -\dot{T}\left(\gamma\, ln\left(\frac{T}{T_0}\right) + \vartheta_0\right) + \Delta\dot{\Psi}_e \tag{A1}$$

where $\Delta\dot{\Psi}_e(t)$ can be calculated from eq. (17) as:

$$\Delta\dot{\Psi}_e = \frac{k_B\dot{T}}{2}\left\langle(\phi - \phi_0)\tilde{r}^2\right\rangle + \frac{k_BT}{2}\left\langle(\dot{\phi} - \dot{\phi}_0)\tilde{r}^2\right\rangle + ptr(\boldsymbol{L}) \tag{A2}$$

Now using the evolution equation for the distribution function, we can write:

$$\left\langle\dot{\phi}\tilde{r}^2\right\rangle = \left\langle\xi_a P_0\tilde{r}^2\right\rangle - \left\langle k_d\phi\tilde{r}^2\right\rangle - \left\langle L_{it}\phi\tilde{r}^2\right\rangle - \left\langle\frac{\partial\phi}{\partial r_i}r_j\tilde{r}^2\right\rangle L_{ij} \tag{A3}$$

Using integration by part on the last term, this equation simplifies to:

$$\left\langle\frac{\partial\phi}{\partial r_i}r_j\tilde{r}^2\right\rangle L_{ij} = -\left\langle\phi\delta_{ij}\tilde{r}^2\right\rangle L_{ij} - \left\langle 2\phi\delta_{ik}\tilde{r}_j\tilde{r}_k\right\rangle L_{ij} \tag{A4}$$

Substituting in (A3) and using the definition of the chain distribution tensor:

$$\boldsymbol{\mu} = \langle P\tilde{\boldsymbol{r}}\otimes\tilde{\boldsymbol{r}}\rangle \quad \text{and} \quad \boldsymbol{\mu}_0 = \langle P_0\tilde{\boldsymbol{r}}\otimes\tilde{\boldsymbol{r}}\rangle, \tag{A5}$$

we obtain:

$$\left\langle\dot{\phi}\tilde{r}^2\right\rangle = \xi_a tr(\boldsymbol{\mu_0}) - \left\langle k_d\phi\tilde{r}^2\right\rangle + 2c\boldsymbol{\mu}:\boldsymbol{L} \tag{A6}$$

Similarly, the time derivative of the chain distribution tensor ϕ_0 from its reference state is:

$$\left\langle \dot{\phi}_0 \tilde{r}^2 \right\rangle = \xi_a tr(\boldsymbol{\mu_0}) - \left\langle k_d \phi_0 \tilde{r}^2 \right\rangle + 2c\boldsymbol{\mu_0}:\boldsymbol{L} \tag{A7}$$

Finally substituting eqs (A6) and (A7) into (A2), allows to express the change in elastic energy as:

$$\Delta\dot{\Psi}_e = \frac{k_B T}{2}\left(2c(\boldsymbol{\mu} - \boldsymbol{\mu_0}):\boldsymbol{L} - \left\langle k_d(\phi - \phi_0)\tilde{r}^2 \right\rangle\right) + \frac{ck_B\dot{T}}{2}\left(tr(\boldsymbol{\mu} - \boldsymbol{\mu}_0)\right) + ptr(\boldsymbol{L}) \tag{A8}$$

which, when plugged into eq (A1) leads to eq. (20) in the main text.

Appendix A.2 Evolution equation for the distribution tensor

Starting from its original definition in eq. (21), let us, for convenience express the time evolution of the tensor $\boldsymbol{\mu}$ in component form as follows:

$$\dot{\mu}_{ij} = \int \dot{P}(\boldsymbol{r})\tilde{r}_i\tilde{r}_j d\boldsymbol{r} = \frac{1}{c}\left(\int \dot{\phi}(\boldsymbol{r})\tilde{r}_i\tilde{r}_j d\boldsymbol{r} - \dot{c}\int P(\boldsymbol{r})\tilde{r}_i\tilde{r}_j d\boldsymbol{r}\right) \tag{A9}$$

Using (10), we then obtain:

$$\dot{\mu}_{ij} = \frac{\xi_a}{c}\mu_{ij}^0 - \left(k_d + L_{kk}\right)\mu_{ij} - L_{lk}M_{klij} - \frac{\dot{c}}{c}\mu_{ij} \tag{A10}$$

where the components of the fourth order tensor M are given by:

$$M_{klij} = \int_r \frac{\partial\phi(\boldsymbol{r})}{\partial r_l}\tilde{r}_k\tilde{r}_i\tilde{r}_j d\boldsymbol{r} \tag{A11}$$

and

$$\overline{\boldsymbol{k}}_{ij} = \int_r k_d(\boldsymbol{r})P(\boldsymbol{r})\tilde{r}_i\tilde{r}_j d\boldsymbol{r} \tag{A12}$$

A simple integration by part then leads $M_{ijkl} = -\left(\delta_{ij}\mu_{lk} + \delta_{jk}\mu_{li} + \delta_{jl}\mu_{ik}\right)$ where we assumed that boundary terms vanished. The evolution equation for $\boldsymbol{\mu}$ therefore take the convenient form:

$$\dot{\mu}_{ij} = \frac{\xi_a}{c}\mu_{ij}^0 - \overline{k}_{d_{ij}} + \left(L_{ik}\mu_{kj} + L_{jk}\mu_{ki}\right) - \frac{\dot{c}}{c}\mu_{ij} \tag{A13}$$

In a tensor notation, this relation can be written as:

$$\dot{\boldsymbol{\mu}} = \frac{\xi_a}{c}\boldsymbol{\mu}^0 - \overline{\boldsymbol{k}}_d - \frac{\dot{c}}{c}\boldsymbol{\mu} + \boldsymbol{L\mu} + (\boldsymbol{L\mu})^T \tag{A14}$$

where the superscript T denotes the transpose operator. Using the fact that the product of a symmetric and antisymmetric tensor vanishes, the term $\boldsymbol{L\mu}$ can be replaced by $\boldsymbol{D\mu}$ where $\boldsymbol{D} = \left(\boldsymbol{L} + \boldsymbol{L}^{\boldsymbol{T}}\right)/2$ is the symmetric rate of deformation tensor. This enables to write:

$$\dot{\boldsymbol{\mu}} = \frac{\xi_a}{c}\boldsymbol{\mu}^{\mathbf{0}} - \overline{\boldsymbol{k}}_d - \frac{\dot{c}}{c}\boldsymbol{\mu} + \mathbf{D}\boldsymbol{\mu} + \boldsymbol{\mu}\boldsymbol{D} \tag{A15}$$

This equation corresponds to eq. (37) in the main text.

Appendix A.3 Recovering the linear viscoelastic model

Under uniaxial tension, $F_{11} = \lambda$, $F_{22} = F_{33} = \lambda^{-1/2}$, and all other components vanish. Substituting $\boldsymbol{F}$ into eq. (50), we obtain

$$\mu_{11}(t) = e^{-k_d t}\lambda^2(t) + \int_0^t k_d\left[\frac{\lambda^2(t)}{\lambda^2(\tau)}\right]e^{-k_d(t-\tau)}\,d\tau \tag{A16}$$

and

$$\mu_{22}(t) = \mu_{33}(t) = e^{-k_d t}\lambda^{-1}(t) + \int_0^t k_d\left[\frac{\lambda^2(t)}{\lambda^2(\tau)}\right]e^{-k_d(t-\tau)}\,d\tau \tag{A17}$$

To obtain the tensile stress σ_{11}, we use the boundary condition that $\sigma_{22} = \sigma_{33} = 0$ to determine the pressure term p. With some simple algebra, we obtain that

$$\frac{\sigma_{11}(t)}{ck_BT} = e^{-k_d t}\left[\lambda^2(t) - \frac{1}{\lambda(t)}\right] + \int_0^t k_d\left[\frac{\lambda^2(t)}{\lambda^2(\tau)} - \frac{\lambda(\tau)}{\lambda(t)}\right]e^{-k_d(t-\tau)}\,d\tau \tag{A18}$$

with small deformation where $\lambda = 1 + \varepsilon$, we can linearize eq. (A18) and obtain the following equation

$$\frac{\sigma_{11}(t)}{ck_BT} = 3\varepsilon(t)e^{-k_d t} + 3\int_0^t k_d[\varepsilon(t) - \varepsilon(\tau)]e^{-k_d(t-\tau)}\,d\tau \tag{A19}$$

$$= 3\varepsilon(t)\int_{-\infty}^{0} k_d e^{-k_d(t-\tau)}\,d\tau + 3\int_{0}^{t} k_d[\varepsilon(t)-\varepsilon(\tau)]e^{-k_d(t-\tau)}\,d\tau$$

We assume the mechanical loading starts at $t = 0$, which implies $\varepsilon(\tau) = 0$ for $\tau < 0$. As a result, eq. (A19) can be casted in the following form:

$$\begin{aligned}\frac{\sigma_{11}(t)}{ck_BT} &= 3\int_{-\infty}^{t} k_d[\varepsilon(t)-\varepsilon(\tau)]e^{-k_d(t-\tau)}\,d\tau \\ &= 3\int_{-\infty}^{t} e^{-k_d(t-\tau)}\frac{d\varepsilon(\tau)}{d\tau}d\tau\end{aligned} \tag{A20}$$

If we recognize that $E_0 = 3ck_BT$ is the instantaneous Young's modulus and $E(t) = E_0 e^{-k_d t}$ is the relaxation modulus, then eq. (A20) can be written as

$$\sigma_{11}(t) = \int_{-\infty}^{t} E(t-\tau)\frac{d\varepsilon(\tau)}{d\tau}d\tau \tag{A21}$$

We have reduced to linear viscoelasticity, specifically a Maxwell model given the form of $E(t)$. Since the mechanical loading starts at $t = 0$ and we allow an instantaneous application of strain, eq. (A21) can also be written as

$$\sigma_{11}(t) = E(t)\varepsilon\left(t = 0^{+}\right) + \int_{0^{+}}^{t} E(t-\tau)\frac{d\varepsilon(\tau)}{d\tau}d\tau \tag{A22}$$